Removal of crude oil films by aqueous detergents

Espig, Sam

Award date:
1997

Awarding institution:
University of Bath

Removal of Crude Oil Films by Aqueous Detergents

submitted by Sam Espig
for the degree of Ph.D. of the University of Bath
1997

ProQuest LLC
789 East Eisenhower Parkway
P.O. Box 1346
Ann Arbor, MI 48106-1346

To Omi

Preface

The work described in this thesis has been carried out in the Department of Chemical Engineering, University of Bath, between October 1993 and October 1996. The work is original unless stated in the text. Neither the present thesis, or any part thereof, has been submitted at any other university.

I have very much enjoyed my time at Bath University and I wish to thank everyone who has helped and supported me throughout this thesis. I am particularly grateful to my supervisor, Dr Michael Bird, for his dedication, advice and encouragement. I would also like to thank Dr Richard Rathbone for his help with the modelling aspects of the work and Dr Matthew Bennett for his guidance.

Financial support from the Engineering and Physical Sciences Research Council (EPSRC) has been invaluable. I am also grateful for the financial and specialist backing provided by International Products Corporation, where particular thanks must go to Mr Charlie Granito.

The technical support provided by the Chemical Engineering Department was greatly appreciated, especially that given by Mr Richard Bull. Mr Colin Wilson was also very helpful in respect of the photographical aspects of the work. In addition, appreciation must go to Mr Harry Motson and Dr Glyn John of ICI Surfactants for their technical product advice.

Sam Espig

Summary

In industry, the cleaning of oily soils from hard surfaces is a common problem. Surfactants are often used to tackle this problem but their application is typically empirical. Further knowledge on the interaction of surfactants with oil films is required. Material published in the literature on the cleaning of oily soils has concentrated on removal from fabrics rather than from hard surfaces, as historically this has been the largest market for surfactant based products. Nonionic surfactants have been identified as the most effective detergents but research work has originated from the area of colloid science concentrating on surface chemistry and primarily the removal of oil droplets rather than oil films. Fouled deposits are also unrepresentative of industry involving manual application. The effects of surfactant composition, concentration, velocity and temperature have been investigated but often only concentrating on an individual parameter, typically temperature.

This study provides an engineering approach to oil removal. Fouling and cleaning rigs have been designed and constructed, crude oil films have been fouled under controlled dynamic conditions and the effect on removal of the above parameters has been determined. Detailed visual removal techniques have provided invaluable information on the mechanisms of removal, confirming roll up as the main surfactant removal mechanism. Removal was found to occur below the critical micelle concentration (cmc), and an optimum cleaning concentration was discovered above the cmc, the reduction of interfacial forces being crucial to removal. At low temperatures further increases above the optimum concentration were detrimental to removal. Gas chromatography of the oil deposit during cleaning has confirmed that there is no selective component removal from the crude oil deposit. The key mechanism involved in removal have been hypothesised, and the 'surface modification' step was found to be rate limiting, with the diffusion boundary layer offering little resistance to removal. Semi empirical models have been developed to describe removal by water and the additional effect of the surfactant.

Contents

LIST OF TABLES

LIST OF FIGURES

Chapter One

To Clean or Not to Clean?

1.1 Introduction

Cleaning is the removal of unwanted deposits from a system. The formation of deposits on process equipment occurs frequently in industry presenting problems such as reduced heat transfer and increased pressure drop. The cleaning of oil films from metal surfaces represents a typical removal problem. Current practice has been developed on an empirical basis. Systems include high pressure steam cleaning, the application of solvents or aqueous based cleaners which are typically a combination of an alkali base and a combination of surfactants.

Cleaning can be costly both to the processor and to the environment and there is surprisingly little published information on the mechanisms of oil film removal. The literature treatment of the principles and mechanisms of oil film removal is unclear and incomplete, specifically with reference to modelling. The majority of the experimental work reported has determined an overall cleaning time rather than production of kinetic curves. Historically work has concentrated on fouling and its reduction rather than on cleaning.

Aqueous cleaning is the most common method of removal. Cleaning overcomes both the soil / soil and the soil / substrate adhesion forces of the deposit by exerting energy on the deposit. This energy is realised either through reaction and subsequent break down of the deposit and / or through reduction of the interfacial forces among the substrate, soil and medium by physical or chemical methods. The substrate can be subjected to the cleaning medium in either flow or static conditions. There are several parameters which will effect the efficiency of any cleaning process; the type of medium and its concentration, temperature and velocity (in a dynamic system). In industry, the selection of these parameters is often done empirically (Romney, [1990]). The following diagram (Figure 1.1) summarises the main parameters that affect removal efficiency.

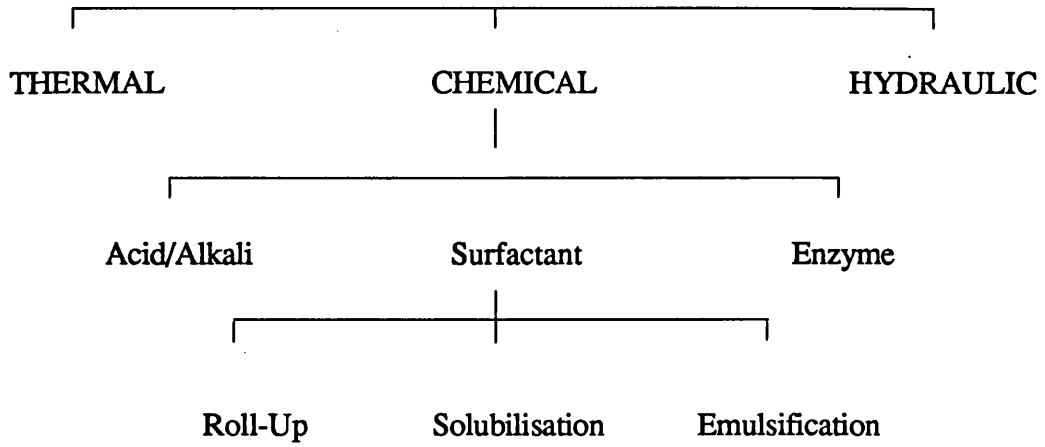

Figure 1.1 The Main Oily Soil Removal Processes

Each of the three main removal processes are important to oil removal and their individual effect has been investigated. If deficient in one the other two become more significant. Kinetic energy is provided in the form of solution velocity and substrate shear stress. The transition from turbulent to laminar flow is generally considered to be crucial although investigation has shown otherwise, (Chapter 6). Thermal energy is important, improving hydraulic and reaction dynamics. Many authors suggest that increased temperatures aid removal. Results presented in this thesis define the effect thoroughly, (Chapter 6). Chemical additives reduce the energy required for deposit removal through deposit reaction and interface modification. Increasing the cleaning agent concentration is generally reported to aid removal, although concentration optima are reported in this study (Chapter 6).

1.2 Detergents

A detergent should be selected specifically for the type of soil to be removed. It has one or more of the following attributes: (adapted from Romney [1990] and The Soap and Detergent Association [1987]

1. Solubilisation- Dissolves organics such as fatty and oily soils
2. Emulsification- Maintains oils and fats dispersed within the cleaning solution
3. Wetting- Reduces of surface and interfacial tensions.
4. Dispersion and suspension- Brings insoluble oils into suspension and prevents their redeposition on cleaned surfaces.

5. Sequestration / chelatation- Combines with calcium and magnesium salts etc. found in hard water to form water soluble compounds.
6. Reaction- Saponifies fatty soils, enzymes digest protein based soils.
7. Neutralisation- Neutralises acid soils.
8. Rinsing- Ensures the cleaned surface is left clear of any trace of soil or detergent.

1.2.1 Types of Detergent

A detergent is defined as "any substance that either alone or in a mixture reduces the work requirement of a cleaning process" (Bourne and Jennings, [1963]). There are many different types of detergent, from solvents to soaps. Aqueous detergents can be categorised into three parts, shown below. For oily soil removal nonionic surfactants are considered to be the most effective (Lange, [1994]) and receive detailed study in this thesis. Voss and Korpi [1972] studied the effect of various detergents and cleaning procedures for oily soil removal from stainless steel.

1.2.2 Acids and Alkalis,

The addition of an acid or alkali to a cleaning solution provides a surplus of H^+ or OH^- ions respectively. The surplus of ions induces reaction of the ions with the deposited soil. Alkalis attack organic material, saponify oily materials and neutralise acidic residues. Conversely acidic solutions are aggressive to base materials and dissolve inorganic oxides. Both processes can leave a large amount of insoluble particulate material (McCoy, [1984]).

1.2.3 Enzymes

Enzymes are complex proteinaceous molecules. Selected enzymes are effective at breaking down certain soils and stains to simpler molecules, which are then more readily removed by detergents. They are typically used at high concentrations or over long exposure times. There are two main types of enzyme used in cleaning: protease and lipase. Protease chemically breaks down polymeric protein soil stains such as blood, egg and cocoa. Lipase hydrolyses triglyceride soils and thereby aid surfactant efficiency (Miller and Raney [1993]). Enzymes are also expensive and unstable at high pHs (above 9) and are rarely used in the breakdown of oily deposits on hard surfaces.

1.2.4 Surfactants

Surfactants (**surface active agents**) are amphiphilic in nature accumulating at interfaces, and have assets that make them very useful cleaning agents. Firstly, they lower the interfacial tension between the cleaning solution and the contacting phase. This reduces the work necessary to create new interface per unit length thus lowering the energy required to disperse a deposit into solution (enhancing roll up and emulsification, Chapter 2). Secondly, at high concentrations the amphiphiles also aggregate promoting solubilisation of the soil (Chapter 2). There are a very wide range of different classes of surfactants that are used in a variety of cleaning applications. Much of the research on surfactants has concentrated on their surface chemistry rather than determining the optimum conditions needed for effective removal.

1.3 Nature of Deposits

There are many different types of soil. These can be categorised into six classes, shown below. The types of soil are often a function of temperature and, for example, are dependent on the soil melting point.

1. Water soluble- Considered easy to remove with clean water but a challenge with dry cleaning techniques.
2. Oily- Primarily hydrocarbon based, no polar group, crude oil, vegetable, motor oil.
3. Greasy- Essentially fatty materials containing polar groups such as esters and carboxylates.
4. Particulate- Soils such as metal oxide alumina and silica clay
5. Bleachable- Oxidizable soils such as stains from fruit, wine, coffee and tea.
6. Protein and starch- Soils such as potato, blood, milk and grass.

Work published concerning oil film removal has only really focused on the removal of oil drops from flat surfaces or individual fibres with the assumption that similar removal mechanisms can be applied to practical situations (Raney and Miller [1993]). This project considers the practical problem of removing oil films from the inside of stainless steel piping.

1.4 Nature of Surface to be Cleaned

The finish of the substrate plays an important role in determining the ease of deposit removal. The rougher the surface the harder soil is to remove. Several investigators have considered the effect of surface roughness on cleaning efficiency. Mahé et al [1988] looked at the effect of the surface roughness of glass on the rinsing of droplets of oil. Three roughnesses were used, 0.1-0.5μm, 1μm, 5-10μm. Results indicated that a surface roughness below 0.1μm had no effect on removal. Above which, removal was increasingly more difficult.

Stainless steel, which is used in this study, is the most commonly used hard surface substrate for detergent analysis, being resilient to the majority of chemical cleaners. A smooth surface roughness has been chosen to minimise the mechanical forces of adhesion, (see Chapter 3).

1.5 Cleanliness Required

The degree of cleanliness required varies substantially from industry to industry. Romney [1990] neatly summarises the target level of cleanliness into three categories; physically clean, chemically clean and microbiologically clean. Physically clean concerns the visual appearance of the surface. Chemically clean is totally free of chemical residuals and microbiologically clean refers to an acceptable level of bacterial contamination. In this study removal is primarily assessed gravimetrically and therefore only considers a physical level of cleanliness with a detection limit of >99% clean which is sufficient for the majority of crude oil based applications.

1.6 Conclusions

Oil cleaning is clearly a complex process the mechanisms of which are poorly explained in the literature. Cleaning efficiency is dependent on the applied process conditions and the type of deposit. In industry, selection of chemical cleaners and thermo-hydraulic conditions is often empirical, applying high concentrations of formulated chemical cocktails which are not specific to the particular application. Although cleaning costs can constitute a significant portion of the overall processing costs, cleaning rarely receives the attention it deserves. Oily film deposits are

tenacious and present a difficult problem to the process industry. Optimising crude oil cleaning and elucidating the mechanisms of removal will improve current understanding and provide benefits to process operations with possible applications to other oil fractions.

1.7 Scope and Aims of the Study

Research undertaken on oil deposit cleaning has not been representative of industry. Little work has concerned the development of models that describe and predict removal. The literature has concentrated in detail on interfacial phenomena rather than from a practical approach, determining optimum conditions of removal.

This thesis has identified an effective industrial nonionic surfactant ($C_{9\text{-}11}E_6$) and concentrated on its singular effect on removal of a crude oil film. Cleanliness can be analysed down to greater than 1% of the original deposit mass, which is equivalent to a visual degree of cleanliness. The effect of additional surfactants and their synergy is beyond the scope of this study but could be tackled in future work, (see Chapter 8). The technique allows change in deposit thickness but this has not been investigated.

The aims of this work are (1) to develop a fouling and cleaning protocol to allow the investigation of the effect of detergents on crude oil films. (2) Produce removal kinetics which can enable determination of the relative importance and significance of key parameters involved in removal: temperature, velocity, concentration. This would facilitate determination of the effect of the surfactant properties on removal (cloud point, micelle shape, etc.). Kinetic and visual analysis would then allow (3) the development of models to describe removal.

1.8 Structure of the Thesis

This thesis is divided into seven subsequent Chapters:

Chapter Two: **Aqueous Detergents.** Describes the action of detergents on oil films and the work undertaken in the literature to enhance current understanding of the mechanisms of removal.

Chapter Three: **Fouling.** Details the mechanisms and processes of adhesion of oily soils to a surface and techniques of deposition reported in the literature.

Chapter Four: **Materials and Methods.** The classification of components and techniques used in the thesis.

Chapter Five: **Development of an Experimental Cleaning System.** A review of previous methods to determine soil removal. Explains the experimental fouling and cleaning protocols developed to determine crude oil film removal kinetics.

Chapter Six: **Experimental Results and Discussion.** Crude oil removal kinetics are examined as a function of velocity, temperature and detergent concentration and composition. The cleaning process is also investigated using visualisation techniques and in terms of crude oil compositional changes during cleaning.

Chapter Seven: **Modelling Removal.** Theoretical and empirical models are developed to describe removal.

Chapter Eight: **Conclusions and Future Work.** Conclusions are drawn from the experimental analysis and areas of future work are examined.

Chapter 2

Aqueous Detergents

2.1 Introduction

Cleaning has been the subject of many investigations from food deposits to oily soils. Oily soils have always received attention but primarily in the form of droplet removal (Lim et al [1991], Kao et al [1989] and Mahé et al [1988]) rather than films and from textiles (Raney [1991] and Thompson, [1992]) rather than from metal surfaces. Early studies were carried out in static baths (Jennings et al [1966]). Subsequent studies investigated the effect of ultrasound (Walker [1985] and Vaccari [1993]) and recent work has concentrated on dynamic systems (Beaudoin et al [1995]). Cox and Matson, [1984] studied the effect of static and dynamic systems on the removal of fatty and oily soils by nonionic surfactants from aluminum and masonite. Analysis determined the time to clean rather than the kinetics of cleaning. Static systems are often used to provide key information on removal mechanisms, but whether this can be applied to dynamic systems using different deposits is questionable.

This Chapter reviews the literature concerning oily soil removal primarily, concentrating on nonionic surfactants. Nonionic surfactants have generally been seen as the most effective detergents for oily soil removal. This Chapter can be broken down into two sections. The first section considers the effect of rinsing and the second the effect of aqueous detergents on the removal of oily soils. Relevant background information on detergents and their properties is provided. Comparisons are drawn between surfactants and alkalis, but little attention is drawn to enzyme cleaners as they are of limited use for the breakdown of oily soils. Particular emphasis is paid to published mechanisms and models proposed in the literature for the removal of oily soils by surfactants.

2.2 Rinsing

Studies concerning the removal of droplets of oil by water are almost nonexistent (Mahé et al [1988]). The rinsing of an insoluble deposit relies solely on the shear forces provided by the rinse solution. However, crude oil removal is strongly oil viscosity dependent, therefore the required fluid shear will also be a strong function of applied water temperature. Adams [1990] wrote a practical paper concerning the removal of crude from the shorelines of the Prince William Sound. Water proved effective especially at higher temperatures. Nevertheless, cleaning was limited to

65°C because of the detrimental effect on the local ecology and the kinetics of oil removal were not reported. Mahé et al [1988] performed a rigorous study rinsing droplets of decane from a glass substrate and found that removal was related to a critical shear stress. Nagarajan and Welker [1992] found high pressure rinsing (up to 210 barg) to be an effective alternative to chlorinated solvents for the particulate removal of oily soils from machined metal alloys. Cleaning efficiency was also found to increase significantly with particle size. These results agree with those of Sterritt [1992], who found that water was a viable alternative to solvent cleaning for flux residues from circuit boards.

Many authors have been interested in the effect of water as a cleaning agent for non-oil applications, with the food industry receiving particular attention. Work is relevant to the current study if deposits are insoluble in water. Jennings et al [1966] dipped insoluble fatty tristearin fouled stainless steel strips into a bath containing water to determine the contribution of the air / liquid interface to removal, (the Marangoni effect). It was determined that the amount of removal depended on the speed and number of immersions made and removal was therefore due to the action of the air liquid interface.

2.2.1 Rinsing Removal Models

Many authors have found that for particulate removal from a hard surface by water flow must be turbulent although the universality of this phenomenon is subject to debate, (Bird [1993]). Cleaver and Yates [1973] considered this event and developed theoretical mechanisms of removal examining the turbulent fluid hydrodynamics of particle removal from a hard surface. They suggested that particle removal occurred as a result of turbulent eruptions occurring in the viscous sublayer. The authors developed a model to relate the bursts to the kinetics of removal. Paulsson [1989] presented a fundamental study considering the removal of clay particles from steel piping using water at 20°C. Reynolds numbers between 8,000 and 80,000 were studied. Shear stress at the wall (τ_w) raised to the power 1.24 best characterised the mechanical effect where rate of change in deposit thickness $\left(-\frac{dl}{dt}\right)$ was given by equation 2.1:

$$-\frac{dl}{dt} = C_1(\tau_w)^{1.24} + C_2 \qquad 2.1$$

Where C_1 and C_2 are dimensional constants.

Mahé et al [1988] developed an elementary model describing oil droplet removal in terms of droplet size, contact angles, interfacial tension and the properties of the rinse water. Plett [1985] presented a paper considering the four phases of rinsing of fluorescein from a plate heat exchanger and the relevant mass transfer mechanisms. Two models were presented to describe removal, one for the transfer of deposit from the sublayer to the bulk by diffusion, and the other for transfer by penetration.

2.3 Aqueous Detergents

2.3.1 Alkalis

Alkaline materials, such as sodium hydroxide can be used alone or as a constituent for more complex cleaning formulations. The presence of alkali salts has the main function of saponifying fatty or oily soils. Alkalis can also enhance certain surfactants, disperse and suspend dirt, provide water softening characteristics, maintain a desired alkalinity and aid in the removal of microorganisms (The Soap and Detergent Association, [1987]). Many workers have studied removal by OH^- ions but primarily on fatty deposits such as tristearin and milk rather than oily soils.

2.3.1.1 Conditions for Alkali Removal

Removal using alkaline solutions is through direct reaction and deposit break down. The effect of temperature upon performance is unclear. It is generally accepted that increased temperature increases removal although some workers imply high cleaning temperatures induce a 'burn on' of the soil (Romney, [1990]). In contrast Barlett, Bird and Howell [1994] found an optimum temperature of 50°C for the cleaning of fatty material fouled on microfiltration membranes using 0.2 wt% sodium hydroxide. Most workers agree that increasing the concentration of NaOH improves removal up to some limit, whereupon subsequent increases have no effect (Bourne and Jennings 1965). However, (Bird 1993) found an optimum concentration of 0.5 wt% when cleaning fatty deposits from stainless steel using sodium hydroxide (Bird [1993]). All workers agree that increasing velocity has a positive effect upon deposit removal (Bird

and Espig 1994). An increased velocity increases the shear stress at the wall and hence the forces upon the deposit. Some workers suggest a minimum Reynolds number below which removal is negligible. This ranges from Jennings et al [1957] with a figure of 25,000 to the Cleaver and Yates [1973] statement that turbulent flow is required before removal occurs. Other workers find steady removal at very low velocities, and in laminar flow regions (Bird, 1993).

2.3.1.2 Alkali Removal Models

Bourne and Jennings, [1963] studied the kinetics of tristearin removal from stainless steel by sodium hydroxide, and found that two species were present. The authors modelled each species removed as a parallel first order reaction with respect to deposit mass, M_d. Gallot-Lavallee and Lalande [1985] proposed an important zero order model for the effect of OH^- concentration on removal, equation 2.2:

$$-\frac{dM_d}{dt} = A\,k_A[OH^-] \qquad 2.2$$

where A = Area

OH^- = Cleaning Agent Hydroxide ion concentration

k_A = Apparent reaction rate

Gallott-Lavalle and Lalande [1985] developed this further suggesting the formation of an intermediate swollen phase. The cleaning process was divided into four separate stages which could be represented by four first order differential equations. Many authors have used this as a basis for further development; Plett [1985], Perlat [1986] and Bird and Fryer [1991]). However, the protein reaction front shelving models are unlikely to be of any use when modelling oil film removal.

2.3.2 Surfactants

Surfactants are useful across a wide range of industries. They have been widely studied, and a large data bank exists in the literature. Surfactant cleaners consist of molecules which are characterised by their individual two component structure, shown in Figure 2.1. Each molecule is schizophrenic; one component, the hydrophilic head, has a strong attraction to the bulk aqueous phase and the other component, the

hydrophobic tail, has repulsion to the bulk phase. The relative size of each of the components determines the surfactant properties.

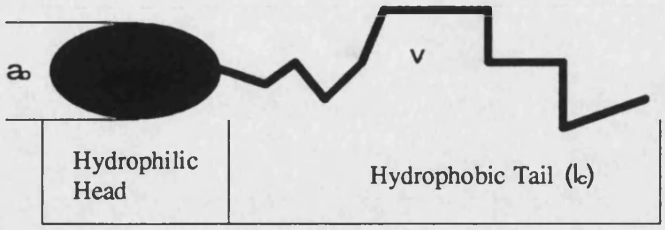

Figure 2.1 Surfactant Molecule

2.3.2.1 Surfactant Aggregation

At equilibrium, surfactant monomers will assume a state of lowest free energy. Since surfactant monomers are amphiphilic they tend to accumulate at interfaces within an aqueous solution. The polar head group having a strong preference to remain in the water and the hydrogen tail favouring leaving the water, see Figure 2.2 (a)-(c). A dynamic equilibrium will exist between monomers dispersed in solution and those aligned at the interface. As the concentration is increased the equilibrium relationship remains constant and more monomers position themselves in solution and at the interface. Initially the monomers will lie flat on the interface but as the interface becomes crowded the monomers will assume a vertical orientation as shown (Porter [1994]) .

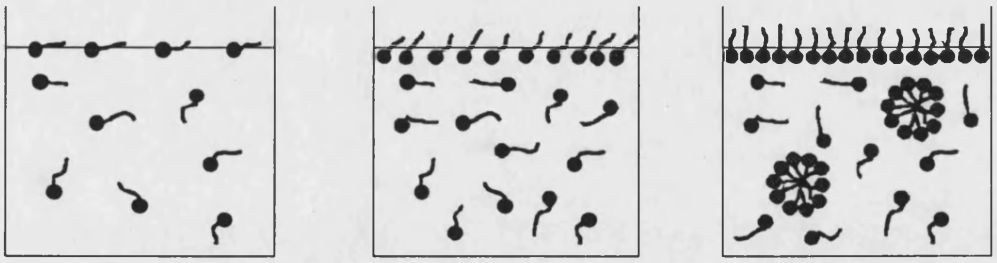

Figure 2.2 (a)-(c) Micelle Aggregation

Eventually a unimolecular layer is formed and the concentration of the solution is known as the critical micelle concentration (cmc). At concentrations above the cmc the surfactant monomers can no longer position themselves at the interface or singly in solution they therefore aggregate forming an ordered structure known as a micelle.

The monomer concentration dispersed will then remain constant, see Figure 2.3 (Israelachvili [1992]).

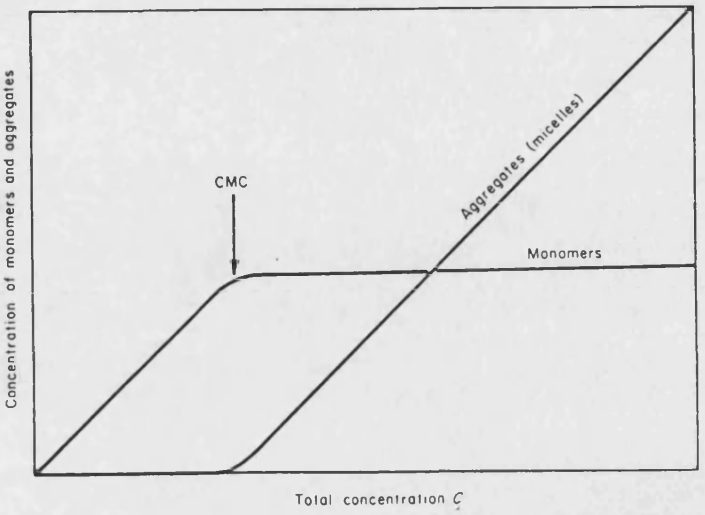

Figure 2.3 Monomer and Aggregate Concentration

This phenomena is due to the hydrophobic effect where the micelle shape formed will be of minimum free energy. This represents a force balance. A force of aggregation, the hydrophobic groups attraction to one another and a force of dissociation, repulsion of individual polar head groups. Monomers within a micelle will be in a dynamic equilibrium with monomers in solution. The rate constant of a monomer surfactant entering a micelle is in the order of 10^{-6} s (Porter, [1994]). The concentration of surfactant monomers aligned at an interface leads to pronounced physical changes to the solution. For example, surface tension is reduced up to the cmc, where it reaches a minimum value, see Figure 2.4 (Clint [1994]). However, with some nonionic surfactants further increases in surfactant concentration above the cmc can lead to a continued reduction in surface tension (Lodhi [1994]).

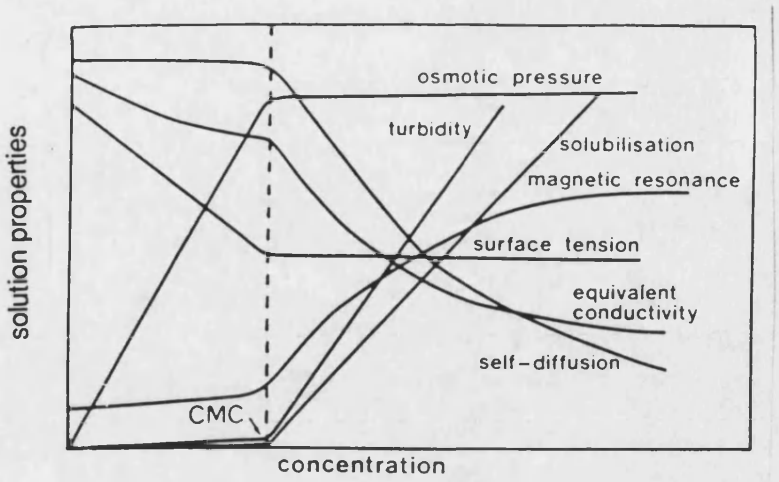

Figure 2.4 Solution Properties

2.3.2.2 Types of Surfactant

Surfactants are usually classified primarily by the charge of their hydrophilic head group. There are four main types: anionic, cationic, nonionic and zwitteronic (or amphoteric).

Anionic surfactants have negatively charged head groups, such as sulphates ($-OSO_3^-$), sulphonates ($-SO_3^-$), and carboxylates ($-OCOO^-$). They are frequently found as ammonium or alkali metal salts (Porter [1994]). Cationic surfactants have positively charged head groups, such as quaternary ammonium ions ($-N(CH_3)_3^+$). Cationic surfactants are often used as fabric softeners binding strongly to negatively charged surfaces. Nonionic surfactants do not have a charged head group, such as the common polyoxyethylene head group ($R-[OCH2CH2]_n-OH$). Unlike the majority of surfactants, nonionics exhibit inverse solubility (i.e. increasing temperature reduces solubility). Zwitteronic surfactants have head groups with a positive and negative charge, such as lecithins ($R-CH_2(PO_4)^-CH_2CH_2N^+(CH_3)_3$). Typically zwitteronic surfactants behave like cationics, nonionics, and anionics at low, intermediate and high pH's respectively. Table 2-1 summarises the main properties of the four main types of surfactant.

Table 2-1 Properties of Surfactants

Property	Anionic	Cationic	Nonionic	Zwitteronic
Charge (hydrophillic)	negative ions	positive ions	no charge	positive & negative ions
Examples	$-OSO_3^-$, $-SO_3^-$, $-OCOO^-$	$-N(CH_3)_3^+$	$R-[OCH_2CH_2]_n-OH$	$R-CH_2(PO_4)^-CH_2CH_2N^+(CH_3)_3$
Ph	sensitive	sensitive	stable	sensitive
Electrolyte	sensitive	sensitive	slightly affected	sensitive
Temperature	minimal effect	minimal effect	sensitive	sensitive
Hard water (Ca, Mg ions)	sensitive	sensitive	not affected	sensitive
Wetting	Good, polar surfaces	Good	Poor	Good/Poor
Solubilisation	Poor	Poor	Good	Good/Poor

2.3.2.3 Micelle Shape

The actual structure and shape of micelles depends upon the geometric packing of the hydrophilic and hydrophobic groups which is equal to $v/a_o\, l_c$ and first proposed by Israelachvili et al [1976]. Where a_o is the area of the hydrophilic group and v/l_c is the area of the hydrophobic group, depicted in Figure 2.1. These parameters are 'effective' areas. When $v/a_o\, l_c < 1/3$ the monomers are cone shaped and spherical micelles are formed, $1/3<v/a_o\, l_c < 1/2$ the monomers are truncated and globular and cylindrical micelles are formed up to when $v/a_o\, l_c > 1$ and inverted micelles are formed. Cox and Matson [1984] varied carbon chain length and ethylene oxide content to determine a general optimum nonionic surfactant for oily soil hard surface cleaning. For concentrated solutions a short carbon chain length was most effective and for dilute solutions a long carbon chain length was most effective. An ethylene oxide content of 50% was recommended.

The packing parameter defines the properties of a surfactant and is a function of many parameters; temperature, electrolyte concentration, pH and addition of cosurfactant. The effects of concentration and temperature are within the scope of this study. The packing parameter is an independent function of concentration for spherical micelles

and dependent for cylindrical micelles. This has been confirmed by measurement (Porter, [1994]). For nonionic surfactants, increasing temperature reduces the hydrogen bonds between the ethylene oxide groups (E) and water (Puvvada and Blankenstein, [1990]). This increase in hydrophobicity effectively decreases a_o and therefore increases the packing parameter. More usually for ionic surfactants, increasing temperature decreases the packing parameter due to increased steric repulsions. A high temperature therefore produces cylindrical and polydispersed micelles for nonionic surfactants, and spherical micelles for ionic surfactants.

2.3.2.4 Nonionic Surfactants

The majority of the experimental data reported in the literature is for nonionic surfactants. This is due to their capacity to remove oily soil from synthetic fabrics and hard surfaces. They exhibit good water solubility, are low foamers and are less sensitive to water hardness than anionic surfactants. They are also required in much lower concentrations than anionic surfactants. According to Scott [1963]) this is due to their particularly low cmcs. Several authors have shown that nonionic surfactants tend to perform best on hydrophobic substrates with non polar soils.

Polyoxyethylenes are the most common nonionic surfactants having a general chemical formula of $C_nH_{(2n+1)}(CH_2CH_2O)_mOH$. The molecule is made up of a saturated alcohol and a series of ethylene oxide groups. They are less susceptible to electrolytes and pH changes because they have no charge. They exhibit inverse temperature solubility and the temperature at which precipitation occurs is called the cloud point. Water solubility and cloud point are linked and both increase as the number of oxyethylene groups increases from 3 to 16 and shorter hydrocarbon chains. Interfacial tensions tend to reach a maximum value at around n=5 and decrease upon further increases.

2.3.2.4.1 Phase diagrams

The phase diagrams of the different classes of surfactants have the same characteristics but vary considerably. When a nonionic surfactant is mixed with water several different types of behaviour may be observed (Schick [1987]).

1. The surfactant may be below its melting point and will be insoluble in water remaining crystalline without swelling appreciably.

2. The surfactant will dissolve in water. Above the cmc micelles are formed with the capacity to solubilise water-insoluble compounds. At higher concentrations liquid crystals are formed, the concentration sequence is as follows: Micellar (L_1)→Hexagonal Phase (H_1)→Lamellar phase (L) → Crystalline surfactant (S) (Figure 2.5).

3. When the aqueous surfactant solution's temperature is increased it will split from a single isotropic phase into a very dilute aqueous phase and a concentrated solution W+L_1. This temperature being called the cloud point.

This study documents the effect of removal above and below the cloud point for an $C_{9\text{-}11}E_6$ alcohol ethoxylate. Assuming $C_{9\text{-}11}E_6$ is equivalent to $C_{10}E_6$ the typical phase diagram is shown in Figure 2.5 (adapted from Schick [1987] and Lange [1994]), the cloud point starting at 60°C. The lamellar phase L although common with most nonionic surfactants is not present with $C_{9\text{-}11}E_6$.

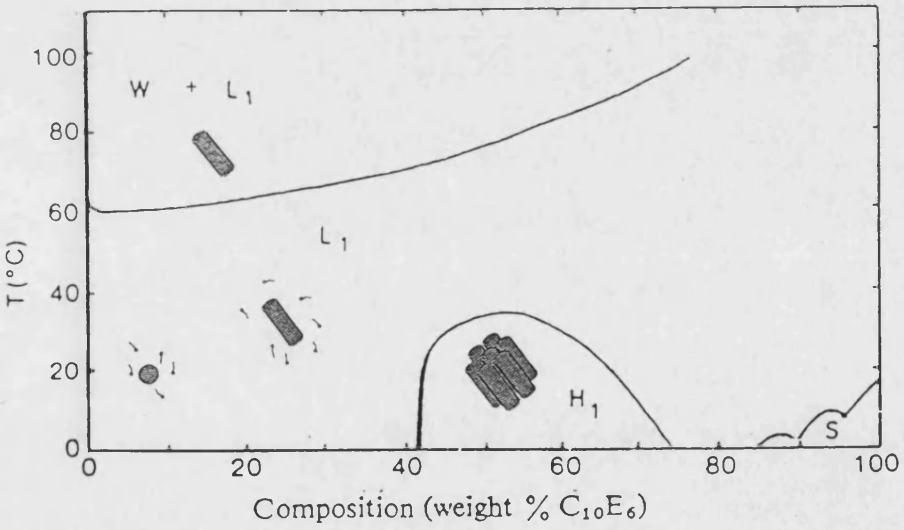

Figure 2.5 $C_{10}E_6$ Phase Diagram

2.3.2.4.2 Phase Inversion Temperature

Increasing temperature increases the packing parameter and hence changes the surfactants properties. The point where $v/a_o\ l_c = 1$ is when the micelles become inverted. This occurs at the phase inversion temperature for nonionic surfactants. At this point the surfactant has a strong solubilising power and ultra low interfacial

tension and is often considered the optimum for detergency. The cloud point and PIT parallel each other. They are both a function of the type of hydrocarbon present. For example an aromatic will lower the cloud point and an aliphatic will increase it.

The PIT cannot be determined within a typical cleaning system because the concentration of oil to surfactant is very low and inverted micelles cannot be formed. Therefore the PIT is calculated by mixing equal quantities of surfactant solution and oil and taking the PIT as the temperature at which separation into a three phase system occurs most rapidly. The PIT may vary with oil content so the content of oil should be reduced and the procedure repeated to determine the new PIT. Through linear regression the theoretical PIT at low oil surfactant concentrations can be estimated (Raney, [1991]).

2.3.2.4.3 Hydrophilic / Lipophilic Balance (HLB)

There have been several attempts to catagorise surfactants the most successful is the Hydrophilic / Lipophilic Balance (HLB), first developed by Grifin [1949], although it is primarily effective for nonionic surfactants. The HLB characterises a surfactant as to its emulsifying properties and is calculated from the chemical structure of the surfactant:

HLB = Molar % of the hydrophilic group divided by 5

Clearly the maximum value is 20, indicating the product has no hydrophobic group and the minimum value is 0 representing a product which is completely water insoluble. Values of 1-7 indicate the formation of water in oil emulsions and 10-20 of oil in water emulsions (Porter [1994]).

2.3.2.5 Anionic and Cationic Surfactants

Anionic and cationic surfactants have ionised hydrophilic groups. Anionics are the largest class of detergents representing 70-75% of total industrial production (Myers, [1988]). The hydrophobic group for an effective anionic detergent is commonly a linear hydrocarbon chain in the range of C_{12}-C_{16} with the polar group at one end (Porter [1994]). Typically, cationics are based on a nitrogen atom carrying the positive charge. The most common types are linear alkylbenzenesulfonate and quaternary ammonium salts for anionic and cation surfactants respectively. Anionics and cationics

generally do not mix. Cationics form insoluble complexes and lose their surfactant properties. Whereas anionic surfactants are detergents cationics act as antiseptic agents (Porter, [1994]).

2.3.2.6 Review of Cleaning Mechanisms

Most cleaning processes can be considered to consist of three primary steps; removal of the soil from the substrate; dispersion of the soil in the deterging medium; and prevention of soil re-deposition on the substrate (Jennings, [1965]). Understanding the mechanisms by which this process occurs is important in the formation of any fundamental kinetic models of cleaning. The rate of removal will depend on many parameters; optimisation of these parameters will reduce the overall cleaning time. The mechanism occurring may vary as a function of surfactant, concentration or thermo-hydraulic conditions (Benton et al [1986]).

2.3.2.6.1 Oily Soil Cleaning Mechanisms

Oil will remain on a substrate as long as the hydrodynamic forces exerted by the cleaning solution on the oil are smaller than the adhesion forces. The adhesion forces have molecular origins which result in the macroscopic quantities such as interfacial tension, contact angle etc. (Mahé et al [1988]). The mechanism by which removal occurs depends largely on the type of soil (section 1.3, Chapter 1) and detergent. There is significant literature on surfactant based removal of oily soil, and it is generally agreed there are four main removal mechanisms:

1. Solubilisation mechanism;
2. Roll-up mechanism;
3. Emulsification mechanism;
4. Oil removal through surface film formation.

The majority of published work only considers the first three (or a combination) of these mechanisms as removal of oil through surface film formation occurs only in exceptional circumstances (non-dynamic conditions). Despite the large amount of literature covering the removal of oil from a solid surface in the presence of surfactant

solutions we still do not fully understand the mechanisms of removal (Kao et al [1989]).

Scott [1963] studied the mechanisms of removal of fatty material mixed with particulate soil. Four mechanisms were observed depending on the material removed, the roll-up mechanism commonly occurred with liquid or molten soils.

2.3.2.6.2 Solubilisation mechanism

Consider an oily soil present on a metal substrate immersed in an aqueous surfactant detergent. The surfactant, above its critical micelle concentration (cmc) simply dissolves the water insoluble oil. The oil or insoluble deposit becomes associated with the surface active molecules to form a micelle as shown in the four diagrams see Figure 2.6(a) - (d). The result is then a thermodynamically stable isotropic solution of oil (solubilisate) normally insoluble or only slightly insoluble in the given solvent (water).

The location of a solubilised molecule within a micelle depends largely on the chemical structure of the solubilisate (Myers [1988]). Typically for an oil deposit or hydrocarbon, the deposit is located in the core of the micelle, (Figure 2.6(a)). Slightly polar materials such as fatty acids, alcohols and esters are usually located in the palisades layer, with the hydrocarbon tail remaining in the micelle core Figure 2.6(b)). With polyoxyethylene nonionic surfactants the polar head can occasionally be very long and large, and the hydrophobic chain is arranged outward into the solution, Figure 2.6(c)). Finally, in non-polar surfactant solutions the configuration of the micelle is reversed. Polar deposits can therefore be attached to the head, Figure 2.6(d)).

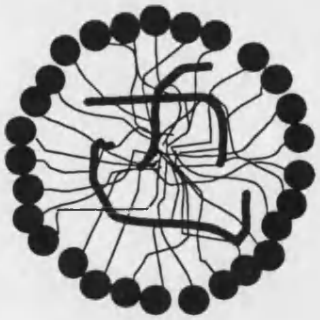

(a) Deposit in the micellar core.

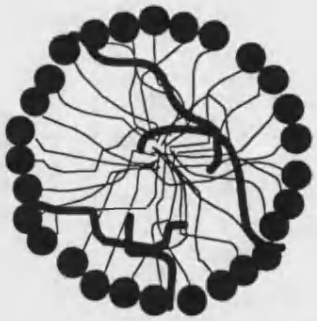

(b) Deposit at the core/palisades interface

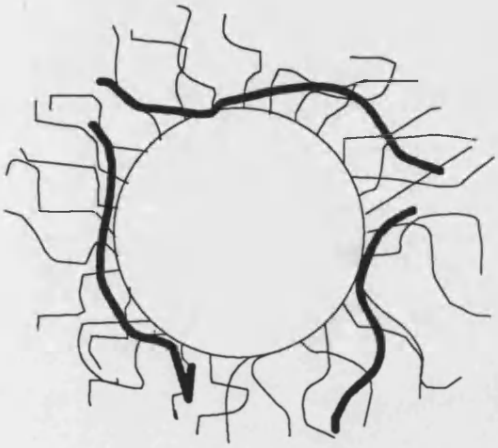

(c) Deposit in the palisades layer.

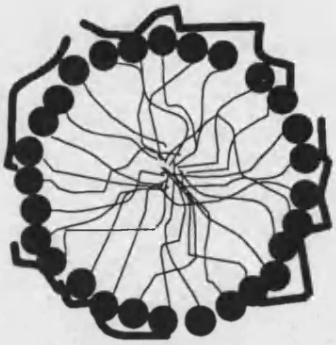

(d) Deposit on the micelle surface

Figure 2.6 Solubilisation Mechanism, Location of Deposit (Myers [1988])

2.3.2.6.3 Conditions effecting Solubilisation

Many authors have reported solubilisation as the most important mechanism for the removal of oily soils from hard surfaces (Carroll, [1981], Lim et al [1991], Sayeed and Schott, 1986, Shaeiwitz et al [1981]). Many workers have found removal to be only significant above the cmc (Lange, [1994], Rosen [1978] and Shaeiwitz et al [1981]). Solubilisation is important for removing oil that cannot be removed through roll-up, (see section 2.3.2.6.4) Optimum conditions occur at several times the cmc for nonionics and even higher for some anionics. Carroll [1981] when cleaning oily soil from textile surfaces found that the rate of solubilisation was proportional to the nonionic surfactant concentration above the cmc. Solubilisation cannot occur in the absence of micelles. However, Jafvert et al [1994] found that when using commercial grade surfactants solubilisation below the cmc was possible. This was put down to monomers with long hydrophobic groups associating below cmc and the extensive dimer and trimer formation. In certain situations the solubilisate (soil) was also found

to enhance micelle formation through the provision of monomers to form additional micelles.

The size and shape of the micelles in solution plays a major part on the rate of adsorption / association of the oil into the micelle. A surfactant forming rod like micelles induces lower oil-liquid interfacial tensions and facilitates the transfer of oil from the substrate to the core of the micelles. Anionics (e.g. sodium lauryl sulphate) tend to produce globular like micelles and hence exhibit low take up rates. Accordingly solubilisation does not contribute significantly to detergency in anionic surfactants as opposed to nonionic surfactants (Rosen [1978]). Chiu and Huang [1993] were able to promote solubilisation of crude oil by increasing micellar size for both nonionic and anionic ethoxylated surfactants. Oetter and Hoffman [1981] were able to relate oil/liquid interfacial tension with decane to micelle shape: above 1 mN/m globular, between 1 and 0.1 mN/m rod like, or below 0.1 mN/m disc like.

Solubilisation is highly dependent upon temperature. Carroll [1981] that found maximum detergency of oily soils occurred suddenly at the cloud point. The authors found that at 15°C (below the cloud point) solubilisation was minimal. Lim and Miller [1991] Raney [1991] (Raney et al [1987]) Thompson [1992] contrast these findings, stating that maximum solubilisation of hydrocarbons from textile surfaces occurs near the PIT which is found well above the surfactant cloud point. Sayeed and Schott [1986] also studied solubilisation of an oily soil, fouled on silica substrates, using a nonionic surfactant. The authors related surfactant temperature effects to the soil melting point. Below the melting point of the soils, solubilisation was found to gradually increase with increasing temperature. At the melting points the solubilisation doubled and tripled when the esters present turned to liquid crystals. Subsequent temperature increases did not have such a large effect. Shaewitz et al [1981] found solubilisation of C_{14}'s from stainless steel increasing with increasing flow rate up to a constant value at higher flow rates.

The class of substrate plays an important role in removal. Nonionics were found to out perform anionics for removal from non-polar substrates (polyester) cleaning but the opposite was true for hydrophilic surfaces (Rosen [1978]). Dillan et al [1979] agrees with these findings stating that nonionics are suited to hydrophobic substances and

non-polar soils. Selective solubilisation occurred for binary hydrocarbon mixtures (Nagarajan and Ruckenstein [1984]). Experimental data showed that the solubilisation capacity of surfactants differs significantly for different oily soil solubilisates. The absorbence of a particular micelle decreased with increasing molecular volume of the solubilisate. The more polar the solubilisate the greater the capacity of the micelle for solubilisation. Aromatic compounds were also solubilised in larger amounts than corresponding saturated hydrocarbons. Chiu and Huang [1993] also propose the occurrence of selective solubilisation of crude oil by a nonionic surfactant. Lim and Miller [1991] suggest that for soils containing more than 10% polar material, solubilisation is likely to be the main mechanism of detergency.

2.3.2.6.4 Roll-up mechanism

Consider a thin oily film deposited on a metal surface, with a contact angle of zero. The film is then immersed in an aqueous surfactant solution. The oily soil will spontaneously form isolated islands on the substrate; this is the roll-up mechanism or roll-back as it is sometimes called, developed by Adam [1937], Figure 2.7. The removal of these islands is then achieved through convection currents within the solution. If a droplet is large, and the contact angle , Figure 2.8, between the oil-liquid interface and the substrate is <90° removal is incomplete with a small droplet remaining on the surface, hydrophobic surfaces. However with the angle >90° droplet removal is total, often with hydrophilic surfaces (Dillan et al, [1979]). Raney and Miller [1993] and Thompson [1992] define the roll-up mechanism as only occurring with complete removal of the oil droplet i.e. <90°. This is contrary to the findings of the majority of workers, (Lange [1994], Myers [1988], Schwartz [1972]). This method of soil removal often occurs when cleaning light loads of oil from metals.

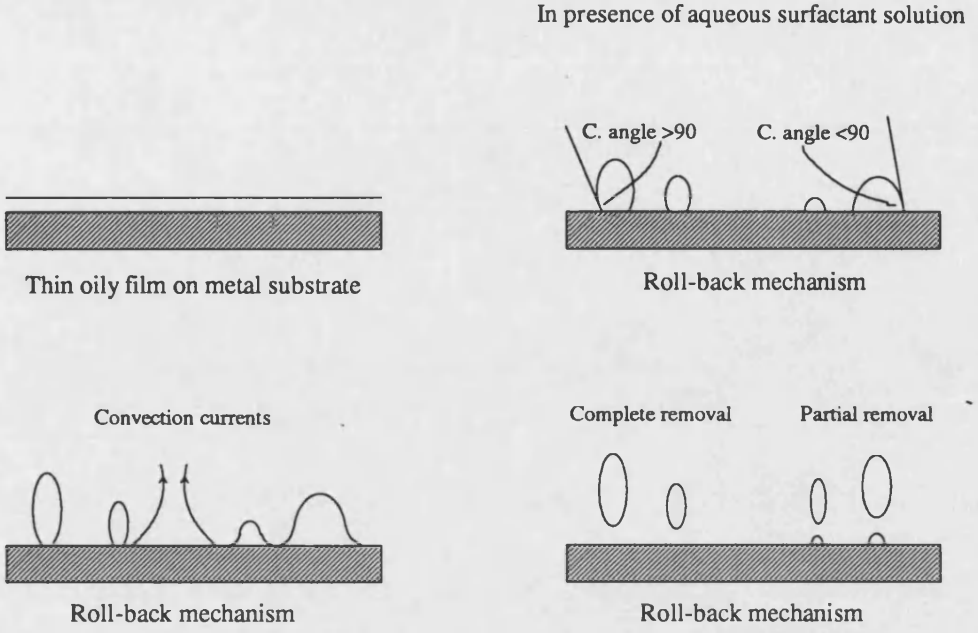

Figure 2.7 Roll-Up Mechanism

When a liquid soil O lies on the surface of a solid substrate S, there is an interfacial tension γ_{OS}, at the soil-substrate interface. The oil droplet forms with the substrate an angle θ, which results from the balance between the forces. The surface tension γ_{SG} between the substrate and the gas phase tends to spread the oil on the surface (to reduce the surface of contact). The interfacial tension γ_{OS} between the oil and the substrate tends to reduce the oil-substrate contact and to re-form the drop. Since the total free energy of any system tends towards a minimum equilibrium condition, equation 2.3 can be written:

$$F = \sum_i \gamma_i (\text{surface area})_i \text{ is a minimum} \qquad \textit{2.3}$$

hence the Young Equation 2.4

$$\gamma_{SG} = \gamma_{OS} + \gamma_{OG} \cos\theta \qquad \textit{2.4}$$

The force balance is shown graphically in Figure 2.8, assuming the vertical component of γ_{og} is assumed to be negligible. The contact angle can be defined as the angle formed in the oil phase (Rosen [1978]) or in the fluid phase (Dillan et al [1979]). Throughout this study the contact angle is defined as the angle formed in the oil phase in common with the majority of authors.

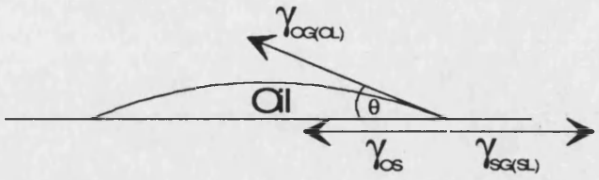

Figure 2.8 Contact Angle

When the substrate and the oil are submerged, the surface tension between the substrate and the gas phase is replaced by the interfacial tension γ_{SL} between the substrate and water, and the surface tension between oil and gas is replaced by the interfacial tension γ_{OL} between the oil and water. The result is usually another contact angle θ'.

If an appropriate surfactant is dissolved in water, the effect is a strong reduction of the substrate-liquid and oil-liquid interfacial tensions, due to the adsorption of surfactant molecules at the liquid-oil and liquid- substrate interfaces. Of course, the oil-substrate interfacial tension is not affected, since water does not diffuse to that interface. The system evolves toward a new equilibrium state, characterised by a higher contact angle. Mechanical action then causes droplets of oil to be removed from the substrate and only a small quantity of oil is left. If the reduction of interfacial tension is so strong that the sum of the oil-liquid and substrate-liquid interfacial tensions reaches the oil-substrate interfacial tension, the contact angle is 180° (cos180°=1) which means that no oil is left on the substrate (spontaneous perfect cleaning).

2.3.2.6.5 Conditions for Roll-up

Roll-up is considered to be the dominant mechanism for anionic surfactants, and has been reported many times (Aronson et al [1983], Dillan [1979], Dillan et al [1979]). Unlike solubilisation, roll-up can occur below the cmc, although this has only been reported for anionics (Raney et al [1987]) (Schott [1972]) and nonionics (Koretskii et al [1983]). Roll-up occurs only with liquid non polar soils and the higher the viscosity of the soil the less effective the mechanism. At low temperatures, removal may well occur by a different mechanism such as emulsification (Miller and Neogi, [1985]) or solubilisation (Benton et al [1986]). High soil substrate bond strengths will also reduce the prominence of the roll-up mechanism.

The roll-up process is often linked to the contact angle the soil forms with the substrate. This concept was pioneered by Adam [1937] and is still widely accepted. Thompson [1992] presents a broad study concerning the removal of four oily soils from a polyester substrate by anionic and nonionic surfactants. A linear relationship was found to exist between the percentage of oil removed and the contact angle made between a drop of the oil and a flat polyester fabric.

Above the cmc, increasing concentration was found to improve the roll-up mechanism at a constant rate (Dillan [1980]). Roll-up was reported to be a function of the values of γ_{ol} and γ_{sl}. Kao et al [1989] confirmed the presence of the roll-up and a secondary diffusional mechanism for the removal of crude oil droplets from a solid silica surface in the presence of a micellar solution. The effect of concentration was not considered. Below the cmc Koretskii et al [1984] found removal of oily soils by nonionic surfactants from stainless steel plates to be equivalent to removal by water alone. The addition of a second surfactant to an effective detergent can be found to enhance or inhibit roll up depending on the circumstances (Aronson et al [1983]). Aronson et al [1983] also found that ionic strength played a significant role. When adding a anionic surfactant to a nonionic surfactant, roll up of mineral oil increasing at high ionic strengths and decreasing at low ionic strengths. The findings could be related to a critical γ_{ol} above which roll-up did not occur. Benton et al [1986] suggested that γ_{sl} was the major factor in determining the rate of roll-up. Dillan et al [1979] found the addition of highly alkaline electrolyte builders and hardness ions promoted emulsification of mineral oil. Dillan believed solubilisation to be of secondary importance in practical systems because of a low surfactant / soil ratio present.

In contrast to solubilisation, the micelle shape is unimportant to removal by roll-up. However, monomer structure effects the rate at which roll-up occurs. Dillan et al [1979] found lower ethoxylated nonionic surfactants performed better than higher ones at low temperatures but this trend was reversed as temperature was increased.

When using a nonionic surfactant there is some confusion in the literature as to true effect of temperature upon removal. The majority of workers agree that an optimum temperature exists which maximises removal, but there is some debate as to whether this occurs at the cloud point or at the phase inversion temperature (PIT). More

recent work suggests it lies at the PIT. The optimum temperature for mineral oil removal from polyester by nonionic surfactants occurs at the cloud point (Dillan et al [1979]). Koretskii et al ([1984]) confirmed this for removal of oil residue from steel plating through vibration by nonionic surfactants. Optimum removal of hydrocarbon soil by nonionic surfactant occurred at the PIT, well above surfactant cloud point (Raney and Miller [1987]). Work by Thompson [1992] for the removal of four oily soils from polyester by anionic and nonionic surfactants found that removal was related to the PIT. Raney [1987] states that the mechanism reported by Dillan et al [1979] [1980] may not be roll-up but a combination of a solubilisation / emulsification mechanism with the process of removal occurring through flow agitation and subsequent emulsification.

2.3.2.6.6 Emulsification mechanism

Emulsification is analogous to roll-up (coarse emulsification ≈ roll-up) occurring below the cmc and is one of the most important mechanisms contributing to oily-greasy soil removal. Solubilisation is often considered to be of secondary importance (Dillan et al [1979]). Consider a thin film of oil on a metal substrate, there can be a tendency for the oil to emulsify (Figure 2.9). Mechanical action is required to break up the insoluble oil into small droplets and disperse it into solution to form a suspension. A surfactant which promotes emulsification reduces the energy required to form an emulsion by absorption at the oil / liquid interface and reduces tension from 20 mN/m to 1 mN/m forming a stable suspension with the continuous phase. An interfacial film will then surround each droplet preventing coalescence with surrounding droplets. Emulsification continues until the residual oil film has become as thin as the diameter of the smallest oil droplet.

Complete detachment of oil drops from flat surfaces has been studied by Mahé et al [1988] who found that in a laminar flow regime detachment occurred at a critical shear stress τ_c, equation 2.5.

$$\tau_c \propto \frac{\gamma_{ol} R_p (\cos\theta_r - \cos\theta_a)}{\mu_l (d_r^2)} \qquad 2.5$$

where μ_l = the viscosity of the continuous phase

R_p = the contact radius

d_r = the drop radius

θ_r = the receding contact angle

θ_a = the advancing contact angle

Although this relationship is specific to the laminar flow regime it's general nature demonstrates the complex interplay of interfacial tension, contact angle and drop size effect as well as introducing the idea that surface roughness (through the parameter θ_r) is important.

A thermodynamic equilibrium exists between the surfactant concentration in water and the surfactant adsorbed on any surface. Increasing the surfactant concentration should increase the rate of adsorption and hence the rate of emulsification. At the cmc, the monomer concentration reaches a maximum and further increases in surfactant concentrations should have no significant benefit.

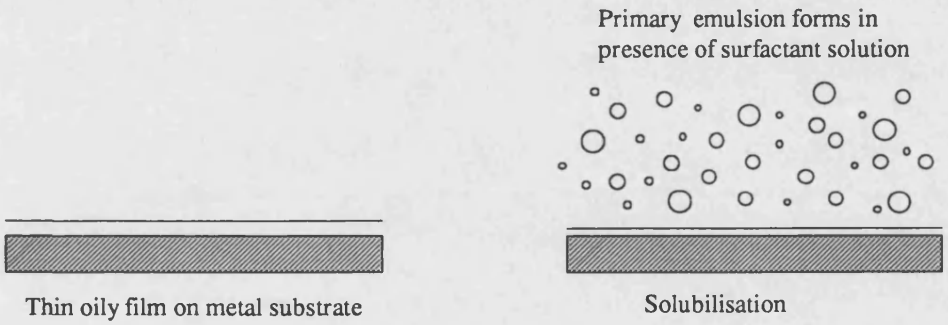

Figure 2.9 Emulsification Mechanism

Cox, [1986], suggested the removal of refined lard, anhydrous lanolin and cetyl alcohol by various surfactants was initially through liquefaction, penetration of the surfactant into the soil, then through emulsification.

2.3.2.6.7 Conditions for emulsification

As with the roll-up mechanism, emulsification is frequently reported to occur below the cmc (Beaudoin et al [1995]) and (Cox et al [1987], Mori et al [1989], Neogi et al [1985], Raney et al [1987], Raney and Miller [1987], Schambil and Schwuger [1987]). Emulsification creates new surface area and therefore requires a minimum in γ_{OL} (Rosen [1978]). This occurs when hydrophobic and hydrophillic (HLB≈8-9) portions of the surfactant balance. For nonionics this occurs at the PIT and for anionics at a specific electrolyte concentration. Optimum efficiency is in the region of

the cmc (Lange, [1994]). A combination of solubilisation and emulsification is often reported, emulsification prominent at low concentrations and solubilisation prominent with an excess of surfactant (Raney and Miller [1993]).

The polarity of the soil is important, the more polar the soil the increase likelihood of removal through emulsification (Aronson et al [1983]). Solid oily soils are removed through emulsification, the lower the temperature the more likely removal is through emulsification or solubilisation rather than roll-up (Otani, et al [1985]).

2.3.2.6.8 Oil removal by surface film formation

As the substrate is immersed into a water bath, the oil film starts to spread over the water. The process is a direct transferal from the substrate to the surface of the bath. The mechanism relies on a free water surface and the rate can therefore be increased by repeatedly dipping the substrate into fresh water. This probably explains the Dupré effect postulated by Bourne and Jennings [1961].

2.3.2.7 Summary

Clearly a considerable amount of data has been produced concerning oily soil removal. Roll up, emulsification and solubilisation have been identified as important removal mechanisms. However the conditions that promote each mechanism have not been reported. This may well be due to the similarity of the mechanisms and the ease with which one could be mistaken for another. Table 2-2 tackles this issue utilising the information available in the literature and the results in this thesis to identify the conditions and parameters that promote each mechanism. The information, although only a generalisation, proposes the most suitable class of surfactant and the optimum conditions of operation for a particular set of removal conditions. For example, roll up is likely to remove large volumes of liquid saturated hydrocarbons which are deposited on hydrophillic surfaces (low substrate bonding) with optimum removal occurring in the region of the cmc at the PIT of the oil / water system.

Table 2-2 Conditions that promote Roll up, Emulsification and Solubilisation

	Roll up	Emulsification	Solubilisation
In terms of Emulsification-	Coarse	Medium	Micro
Quantity of oil to be removed-	large amount	large amount	residue
Soil characteristics-	Liquid, low viscosity	Solids soils	-
Soil charge-	non polar	polar	polar
Substrate-	low substrate bonding	high substrate bonding	high substrate bonding
Surfactant class-	nonionic or anionic	nonionic or anionic	nonionic
Optimal Conc-	Region of cmc	Region of cmc	Several times cmc
Required micelle shape-	Spherical / globular	Spherical / globular	Rod like, large vol.
Optimal Temperature-	PIT, (high)	PIT, (lower)	Cloud point, (low)
Phase (inc. oil)-	two	two	one
Velocity-	increases always improve removal		

N.B. There is some debate as to the optimum temperatures.

2.3.2.8 Surfactant Removal Models

Within the literature there are few mathematical models describing oily soil removal by surfactants. Workers prefer to express the removal mechanism in text. However, Shaeiwitz et al [1981] described the solubilisation mechanism in equation steps. At low temperatures five steps were proposed with micelle desorption and diffusion rate limiting. At higher temperatures the solubilisation was governed by the formation of a liquid crystalline phase at the fatty acid interface. The mechanism being described in terms of two steps: dissociation from the surface and diffusion into the flow in solution. Carroll [1981] described the mechanistic route for highly insoluble soils to be adsorption-desorption of the micelles at the oil/water interface rather than the diffusion of the molecules of oil into the micelle. The limiting step was found to be the adsorption of the micelle.

The roll-up mechanism is often investigated using single droplets of oil rather than oil films. Mechanisms are generally described in terms of contact angle, the droplet rolling

up when $\gamma_{Ol} \cos\theta + \gamma_{OS} - \gamma_{SG} > 0$. Within a flow system determination of these parameters is very difficult with the additional effects of surface shear.

The combination of removal mechanisms is common. Novel work undertaken by Thompson [1992] resolved the cleaning of a radioactive oily soil (squalane) from polyester into the existence of two removal mechanisms; roll-up and emulsification. Varying the composition of the detergent $C_{12}E_3$ produced two optima for the removal of the oily soil indicating the presence of the two mechanisms. Thompson [1992] distinguishes the two processes by the work of adhesion (W_a- roll-up) to the work of cohesion (W_c- emulsification) and expresses this in a mathematical form, equations 2.6 and 2.7:

$$W_a = \gamma_{O/l} (1+\cos\theta) \qquad 2.6$$

$$W_c = 2\gamma_{O/l} \qquad 2.7$$

It is interesting to note Miller and Raney [1993] contrast these findings suggesting the removal of oily soils from polyester is by solubilisation-emulsification mechanisms. It seems further work is required to verify the actual removal mechanism. Cox, 1986 proposed two mechanisms for the removal of solid organic soils; liquefaction and emulsification.

2.3.2.8.1 Interfacial Forces

Breaking of the interface can have an important benefit on the removal of deposits. Bourne and Jennings, [1961], undertook a fundamental study of the removal of radioactive tristearin from stainless steel plates by 0.03M sodium hydroxide subjecting test strips to a number of washes. Results indicated two removal mechanisms, the more powerful one was time-independent and arose from the air-detergent interface (the Dupré effect). This was later confirmed by Jennings et al [1966] who found that when cleaning a metal plate by continuous immersion the removal was found to be also an air-water interfacial effect.

2.3.2.9 Re-deposition

Re-deposition is soiling of the substrate during the cleaning process. Once the soil has been removed through cleaning it is then re-deposited onto the substrate. This

process occurs commonly with oily soils because they contain more than one component and each component is removed at varying times during the cleaning process. Re-deposition occurs mainly with solubilised particles that have deflocculated and particles removed by the roll-back mechanisms. In both cases particles are subject to hydraulic currents, before colliding and adhering to the substrate.

2.3.3 Formulations

Household hard surface cleaners are usually lower in active ingredients and alkalinity than their industrial counterparts, relying on the additional mechanical action of scrubbing. When formulating a hard surface cleaner the main objective is not only to removal the soil, but to leave the surface intact and free from cleaning agent residue. Formulations need to be specific to the surface and soil. The use of fully biodegradable product surfactants and non-toxic solvents is preferred.

Industrial formulations can be liquid or powder, with liquid formulations becoming increasingly more popular. In industry the most common soils removed from metal surfaces are fatty greases, mineral oils and lubricants. These require highly active cleaning compounds, high temperatures (60-90°C) and mechanical energy. Typically aqueous detergent cleaning compounds are made up of anionic, nonionic surfactant and alkali salts and applied at temperatures between 50 and 94°C (Lange, [1994]). For example a highly alkaline detergent for steel surfaces would have the following active ingredients: octylphenol, sodium metasilicate, tetrasodium pyrophosphate, sodium hydroxide and sodium carbonate (Lange, [1994]). Anionic surfactants tend to supplement the nonionic surfactants providing a strong synergy (Porter [1994]). Cationic cleaners have not been studied because they are used more commonly as fabric softeners and as antiseptic agents than detergent additives. Alkali cleaners react with deposits, saponifying the fats and oils. This study considers the effect of each of the main compounds, with particular emphasis on the nonionic surfactant which has been found to provide the majority of the cleaning power.

2.3.4 Choice of Cleaning Chemicals

2.3.4.1 Nonionic Surfactants

The two main types of non-ionic surfactants are alcohol ethoxylates and alkylphenol ethoxylates. The alcohol ethoxylate class was chosen for the study because it is considered excellent at liquid oily soil removal and a more effective detergent than the alkylphenol (Lange, [1994]). Both classes are similarly efficient wetting agents. Alcohol ethoxylates are also the most common and widely studied having a significant supply of published data.

There are many types of alcohol ethoxylates and deciding on the most appropriate compound was a difficult task. However, it has been determined that for efficient detergency a 60-70 wt% of ethylene oxide and a molecular weight of between 200 and 350 is required (Scott 1963) (Lange 1994). Three surfactants were chosen within this range; $C_{10}E_7$, $C_{13}E_{6.5}$, and $C_{9\text{-}11}E_6$ (ICI Surfactants, Synperonic 10, 13 and 91 series). The surfactants chosen are commercially available so any results produced could be directly beneficial to industry. Limited laboratory tests were then performed on thin stainless steel plating fouled with crude oil. The tests were performed in an ultrasonic bath observing visually the effect of each detergent at 1 v/v%, 50°C, noting the time for 50% of the free surface of the film to be removed. The surfactants performed similarly but $C_{9\text{-}11}E_6$ having an average 62.6 wt% of ethylene oxide was found to be the most proficient and hence chosen for the subsequent cleaning analysis.

2.3.4.2 Anionic Surfactants

Anionics are the most common surfactants in almost every type of commercial formulation, but they are not compatible with cationic cleaners. Sodium lauryl sulphate was selected for the study and is one of the most commonly used anionic cleaners. It is used in heavy duty liquid cleaners in conjunction with non-ionics, often in shampoos. It is an excellent wetting agent with good emulsifying properties.

2.3.4.3 Alkali Cleaners

Sodium Hydroxide has been chosen as a typical the alkali cleaner for result production. It is used in conjunction with anionic surfactants to form detergent formulations for oil deposit removal where the purpose of the OH^- ion is to saponify fats and oils. In industry it is the most commonly used alkali cleaner having many

applications from disinfection to neutralisation of acidic deposits. It also benefits from being cheap and readily available in large quantities.

2.3.4.4 Formulations

There are thousands of different commercially available detergent formulations. In general they are designed to remove a wide variety of soils from food to petroleum greases and oils. Rarely are detergent cocktails specific to removal of a particular soil. *Micro* (International Products Corporation) has been selected to be used in the study. It is primarily a laboratory cleaner but has wide cleaning applications within industry. Primarily containing anionic surfactants and supplemented by quaternary ammonium salts it is an effective hard surface formulation.

Chapter 3

Fouling

3.1 Introduction

Fouling is defined as the deposition, crystallisation or growth of unwanted material on surfaces. Understanding the processes of adhesion of oil films to a surface is an important prerequisite prior to undertaking any cleaning examination. Fouling is a function of many process parameters: temperature of substrate and fluid, flow rate, concentration, surface roughness etc.. The majority of the literature has concentrated reaction fouling in heat exchangers and its reduction although more recently cleaning has been receiving more attention. The build up of oil deposits on metal surfaces is a large problem presenting difficulties in equipment inspection, increasing pressure drop, reduce heat transfer etc.. Costs are significant but difficult to compute, but sizeable, for example in 1985 Garrett-Price determined the annual costs of fouling and corrosion in the United States to be between $3 and $10 billion.

3.2 Fouling Mechanisms

The fouling can be the result of one or a number of mechanisms, (Bott, [1990]). It is generally accepted that fouling processes may be classified into seven groups:

1. Crystallisation and scaling;
2. Particle deposition;
3. Accumulation of biological material;
4. Chemical reaction;
5. Corrosion of the heat transfer surface ;
6. Solidification of process fluid on the surface;
7. Mixed systems and the interaction of mechanisms listed in 1-6 above.

Typically hydrocarbon deposition is slow occurring at high temperatures and pressures through chemical reaction. Whereas food fouling occurs in a matter of minutes primarily through crystallisation and also chemical reaction. The mechanics of oil fouling at high temperatures is well understood (Phillips [1996]). Fouling within this study occurs at room temperature and is through surface forces and solidification induced by evaporation rather than through coking, cracking and polymerisation. The development of a fouling layer can be split into three distinct stages, (Bott, [1990]).

Stage 1. There is little evidence of fouling, this period representing an initiation or conditioning period. This period lasts varying periods of time from a matter of minutes in the food industry to several weeks or months in the heavy oil industry.

Stage 2. Here deposit growth begins, growth is steady and constant.

Stage 3. The final stage, fouling is asymptotic, the resistance reaching an ultimate value. The typical fouling curve, Figure 3.1, obtained is depicted below.

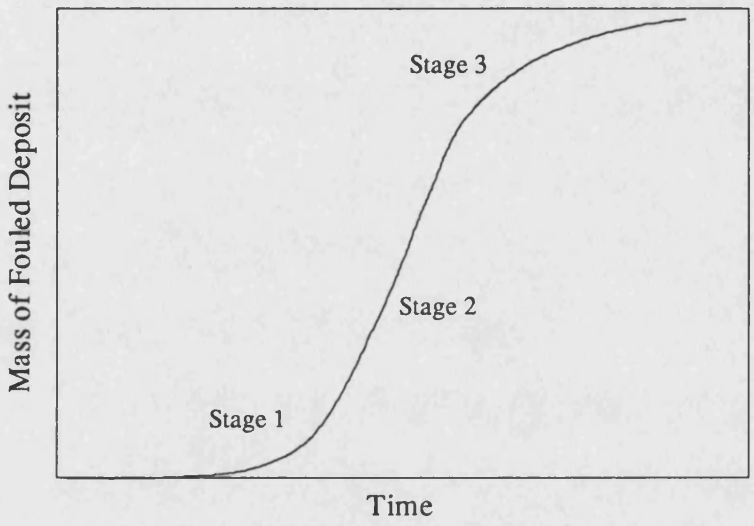

Figure 3.1 Typical Fouling Curve

The fundamental mechanisms by which the foulant arrives at the surface are as follows:

1. The substances or fluid that contribute to the fouling layer move from the bulk fluid to the surface crossing the boundary layer.

2. At the fluid/surface interface they are subjected to interfacial forces and conditions particular to the local surface and flow.

3. Deposition of the foulant.

4. The foulant once deposited on the surface is then vulnerable to shearing forces of the fluid whether they be natural or forced.

Kern and Seaton [1959] developed a fundamental model to describe hydrocarbon fouling hypothesising that the fouled layer thickness, l, was a balance between removal as well as deposition fluxes, equation 3.1. Where C_3 and C_4 are proportionality

constants, G the mass flow rate of the fluid, h the 'dirt content' and τ_w the surface shear stress.

$$\frac{dl}{dt} = C_3 G h - C_4 l \tau_w \qquad 3.1$$

where $C_3 G h$ = deposition flux

$C_4 l \tau_w$ = removal flux

3.3 Crude Oil

An Arabian light crude oil has been chosen as the foulant to produce oil films within this study, API 26.8. Since crude oil is a complex mixture of hydrocarbons, results should provide fundamental information on the removal of oil films by aqueous detergents with the applicability to a wide variety of oils. Crude oil has not received much attention in the literature except concerning enhanced oil recovery. It is, however, a common tenacious deposit found in industry.

The main constituents of the crude oil are saturated hydrocarbons (well over 97% for light crudes, Speight [1980]) but variable amounts of compounds such as sulphur, nitrogen, and oxygen can be detected. Crude oil is classified by its specific gravity or API. The proportions of the elements in crude oil vary only over fairly narrow limits but the physical properties vary significantly from well to well. For details of the crude oil composition refer to Chapter 4.

3.4 Forming a reproducible deposit experimentally

There are many ways of forming soil deposits in the laboratory. Common with each method must be ease of reproducibility. Oily soils are often manually deposited on the substrate (Dillan, Goddard and McKenzie, [1979], and Cox and Matson, [1984], Mahé et al [1988] Yatagai et al [1992] Prieto et al [1996]). Cox and Matson, [1984], applied grease-carbon onto 100 mm × 400 mm sheets of 3 mm masonite using a brush, smoothing out the deposit with a stretched strip of mohair cloth. Reproducibility was verified using a colorimeter, measuring the reflectance of each plate before cleaning. Prieto et al [1996] heated the substrate to 65°C then pipetted the oil and dispersed it with a roller. Alternatively melting the soil to give a uniform

layer is a common technique, Bourne and Jennings, [1961], melted tristearin in a hot-air oven forming smooth deposits on stainless steel . Cox and Matson [1984] melted black wax to give an even layer. Beaudoin et al [1995] used a novel technique fouling the substrate through disc spinning the oily soil. The industrial relevance and applicability of the above techniques has to be questioned. Fouled films deposited in a flow system are more industrially relevant but up until now this has only been undertaken in the food area (Bird [1993]).

Producing a uniform oil film in a flow system is a difficult task. It was found that films produced vertically at room temperature, under gravity, and left overnight for the light ends to evaporate were the most effective. The films produced were even and gave minimal scatter upon further cleaning analysis.

3.5 Adhesion

The forces of adhesion of the crude oil to the substrate have to be overcome during the cleaning process to remove the fouled layer from the substrate. The attractive mechanisms can be broken down into the presence of absence of solid or liquid material bridges, (Hauser and Sommer [1990]), Figure 3.2. Solid bridges are formed by the crystallisation of dissolved materials. Fluid bridges result from capillary forces or are due to high viscosity materials. Without material bridges, van der Waals and electrostatic forces prevail.

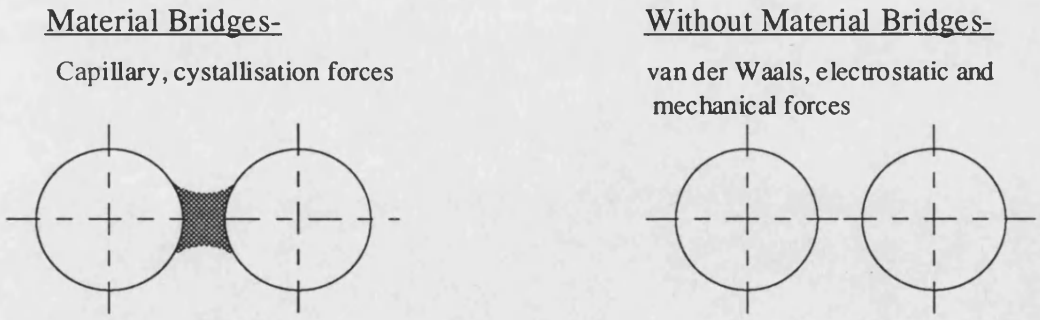

Figure 3.2 Adhesion Mechanisms

Adhesion of both solid and liquid soils to solid substrates is primary due to van der Waals forces with electrical forces being less important (Carroll [1993]). The electrical forces are dependent on pH, composition of the crude oil, etc. (Hirasaki [1988]). Non polar soils (hydrocarbons) are more difficult to remove from hydrophobic (polyester)

surfaces than hydrophilic surfaces (cotton, glass). Conversely polar soils (clay) are more difficult to remove from hydrophilic surfaces than hydrophobic surfaces (Rosen, [1978]). Purely mechanical forces also may hold soils to substrate but these appear to be significant only for soils when the substrate is of a fibrous nature or a substrate of high surface roughness. Since the project is concerned primarily with the chemical effect of detergents, mechanical forces have been minimised by using a smoothed polished stainless steel surface.

Since the Arabian crude is a light fraction it is fair to assume that the oil is effectively non polar. Stainless steel is hydrophilic and lipophilic but the substrate is more strongly lipophilic (for the crude oil) than hydrophillic, therefore removal of the crude film presents a difficult cleaning problem. There are two types of van der Waals bonding; dipole - dipole bonding and transient dipole bonding. Since the crude does not contain a large proportion of electronegative substances like O, Cl and F, dipole - dipole adhesion will not prevail. Transient dipole will provide the strong adhesion force for oil - oil and oil - substrate bonding.

The attraction is due to molecular polarisation. The dipole moments are induced by the electric field emanating from molecules nearby. For non-polar molecules this occurs due to displacement of negatively charged electron clouds. The contact angle the oil forms on the surface of the oil will be a strong indication to the force of attraction to the steel. The oil's viscosity will only define the time the oil will take to assume the equilibrium shape rather than being a function of the attraction.

3.6 Removal

Oil deposit removal is usually carried out by either mechanical or either chemical means. Chemical treatment, although more expensive, does not require costly equipment disassembly. The cocktails require specialist knowledge in application and disposal to remove the deposit rather than corrode the substrate. Mechanical cleaning is through high pressure water or steam jets depending on whether the deposit requires thermal loosening. The process uses large quantities of water and can be hazardous often operating at very high pressures.

3.7 Conclusion

Fouling has been studied in great detail over the last 30 years. Cleaning, however, has received little attention. Of the research studying the removal of oily soils the deposits used have not been representative of industry, often the deposit was applied manually. In this study, oily films are produced through a flow system yielding more uniform and reproducible deposits, representative of those found in industry. The main force of attraction through van der Waals transient dipoles.

Chapter Four

Materials and Methods

4.1 Introduction

This Chapter covers the fundamental components and techniques used in this thesis that are outside the experimental protocol Chapter 5. The Chapter is divided into three sections covering the classification of detergents, crude oils, and the test piece surface. The properties of the selected nonionic surfactant ($C_{9\text{-}11}E_6$) as a function of temperature have been determined, investigating the effect of viscosity, density and micelle size. Important crude oil properties of density, viscosity and composition have also been determined. The procedure used to analyse crude oil composition variation with cleaning is detailed. The stainless steel test section has been examined with respect to surface roughness.

4.2 Detergent Classification

4.2.1 $C_{9\text{-}11}E_6$ Structure

$C_{9\text{-}11}E_6$ is a mixture of polyoxyethylene nonionic surfactants containing 13-23% C_9's, 36-48% C_{10}'s and 33-43% C_{11}'s with an average 6 moles of ethylene oxide (*ICI Surfactants, Wilton*). Its average structure, $C_{10}H_{21}(CH_2CH_2O)_6OH$ ($C_{10}E_6$), is shown in Figure 4.1 (adapted from Lodhi, [1994]). It is different from the typical shape of a surfactant molecule. Instead of the hydrophilic portion being small and compact it is in the shape of a long chain similar to the hydrophobic portion. The surfactant is nonionic and will not exhibit any electrical effect, i.e. strong adsorption on to charged surfaces.

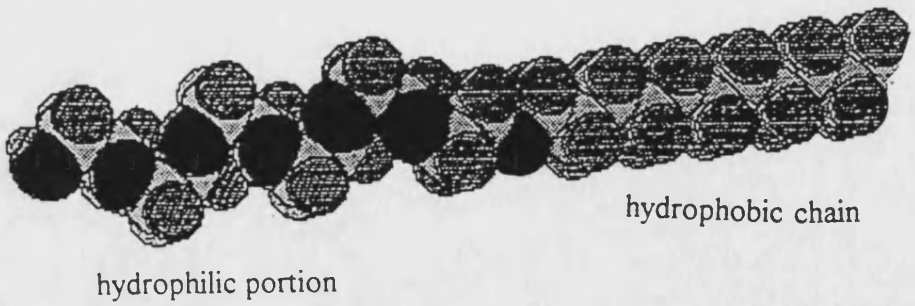

Figure 4.1 $C_{10}E_6$ Structure

4.2.2 $C_{9\text{-}11}E_6$ Density measurement

The density variation of $C_{9\text{-}11}E_6$ with temperature has been determined using a 25 ml Gay-Lussac pyknometer, in accordance with BS 733 [1987], results are reported in Figure 4.2. Refer to Appendix A for details. Although the neat densities of $C_{9\text{-}11}E_6$ and water are very close the solutions cannot be assumed to be that of water as the surfactant molecules may pack differently around water molecules compared to themselves.

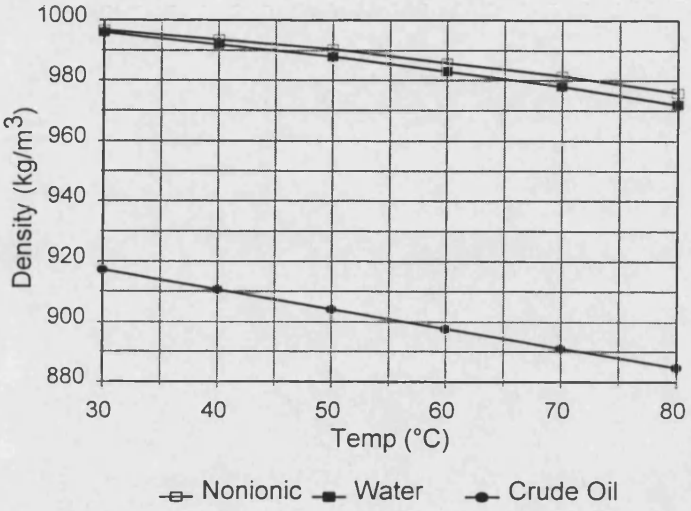

Figure 4.2 5v/v% $C_{9\text{-}11}E_6$,, Water and Crude Oil Densities

4.2.3 $C_{9\text{-}11}E_6$ Viscosity Determination

The viscosity of the nonionic surfactant $C_{9\text{-}11}E_6$ has been determined in accordance to BS 188 [1977]. The results are depicted in Figure 4.3, for details refer to appendix A. As expected viscosity is a strong function of temperature, generally decreasing with increasing temperature. Additional surfactant always increases viscosity. However, the rate of increase is much more significant below and approaching the cloud point (57°C) than above. At 30°C the solution viscosity increases 52% from water to 5 v/v% $C_{9\text{-}11}E_6$ compared to 142% at 50°C and 16% at 70°C. The viscosity of a detergent solution can gives an indication as to the structure of the micelles in solution (Porter, [1994]). Spherical micelles show no appreciable increase in viscosity with concentration, however, rodlike polydisperse micelles show a significant increase. This suggests the existence of spherical micelles at 30 and 40°C and rodlike micelles at 50°C which is confirmed later in section 4.2.6.

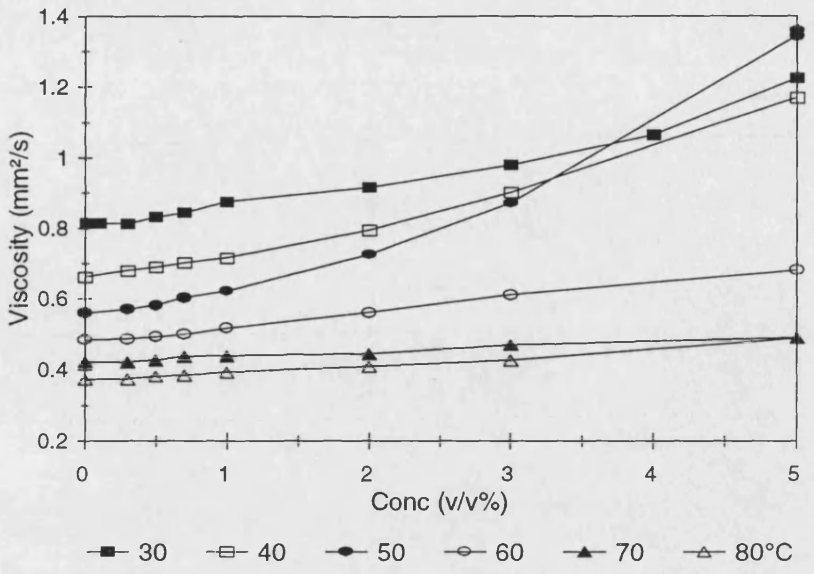

Figure 4.3 $C_{9-11}E_6$ Kinematic viscosity variation with concentration from 30-80°C

4.2.4 Surface Tension Measurements, Cmc Determination

Surface tension is defined as the force required to create new unit surface area and can be used to define the effectiveness of a particular surfactant at reducing interfacial forces. Due to the significant changes in solution properties as a function of surfactant concentration there are many methods to calculate the cmc, measurement of conductivity, turbidity, surface tension etc. (Tadros [1984]). The Whilhelmy Plate procedure, measuring surface tension is the most popular and has been used, see Appendix A. Results portraying the effect of the addition of $C_{9-11}E_6$ on surface tension are presented graphically in Figure 4.4. For ease of differentiation between each surface tension curve determined at a different temperature, data produced at 30°C has had 5 mN/m added and data produced at 40°C has had 10 mN/m added and so on.

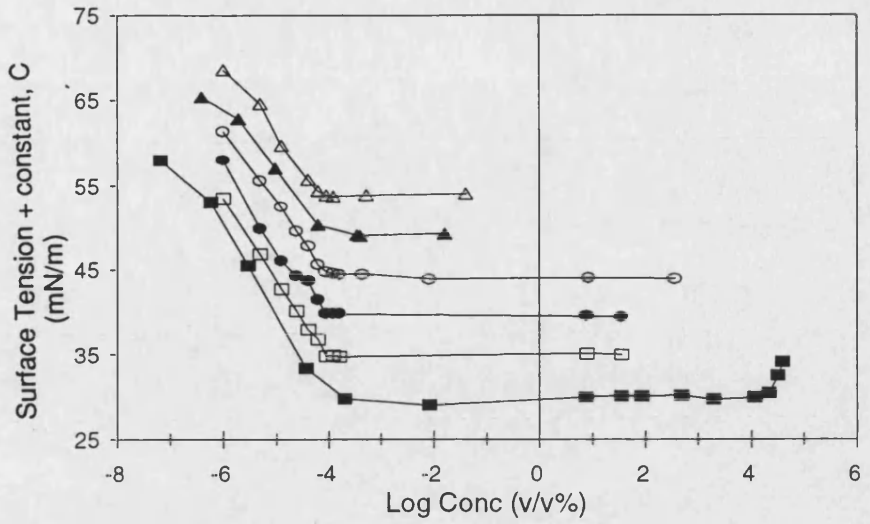

Figure 4.4 Variation of Surface Tension with Concentration over 30-80°C, $C_{9-11}E_6$

As expected there is a linear relationship between surface tension, γ, and log concentration of $C_{9-11}E_6$ below the cmc. Typical of nonionic surfactants this does not apply at very low concentrations where the surface tension begins to plateau off. This is especially noticeable with the curve produced at 20°C. The linear portion of the curve is a consequence of the surface becoming saturated with surfactant molecules. Any further addition of surfactant packs the molecules more tightly at the surface until the cmc is reached and the molecules are perpendicular to the interface (Clint [1994]). Occasionally with mixed surfactant systems a 'double cmc' is obtained corresponding to each of the individual surfactants cmc but with $C_{9-11}E_6$ a specific cmc is obtained, probably due to the fact that surfactant distribution is over a small range of hydrocarbon chain length. Table 4.1 summarises the results. As expected the cmc's decrease slightly with increasing temperature rather than increase as is the case for ionic surfactants.

Table 4.1 $C_{9-11}E_6$ Cmc

Temp (°C)	γ_{cmc} (mN/m)	cmc (v/v%)	cmc (mol/dm^3)	γ_{water} (mN/m)
20	29.9	0.0183	0.00043	71.5
30	29.8	0.0178	0.00042	71.0
40	29.6	0.0173	0.00041	69.2
50	29.5	0.0171	0.00040	68.2
60	29.2	0.0166	0.00039	67.4
66	28.9	0.0152	0.00036	65.1

4.2.5 Cloud Point Curve Determination

The majority of nonionic surfactants exhibit reverse solubility with temperature. The cloud point is the temperature at which the surfactant precipitates into a surfactant rich and a surfactant lean phase. This phase boundary is a function of concentration and is called the cloud point curve. It is identified by the clouding of the detergent solution and is characterised by a lower critical point which is defined as the cloud point.

The cloud point has been determined experimentally for $C_{9-11}E_6$. Detergent solutions of known concentrations were sealed in clear tubes and submerged in a thermostatically controlled water bath, (± 0.5°C). The temperature was then gradually increased and the temperatures at which each solution became opaque were noted. The temperature was then decreased and temperatures at which the solutions became clear were noted. The cloud point was taken as the average of the two temperatures. The point of clouding was not particularly well defined, this is probably due to fact that $C_{9-11}E_6$ is not a pure component. The results are depicted in Figure 4.5. The cloud point of $C_{9-11}E_6$ is clearly 57°C which is 3° lower than pure $C_{10}E_6$ (Schick [1987]) indicating a higher proportion of the $C_{9-11}E_6$ is made up of the longer hydrophobic chain (C_{11}) since increasing hydrophobic chain length decreases the cloud point. This agrees with the composition breakdown of $C_{9-11}E_6$ detailed in section 4.2.1.

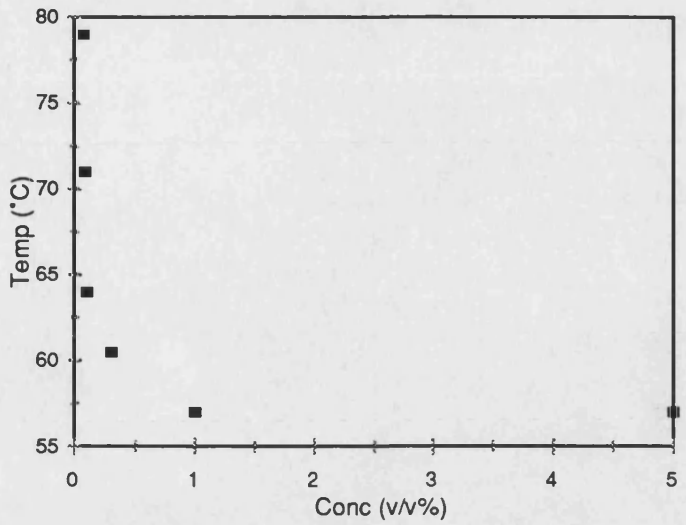

Figure 4.5 Cloud Point Curve for $C_{9-11}E_6$

4.2.6 Micelles in Solution

Cleaning performance has been shown to be affected by the size, shape and quantity of micelles in solution. It is therefore important to be able to predict micelle dimensions and aggregation number for a particular set of process conditions. This is especially crucial with nonionic surfactants since temperature has a dramatic effect upon micelle structure.

There are many practical techniques for micelle size determination but there is often a wide variation in the reported results. Clint [1994] suggests steady state fluorescence quenching and small angle neutron scattering are the most effective. Theoretical approximations have also been developed by Nagarjan and Ruckenstein [1991] and Puvvada and Blankschtein [1992], considering the equilibrium relationship between a monomer in solution and monomers contained within a micelle. These have been utilised to predict micelle size with temperature for the $C_{9-11}E_6$ solution.

4.2.6.1 Prediction of Micelle Self Assembly

Within an aqueous surfactant solution an equilibrium will exist between the monomers within a micelle and the singly dispersed monomers in solution. This is shown in Figure 4.6.

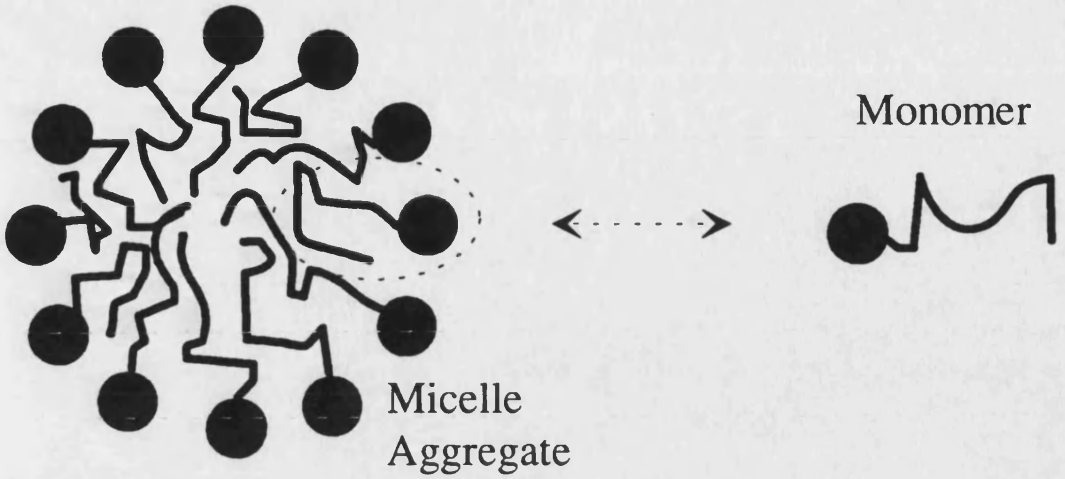

Figure 4.6 Micelle Equilibrium Relationship

At equilibrium, the chemical potential of the individual monomer will equal the chemical potential of the monomer present within a micelle and the Gibbs Free Energy of the monomers will be at a minimum. This can be represented as:

$$\psi = \mu_g^0 + k_b\,T\,\ln X_g = g\left[\mu_1^0 + k_b\,T\,\ln X_1\right] \qquad 4.1$$

where ψ = chemical potential

k_b = Boltzmann's constant

g = aggregation number

μ = Gibbs Free Energy

X = Mole fraction

X_{total} = $X_1 + (g\,X_g)$

By manipulation of Gibbs Free Energy equation 4.1 the following is obtained.

$$X_g = X_1^g \exp\left(-\frac{g\,\Delta\mu_g^0}{k_b\,T}\right) \qquad 4.2$$

The semi-empirical correlations Nagarajan and Ruckenstein, [1991] estimated the difference in free energy ($\Delta\mu_g$) between an individual monomer (X_1) and a monomer within a micelle (X_g). It is then possible to determine the value of g, the monomer aggregation number, where X_g is a maximum. This value of g then specifies the equilibrium aggregate shape for the particular conditions.

This procedure has been applied to $C_{9\text{-}11}E_6$ assuming the C_9-C_{11} distributions of hydrocarbons chain is equivalent of C_{10} and an average of 6 polyoxyethylene groups. Figure 4.7 shows the variation of X_g with aggregation number g for $C_{10}E_6$ at 1°C, the predicted equilibrium aggregation number being 58 monomers.

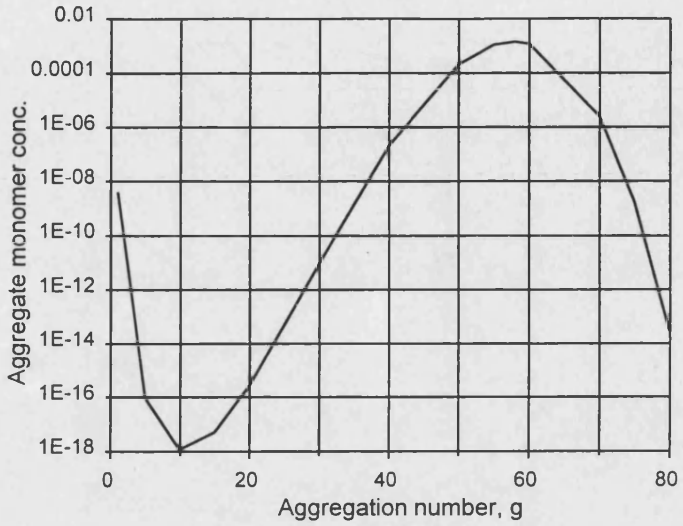

Figure 4.7 Aggregation Monomer Conc against Aggregation Number

The predicted shape is independent of concentration. Increases in concentration produce more micelles of the same shape. At high concentration the micelles in solution become crowded and interfere with each other making this assumption inappropriate.

4.2.6.1.1 Estimation of $\Delta\mu_g$ for nonionic monomers

Calculation of the difference in free energy ($\Delta\mu_g$) of $C_{10}E_6$ was broken down into 4 key steps for nonionic monomers. The semi-empirical correlations used to determine the surfactant properties and each step can be found in Appendix A.

1) The first step is to estimate the free energy of transfer of the hydrocarbon chain $\left(\Delta\mu_g^0\right)_{tr}$ of the surfactant from water into the hydrocarbon core of the aggregate. The relationship is linearly dependent on the number of carbon atoms in the hydrocarbon chain. This is the driving force for aggregation.

2) The hydrophilic end of the hydrophobic tail is compelled to remain at the polar water interface causing a free energy of deformation $\left(\Delta\mu_g^0\right)_{def}$.

3) Formation of the micelle produces a hydrophobic / water interface between the polar heads. This free energy difference $\left(\Delta\mu_g^0\right)_{\text{int}}$ is accounted for as the product of the area of the interface and macroscopic interfacial tension of the hydrophobic / water interface.

4) Finally, micelle aggregation produces a steric repulsion of the polar head groups $\left(\Delta\mu_g^0\right)_{steric}$. The work of Nagarajan and Ruckenstein [1991] assumes that the head groups are compact in nature acting as hard particles with a definable core. For polyoxyethylene head groups having a long chain head structure this is not valid. To account for this a correlation produced by Puvvada and Blankschtein [1992] is utilised.

The overall difference in Free Energy of an individual monomer and a monomer within a micelle in then obtained by summing the individual contributions, equation 4.3:

$$\frac{\Delta\mu_g^0}{k_b\,\mathrm{T}} = \frac{\left(\Delta\mu_g^0\right)_{tr}}{k_b\,\mathrm{T}} + \frac{\left(\Delta\mu_g^0\right)_{def}}{k_b\,\mathrm{T}} + \frac{\left(\Delta\mu_g^0\right)_{\text{int}}}{k_b\,\mathrm{T}} + \frac{\left(\Delta\mu_g^0\right)_{steric}}{k_b\,\mathrm{T}} \qquad 4.3$$

4.2.6.1.2 The geometry of the micelles.

The free energy difference is a function of the aggregate shape. The two shapes considered in this routine are spherical (see equations 4.4, 4.5 and 4.6) and globular micelles (see equations 4.7, 4.8, 4.9 and 4.10). Rodlike micelles and hence polydispersity has been predicted but the procedure is complex (Nagarajan and Ruckenstein [1991]).

Spherical Micelles

$$V_g = \frac{4\pi\left(\mathrm{R}_s\right)^3}{3} = \mathrm{g}\,v_s \qquad 4.4$$

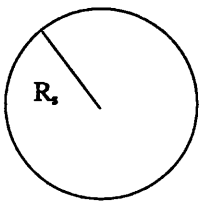

$$A_g = 4\pi\left(R_s\right)^2 = \mathrm{g}\,a \qquad 4.5$$

$$P = \frac{V_g}{A_g\,\mathrm{R}_s} = \frac{v_s}{\mathrm{a}\,\mathrm{R}_s} \qquad 4\,6$$

where R_s = radius of hydrophobic core of the micelle

v_s = volume of the hydrophobic tail of the surfactant molecule

A_g = aggregate surface area

a = aggregate surface area per surfactant molecule

P = packing parameter

Globular Micelles

$$E = \left[1 - \left(\frac{R_s}{b}\right)^2\right]^{1/2} \qquad 4.7$$

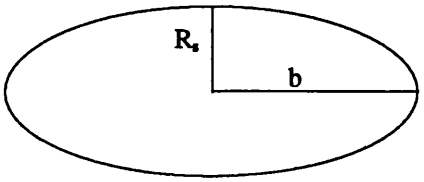

$$V_g = \frac{4\pi (R_s)^2 b}{3} = g\, v_s \qquad 4.8$$

$$A_g = 2\pi (R_s)^2 \left[1 + \frac{\sin^{-1} E}{E(1-E^2)^{0.5}}\right] = g\, a \qquad 4.9$$

$$P = \frac{V_g}{A_g R_s} = \frac{v_s}{a R_s} \qquad 4.10$$

where E = Eccentricity factor (account for deviation from spherical shape)

b = Length of semi-major axis

4.2.6.1.3 Micelle Shape Experimental and Predicted

The table below compares the predicted aggregation numbers against the experimental aggregation number which were determined using time resolved fluorescence (Alami et al [1993]). A good agreement is obtained as shown in Table 4.2.

Table 4.2 Experimental and Predicted Micelle Structure

Surfactant	Temp	Experimental		Predicted	
	°C	Aggreg No.	Shape	Aggreg No.	Shape
$C_{10}E_6$	1			58	globular
$C_{10}E_6$	10			63	globular
$C_{10}E_6$	15	85	globular		
$C_{10}E_6$	20			68	globular
$C_{10}E_6$	25	100	globular		
$C_{10}E_6$	30			92	approaching rodlike
$C_{10}E_6$	35	150	approaching rodlike		

For $C_{10}E_6$ the maximum aggregation for a spherical micelle is calculated to be 40. Thus indicating the existence of globular micelles even at the low temperatures.

Figure 4.8 depicts the variation of aggregation number with temperature. The black squares representing the predicted data and the clear rectangles representing the experimentally determined data. A good correlation can be observed. The curve is an exponential fit to both sets of data.

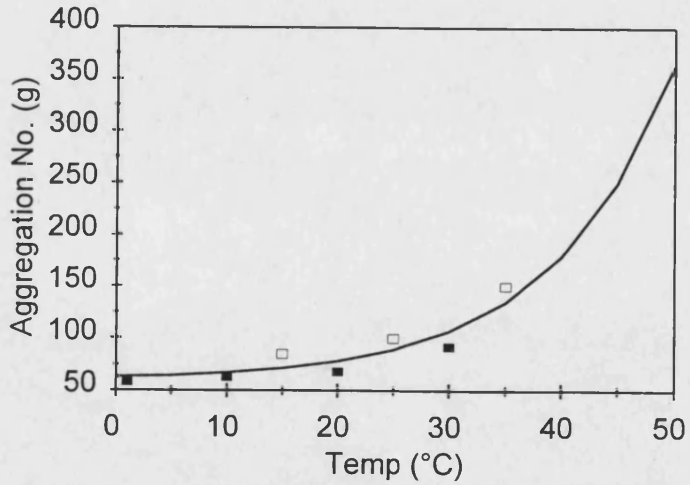

Figure 4.8 Plot of Aggregation Number versus Temperature

Using the curve fit, average aggregation number, micelle shape and core dimensions for experimental conditions are depicted in Table 4.3. Micelle sizes above 50°C are

not presented because the results have been produced at 10°C intervals and at 57°C the surfactant starts to precipitate (cloud point).

Table 4.3 $C_{10}E_6$ Micelle size and shape

Surfactant	Temp °C	Average Agregation No.	Core dimensions Width (Å)	Length (Å)
$C_{10}E_6$	30	107	28	60
$C_{10}E_6$	40	179	28	96
$C_{10}E_6$	50	363	28	187

4.3 Crude Oil Classification

4.3.1 Crude Oil Density measurement

The density of the crude oil and the detergent were determined using the same technique, (section 4.2.2) taken from BS 733 [1987]. At 20°C the density of the neat crude oil was determined to be 891 kg/m^3 with an API gravity of 26.8. The API of a crude is a common way of classifying oils and is defined by equation 4.11.

$$\text{API gravity} = \frac{141.5}{\text{S.G.}60°/60°\text{F}} - 131.5 \qquad 4.11$$

It does not uniquely define the quality of the crude but provides an estimation. Increased amounts of aromatics result in an increase in the density of petroleum. Increased saturated compounds result in a decrease in density. API also indicates sulphur content, the higher the API the larger the sulphur content of the oil.

After fouling, the crude oil density increased to 924 kg/m^3 having an API gravity of 21.1. Samples of the fouled oil film were obtained by centrifuging the fouled test piece, (see section 6.3.1, Chapter 6). Calculating the density variation with respect to temperature up to a value of 80°C proved difficult and inaccurate using a pyknometer, for this reason the coefficient of thermal expansion was used and for a petroleum fuel of API range 15.0-34.9 this value is equal to 0.00072/°C (Perry and Green [1984]). The results are found in section 4.2.2, Figure 4.2.

4.3.2 Crude Oil Viscosity measurement

The viscosity of the fouled crude oil film was determined using a plate - plate Bohlin rheometer (Lund, Sweden) results are portrayed in Figure 4.9 with further details presented in Appendix A. As expected, the viscosity decreases significantly with temperature but at a reducing rate.

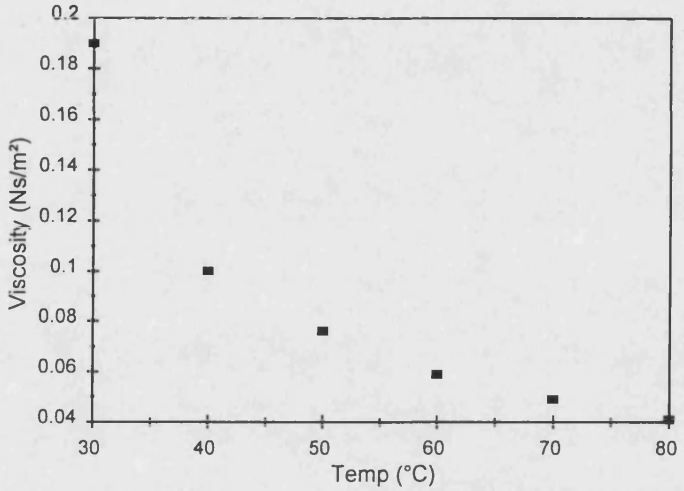

Figure 4.9 Change in Viscosity with Temperature of the Crude Oil

4.3.3 Crude Oil Composition

Crude oil is a mixture of hydrocarbons ranging from light aliphatic paraffins, methane and ethane to very heavy asphaltenes, cokes and wax crystals. The complex nature of the oil makes it almost impossible to determine the composition in terms of component substances. It has therefore been characterised in terms of boiling range distribution through the standard test method ASTM D5307 [1992], see Appendix A. The method uses gas chromatography and will report boiling ranges up to 538°C (1000°F), above 538°C material is reported as a residue. This technique is used to determine possible composition changes in the crude occurring during cleaning time. Findings are reported in Chapter 6. The resulting chromatogram for the pure untreated crude is shown in Figure 4.10. The calculated boiling point distribution curve is portrayed in Figure 4.11, the straight line indicates an even spread of hydrocarbons. A residual mass of 17.5 % was estimated.

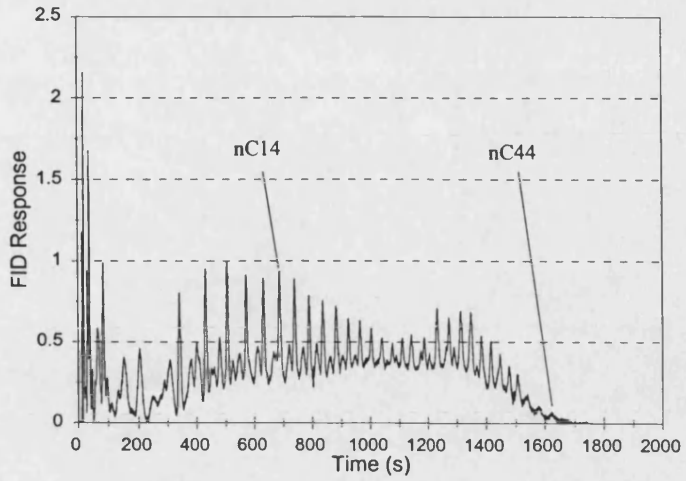

Figure 4.10 Raw Crude Oil Gas Chromatogram
Crude Oil Residue = 18%

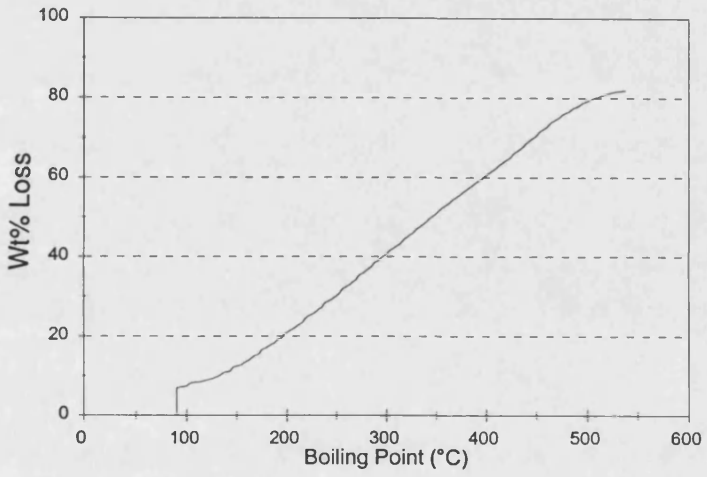

Figure 4.11 Crude Oil Boiling Distribution Curve

4.4 Surface Classification

The surface roughness of a substrate can play an important role in determining its cleaning properties, and is therefore important to characterise. The test piece and lead up tubing was 0.5" (12.7 mm) O.D. 0.01" (0.25 mm) wall thickness seamless cryogenic 304 stainless steel (*Tube Sales Ltd, Southampton*). Surface roughness measurements were made using a *Taylor-Hobson Talysurf-50* machine. An average arithmetic mean roughness value (R_a) of 0.43 μm for native and 0.42 μm for cleaned tubing was calculated. Readings were taken over 5 runs of 15 mm using a 0.8 μm stylus.

4.5 Water Classification

Unless otherwise stated, water used in the experiments was pre-softened to have a conductivity of 260 μS/cm and purified using an *Elga Intercept ROS* reverse osmosis machine to 20 μS/cm, typical of bulk industrial water purification. Hard water was used direct from the mains having a conductivity of 600 μS/cm.

Chapter Five

Development of an Experimental Cleaning System

5.1 Introduction

In this Chapter the design of an experimental protocol to determine oil film removal kinetics is presented. Measurement techniques from the literature are reported and critically appraised as to their applicability to oil film removal. Gravimetric analysis is shown to be the most suitable detection technique. Design and construction of experimental rigs is then detailed, reviewing the apparatus that has been utilised by other workers. The protocol is thoroughly assessed analysing the inherent errors and the reproducibility of the technique.

The protocol developed should be widely applicable and is a key development arising from this study. Potentially the protocol allows assessment of the effect of any detergent on a wide variety of oily soils. Unlike many previous studies the resulting removal curves are very accurate with minimal data scatter. The technique also allows deposit composition determination with cleaning time which has not been reported before. Additionally, video visualisation provides invaluable information on the oil removal mechanisms.

5.2 Cleaning Measurement Techniques

Obtaining a quantitative measure of cleaning efficiency is particularly important as it determines the validity of all results and conclusions subsequently derived. The chosen measurement technique must provide accurate cleaning kinetics as opposed to merely overall cleaning times. In the literature, there are principally two approaches to evaluating a level of cleanliness; direct and indirect methods (Paulsson, [1989]). The direct methods measure the amount of deposit remaining on the surface, and the indirect methods measure the amount of deposit removed from the surface (by effluent analysis). In choosing a technique there are several important factors to consider:

1. What is the lowest detection limit of the technique?

2. How accurate and reproducible is the technique?

3. Is the length of time taken for analysis reasonable?

4. Does the procedure present any laboratory hazards?

Oil film cleaning is particularly difficult to assess since removal is through unstable droplets which tend to coalesce. The high hydrocarbon content of the oil can also present difficulties in differentiating between the cleaner and the removed oil fraction. Whatever technique is chosen, it should be remembered that acceptable levels of cleanliness within the oil industry are often less stringent than some other applications, such as disinfection and biofilm removal studies.

5.2.1 Direct Methods

The following section details the main direct methods that are applicable for analysing the rate of oil film removal.

5.2.1.1 Visual methods

Most visual methods are simple to undertake, but do not provide a quantitative appraisal of the rate of removal, and therefore have no interest for kinetic removal studies.

5.2.1.2 Optical methods

Relating the amount of light a substrate reflects to the oily soil cleanliness of the sample was a common technique used by many authors (Comelles et al [1986], Cox and Matson [1984], and Johnson [1984]). Cox and Matson [1984] measured the reflectance of soiled samples of wax and grease fouled on masonite and aluminium before and after cleaning using a standard colorimeter. Results were expressed in terms of a 'relative cleaning performance' of surfactants. The accuracy of the technique was improved by using a transparent substrate. Pohlman, Werden and Marziniak [1972] precisely determined the distribution of contaminants on a glass plate by passing light through the plate onto a photoelectric cell.

The use of optical methods for the assessment of oily films formed on metal surfaces is inappropriate. The procedure is inaccurate, as it cannot evaluate soil depth. In addition the detergent solution must be translucent.

5.2.1.3 Dry weight method

This method has been used frequently and involves weighing the substrate before cleaning and re-weighing it subsequent to drying and removing any moisture present (Cox, [1986], Paciej et al [1993] and Prieto et al [1996]). The procedure is simple and easy to set up. It has not been widely applied, mainly because it not possible to follow the removal process continuously due to the drying stage and the Dupré effect (Chapter 2). Problems also arise in producing an oil deposit which has a weight significant compared to that of the substrate. This allows detection of the deposit when only 5% or more of the original mass is present. Hegg, Castberg and Lund [1985] suggest this method can be used to study fouling down to levels of 0.2-3 g/m^2 of fouled deposit.

5.2.1.4 Radiological method

This technique involves labelling the deposit with a radioactive tracer. The radioactivity detected gives a direct indication of the amount of deposit remaining, the counter measuring the reactivity of the deposit. This method relies upon the tracer having no effect on the rate of removal of the oil and the radioactivity lost from the surface representative of whole mass of deposit removed. This procedure was the most popular technique for many years (Voss and Korpi [1972], Scott [1963] and Chan et al [1976]). It popularity was due to its ease of application and sensitivity in detecting contaminants present in extremely small amounts or located in crevices or channels. However, due to its hazardous nature and the growth of environmental concerns its use is now minimal.

Bourne and Jennings [1965] measured the reduction in radioactivity of pure films of tristearin as they were removed from stainless steel by a circulation cleaning system. The technique was found to be accurate and reproducible. Bulat [1955] used a chromium oxide isotope to label a medium heavy lubricating oil. He evaluated the efficiency of ultrasonic equipment compared to various cleaning alternatives; vapour degreasing , agitation, brushing etc. Voss and Korpi [1972], measured radioactive labelled oil di (2-ethylhexyl) sebate films to compare different cleaning methods. Detection was accurate down to $4.65\times10^{-6} g/m^2$ of oil contaminant. This technique is making a comeback and has been used recently by Thompson [1994] to analyse oily

soil removal kinetics, although, with the problems of contamination and disposal it's use is likely to remain limited.

5.2.1.5 Ultrasonic Sensors.

A new technique has been developed for the measurement of the thickness of deposits in pipework (Withers, [1994]). Two transducers are mounted one on either side of the piping, one which is used to transmit an ultrasonic beam through the product the other to receive it. The intensity of the received beam is proportional to the thickness of deposit. The prototype sensor was able to detect the presence of deposits down to a minimum thickness of 0.1 mm over a temperature range of 20-140°C. Unfortunately the use of these sensors is in its infancy, and a commercially available sensor to determine deposit thickness is unlikely to be available for some time.

5.2.2 Indirect Techniques

The main indirect techniques applicable to oil removal are detailed below. A common problem with all techniques is that the mass of the deposit removed forms only a very small proportion of the overall mass of the solution and therefore the concentration of the deposit in the effluent is very small. This is especially true for moderate or high flow rates even though the rate of deposit removed is often increased. This class of techniques detect the change in physical property of the effluent when it contains the removed soil. Indirect techniques also depend upon the removed soil being spread evenly throughout the solution and not in particulates (which is a particular problem with oily soils, since they tend to coalesce).

5.2.2.1 Absorption method

Chemicals absorb energy from at least one region of the electromagnetic spectrum. Spectrophotometry involves the measurement of the energies of absorption across the electromagnetic spectrum in a precise analytical procedure (Harris and Bashford [1987]). The exact energy of absorption of a peak can be then related to the concentration of the component in solution. In the case of the oil, water and detergent effluent, a peak present in the absorption spectrum produced would have to be characteristic of the oil deposit removed. The energy content of the peak would

then indicate the oil concentration in the effluent and hence the rate of removal from the surface (Koretskii et al [1983] and Southworth et al [1983]).

Two problems exist with this method. Firstly, the detergent present within the solution is likely to have a hydrocarbon content. This may lead to an overlap between the spectrum produced by the removed oil, and the spectrum produced by the hydrocarbon(s) present within the detergent. A wavelength that is representative solely of the removed oil would need to be determined. Secondly, for every detergent concentration used, calibration of the energies of absorption of the chosen wavelength would be required before deposit concentration calculation would be possible. Additional difficulties would also exist if the removal oil fraction changed composition during the cleaning process.

5.2.2.2 Conductivity methods

There are two methods of analysing a fluids conductivity, determining either the electrical or the thermal conductivity.

(a) Electrical Conductivity

An electrical conductivity probe measures the ionic strength of the solution. The concentration of the oil in the stream is proportional to the ionic strength of the solution. The problem with this technique is that water is a very good electrical conductor, and hence a slight increase or decrease in the presence of oil in the solution is unlikely to provide a large change in the conductivity of the solution. Belyakov and Sagdeev [1988] measured the oil content in water rich emulsions but only down to concentrations of 5 wt% oil.

(b) Thermal Conductivity

A thermal conductivity probe measures the heat transfer from a probe into the effluent solution. This physical property is a function of the concentration of oil in solution.

Both methods of measuring conductivity methods have the same similar disadvantages, the main one being that conductivity is influenced by many other factors; temperature, cleaning agent, pressure and presence of micelles which leads to lengthy probe calibration procedures.

5.2.2.3 Capacitance

This method measures the dielectric properties of the effluent stream and relates them to the concentration of the oil in the solution. Problems occur when applying this technique to a three component system; with oil, detergent and water. For each detergent concentration, lengthy calibrations would be required. Chahine and Bose [1983] used time domain spectroscopy for the analysis of dielectric properties of water/oil emulsions. However, the study used much higher concentrations of oil in water; volume fractions of 90% to 99%.

5.2.2.4 Nephelometry

The intensity of a light beam passing through the effluent stream, turbidity, can in principle be related to the content of oil in solution. Turbidity is however commonly a non-linear function of the concentration. The technique is very sensitive at low concentrations. However, when oil drops suspended in solution large, light scattering occurs and readings will fluctuate. Unfortunately, turbidity measurements are effected by other parameters; temperature, velocity of effluent solution and concentration of detergent in solution. Nevertheless, this method was developed by Gallot-Lavellee, Lalande and Corrieu [1984] to study the removal of milk deposits in a plate heat exchanger. However, calibration was found to be difficult and time consuming.

5.2.2.5 Radiological methods

This method is the same as the direct radiological technique, except that the counter monitors the radioactivity of the effluent stream as opposed to that of the deposit remaining (Raney [1991]). This technique has not been as commonly used as the direct radiological technique but in common with that technique, high sensitivity and accuracy are possible. Once again, the hazardous nature of the radioactive solutions means that its use is now minimal.

5.2.2.6 Total Organic Carbon (TOC) Analysis

A TOC analyser measures the amount of organic carbon in solution, theoretically, down to 10 ppb. An injected sample is completely oxidised to form CO_2 with the amount of CO_2 produced being proportional to the amount of carbon in the sample.

The technique has not been described in the literature for determining oil film removal kinetics. This is probably due to the high carbon content of many detergents which leads to a high background count. However, because of the methods high degree of sensitivity it has been assessed in this study in evaluating crude oil removal kinetics. Initially, the technique was used to assess rinsing where there is only a very small contamination level of carbon (0.5 ppm). Even for removal by water, the method was found to be ineffective. The results were unstable, even using a homogeniser provided an unacceptable variation.

5.2.3 Conclusion

The type of measurement technique workers have utilised varies enormously. Direct techniques have been used more extensively than indirect techniques. The use of indirect techniques is limited for oily soil removal because of the difficulties in differentiating between the oil and the hydrocarbon content of the detergent. They are also inaccurate, as they involve lengthy calibration procedures relative to the detergent concentration. Radioactivity is probably the most effective procedure for assessing oily soil removal kinetics providing very high sensitivity with low cost. However, its use has declined due to environmental concerns, but for workers with suitable experimental laboratories its use has continued. The ultrasonic detection technique shows a lot of potential, but unfortunately the system is only in the early stages of development.

The gravimetric technique provides the best solution for the assessment of removal kinetics. By using a thin stainless steel substrate (1 hundreth of an inch thick) and an accurate balance (±1 mg) a deposit of 40 g/m^2 can be detected to greater than 99% clean.

5.3 Rig Design

5.3.1 Apparatus Review

Oily soil removal has been extensively described in the literature. However, few authors have produced kinetic cleaning curves. Several types of apparatus have been used for the analysis, these can be divided into two categories: batch and continuous systems. For the purpose of this study, a batch cleaning system is defined as an

apparatus where the cleaning solution is in constant contact with the deposit, typically a stirred tank, conversely a continuous system is defined where the cleaning solution is constantly replenished, typically a spray unit. The advantages and disadvantages of each of the two types are now discussed.

5.3.1.1 Batch Cleaning Systems

Batch cleaning systems for oily soils are simple, easy to setup and have been used by the majority of authors. The apparatus structure varies significantly from static tanks and rotating disks to tergotometers. Cleaning analysis is generally performed using optical techniques or gravimetrically. Experiments in static tanks generally do not directly measure removal but investigate contact angles and the variation in dynamic interfacial and surface tension with detergent and electrolyte concentration and temperature, with a view to determining the conditions for minimising surface tensions (Nasr-El-Din and Taylor [1992], Lim and Miller [1991], Herd et al [1992] and Ogino and Agui [1976]). Stirred tanks have been used to investigate the removal of oily soils from flat plates (Yatagai et al [1992]) (Paciej et al [1993]) (Aronson et al [1983]). Stirred tanks have limited use because the shear force on the surface of the plate is difficult to calculate and reproduce. The conditions also are not typical of an industrial cleaning system. Rotating disks or plates overcome the problem of fluid dynamics (Beaudoin et al [1995]). Semi empirical correlations provide accurate determination of the shear force on the surface.

5.3.1.2 Continuous Cleaning Systems

Spray systems are commonly used in industry, and laboratory size units have been used to assess cleaning efficiency (Prieto et al [1996], Sterritt [1992] and Nagarajan and Welker [1992]). Oil deposit analysis is difficult, and gravimetric and radiological techniques provide the best options. Tubular equipment has been successfully used by a number of workers for a variety of deposits (Bird [1993]) (Plett [1985]), although oily soil removal has received little attention. Bourne and Jennings [1965] undertook pioneering work investigating the kinetics of removal of radioactive tristearin in a circulation cleaning system. Mahé et al [1988] accurately studied the shearing of alcane droplets by detergent solutions. Tubular systems have the advantage that the thermo-hydraulic conditions can be precisely controlled allowing excellent

reproducibility. More over, the technique can be easily operated at conditions that represent those occurring industrially.

5.3.2 Test Piece Design

A continuous tubular test piece was chosen as it allows control of process variables, and flow visualisation within a glass cell. The test piece was designed to be of minimal mass, 1/100 inch thick, (0.254 mm, 304 stainless steel tubing) to enhance the gravimetric analysis. Preliminary plate studies indicated an average fouled coverage of 40 g/m^2 crude oil, a test piece length of 13.5 cm was therefore specified which gave detection greater than 99% removal (assuming a balance accuracy of ±1 mg). A second test piece was constructed to allow visualisation of the cleaning process within a glass cell. Two semi circular pieces were created by cutting a horizontal cross section along the length of an existing test piece.

It was important that each test piece fitted flush into the fouling and cleaning equipment. The connecting tubing before the test piece was the same ID and OD to reduce the effects of contraction or expansion of the flow due to the join. The normal twin ferrule type tubing union connection could not be used to couple the test piece to the fouling and cleaning equipment. The union damaged the internal surface and once applied left the twin ferrules permanently attached to the tubing. Selecting an alternative was difficult due to the vulnerable nature of the thin walled tubing. *Swagelok Ultra Torr* unions were selected (Figure 5-1), the fittings have rubber rings which upon tightening grab either side of the join to form a leak tight seal. The unions were bored through to allow quick release of the test piece by pushing the union back over the join. The experimental apparatus was then designed around the test piece with the intention of:

1. Producing uniform fouled oil films on the inside of the stainless steel test pieces

2. Cleaning the test pieces under controlled thermo hydraulic conditions.

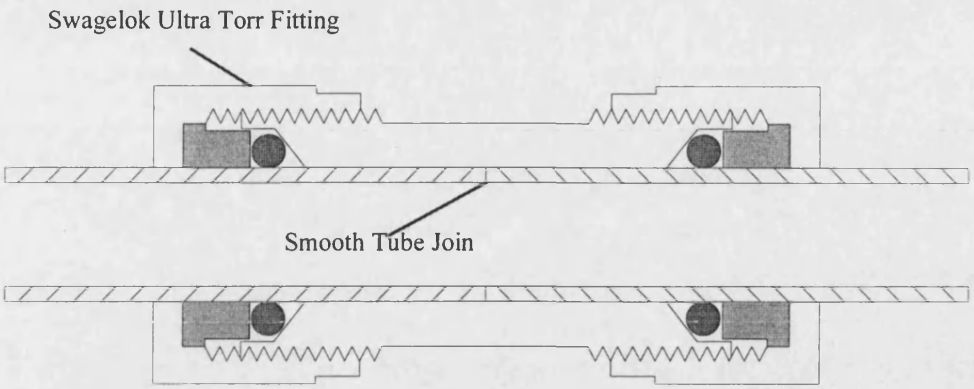

Figure 5-1 Union Connection of Test Piece

5.3.3 Materials of construction

The harshest constituent of the majority of chemical cleaners is sodium hydroxide. Sodium hydroxide is corrosive and can react with many of the commonly used construction materials such as tin, lead, brass, aluminium and mild steel. Aluminium evolves dangerous amounts of hydrogen upon contact with the hydroxyl ion, equation 5.1.

$$Al + OH^- + H_2O = AlO_2^- + \tfrac{3}{2}H_2 \qquad 5.1$$

Care was therefore taken not to use any of these materials in the construction of the rigs. Stainless steel (all classes), polyethylene, copper, and glass were used as suitable alternatives.

5.3.4 Experimental Apparatus

Several different rig designs were investigated and it was decided that separate fouling and cleaning rigs were necessary. This was mainly, due to the possible problems of cross contamination between the oil and the cleaning solution.

5.3.4.1 Fouling Rig

Before fouling began each test piece and the lead up tubing (Figures 5-2(a)-(c)) was rigorously cleaned. The tubes were initially brushed with a pipe cleaner using *Jizermizer* cleaning solvent to remove any visible crude deposits. They were then cleaned using $C_{9\text{-}11}E_6$ at ≈50°C for approximately 15 minutes and subsequently rinsed four times using reverse osmosis (RO) water. The internal surface of the tubes were

then subjected to the water break test to give an indication of cleanliness of the surface. Finally the tubes were oven dried at 50°C and weighed.

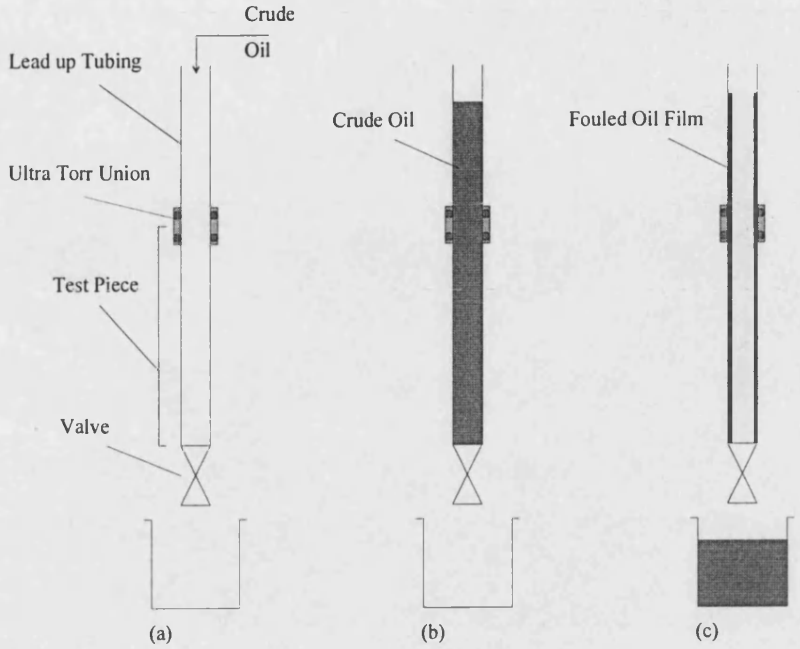

Figures 5-2(a)-(c) Test Piece Fouling Procedure

The apparatus used to foul the test pieces is shown in Figures 5-2(a)-(c). Test pieces are mounted vertically in a rack. A valve is attached to the lower end of each test piece and a section of lead up tubing of the same O.D. and I.D. is connected to the upper part of each test piece Figures 5-2(a). The join is made by an *Ultra Torr* union. Crude oil, mixed on a mill and regulated to 18°C is then gravity fed into each test piece with the valves closed Figures 5-2(b) and left for 5 minutes. The valves are then opened and the oil is allowed to drain, the apparatus is then left overnight for 16-18 hours prior to cleaning. The procedure was carried out in a fume cupboard and fourteen identical test pieces were typically fouled in one session. Maintaining the temperature of the applied crude oil at 18°C was very important as the temperature was a strong function of the crude oil thickness. The semi circular test pieces used for cleaning visualisation were fouled using the same technique, except that they were mounted inside an additional tube and then fouled.

5.3.4.2 The Fouled Oil Film

The change in crude oil mass of the test piece over the 16-18 hour fouling period was investigated (Figure 5-3). The fouling apparatus was suspended on an analytical

balance in the fume cupboard and the test piece was fouled using the same program. The fouling occurs in two stages, initially the crude oil reaches an equilibrium condition where the van der Waals forces of adhesion balance the gravitational forces of removal. The van der Waals forces are primarily due to transient dipole rather than dipole-dipole electrostatic attraction (Chapter 3). The crude oil principally contains molecules of hydrogen and carbon as opposed to polar molecules containing electro-negative elements. The second stage is evaporation, where the light ends up to the equivalent of nC_{13} are removed. The first stage is fast and lasts about 5 minutes, the second stage continues until the test piece is cleaned (Figure 5-3).

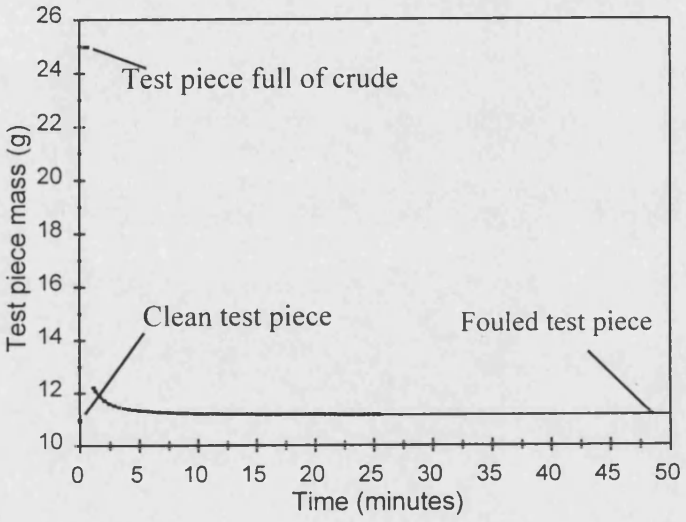

Figure 5-3 Fouling of Test Piece

The resulting oil films on each of the test pieces are inspected before cleaning. Oil film masses between 33.6 g/m^2 and 38.4 g/m^2 with an average of 36 g/m^2 were accepted for cleaning experimentation. Differences in deposit thickness are probably due to variation in the cleanliness of the test piece surface prior to fouling, rather than oil variations. Selecting test pieces within the deposition range reduces this inaccuracy and improves the results of subsequent cleaning analysis.

The crude oil has been analysed both before and after fouling using a gas chromatograph (GC). Figure 4.10 in Chapter 4 and Figure 5-4 depicts the chromatogram for the raw crude and the fouled crude oil respectively. The fouled deposit is of the same composition as the raw crude oil except that hydrocarbons below nC_{14} have evaporated. Samples of the oil fouled on a test piece were obtained

by spinning a fouled test piece in a centrifuge at 5,000 rpm. The collected oil could then be analysed using the gas chromatogram (Chapter 4).

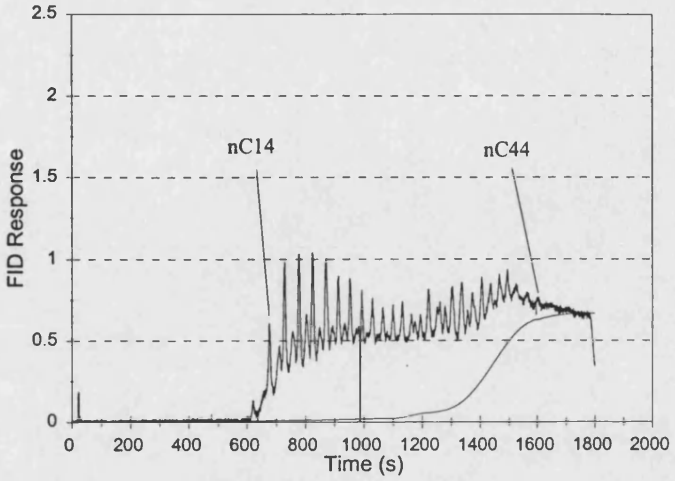

Figure 5-4 Gas Chromatogram of Crude Oil after Fouling
Crude Oil Residue = 46 wt%

5.3.4.3 Cleaning Rig

5.3.4.3.1 Design Criteria

Having decided upon a gravimetric cleaning analysis technique and the dimensions of the test piece, the cleaning rig was constructed to meet the following design criteria- accurate control of (i) the cleaning time; (ii) the detergent type; (iii) the detergent concentration; (iv) the detergent temperature; (v) the detergent flowrate. Each test piece also required subsequent rinsing and air drying.

5.3.4.3.2 Temperature Control

The cleaning rig was required to run over a wide range of detergent temperatures (30-80°C) with an accuracy of ±0.5°C. A water bath was constructed to control the process stream up to 70°C and the extra 10°C heat boost was provided by an oil bath. In the design of the water bath two variables were specified: a 200 litre water bath and a maximum of 30 minutes to heat up a full cleaning reservoir of 150 litres to 50°C. Assuming a detergent flowrate of 10 l/min, a temperature approach of 5°C and an overall heat transfer coefficient of 600 W/m² °C (Walas, [1988]) a heat duty of 18 kW was estimated for a practicable 30 metre length of copper piping.

Construction and Operation

A photograph of the cleaning rig is shown in Figure 5-5 and a simplified flowsheet of the cleaning rig is depicted in Figure 5-6 the bold line indicating the main process line. The apparatus has been designed specifically for this application. The cleaning tank has a volume of 150 litres allowing multiple cleaning runs. It is connected to a centrifugal pump, P-01, capable of developing 40 l/min water at 4 bara (*Lowara Ltd.*). Regulating the valve on the recycle line, V-02, allows rough adjustment of quantity of fluid passing to the rotameters. The needle valve, V-03, provides fine adjustment of the flow. Only one of the rotameters is in use at any time, this depends on the flow to be measured. One of the rotameters has been calibrated to 0-1 l/min and the other 1-10 l/min.

Heat is provided to the process stream through the water and oil baths. The water bath is a simple stirred tank heat exchanger its design has been discussed earlier section 5.3.4.3. It consists of two copper coils which surround six thermostatically controlled 3 kW immersion heaters and a stirrer. The larger of the coils, 30 m long, carries the process fluid and the smaller coil, 10 m long, carries cooling mains water. The amount of heat transferred to the process stream can be controlled through the speed of the stirrer and the setting of the thermostat. Cooling can be supplied through valve, V-06. This setup allows the process fluid to be maintained to ±0.5°C over 30-70°C. When temperatures higher than 70°C are required the oil bath is utilised and process fluid temperatures up to 80°C can be obtained. Temperature is monitored by Pt100 resistance probes, which provide accurate and quick response to 0.1°C, they are denoted by TI in Figure 5-6.

From the oil bath the main process stream divides into two separate lines. The flow into each line is controlled by valve, V-07. One line is used when recycling the process fluid back to the cleaning tank, the other when cleaning a test piece. The two lines then combine and a 3-way valve, V-14 directs the resultant stream to drain or recycles it back to the cleaning tank. To ensure fully developed flow entering the test piece the lead up tubing was at least 50 pipe diameters long (Kay and Nedderman, [1988]).

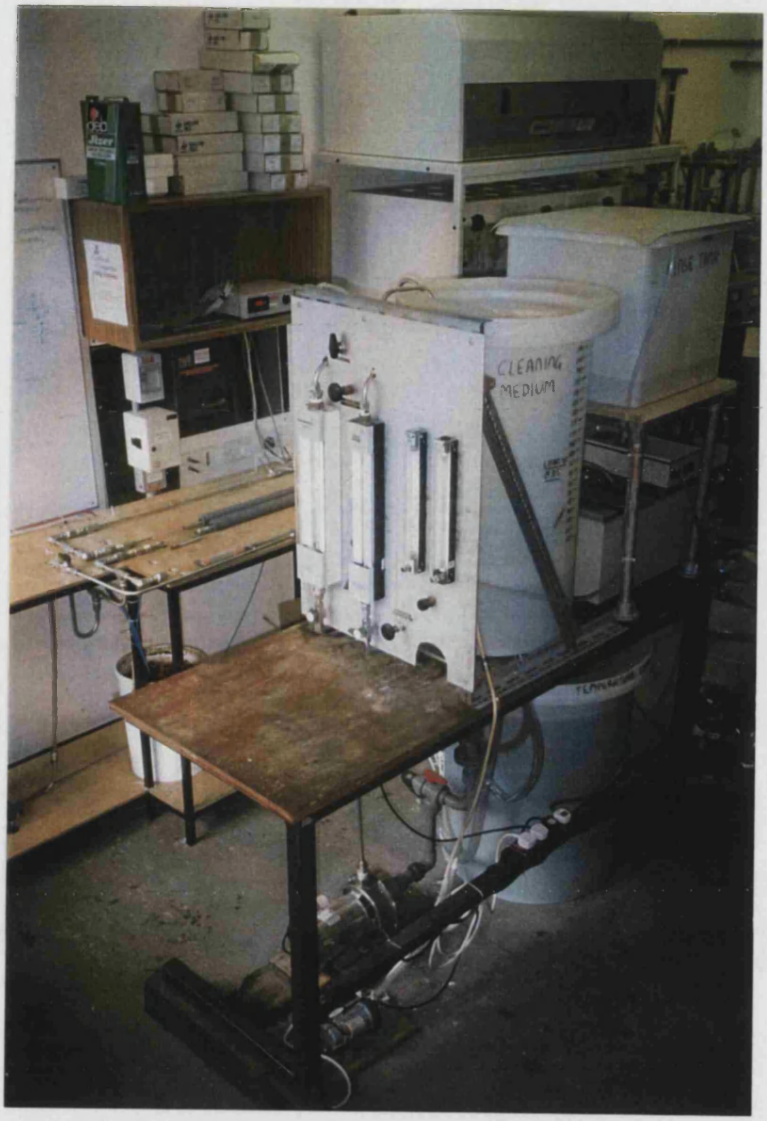

Figure 5-5 Photograph of Cleaning Rig

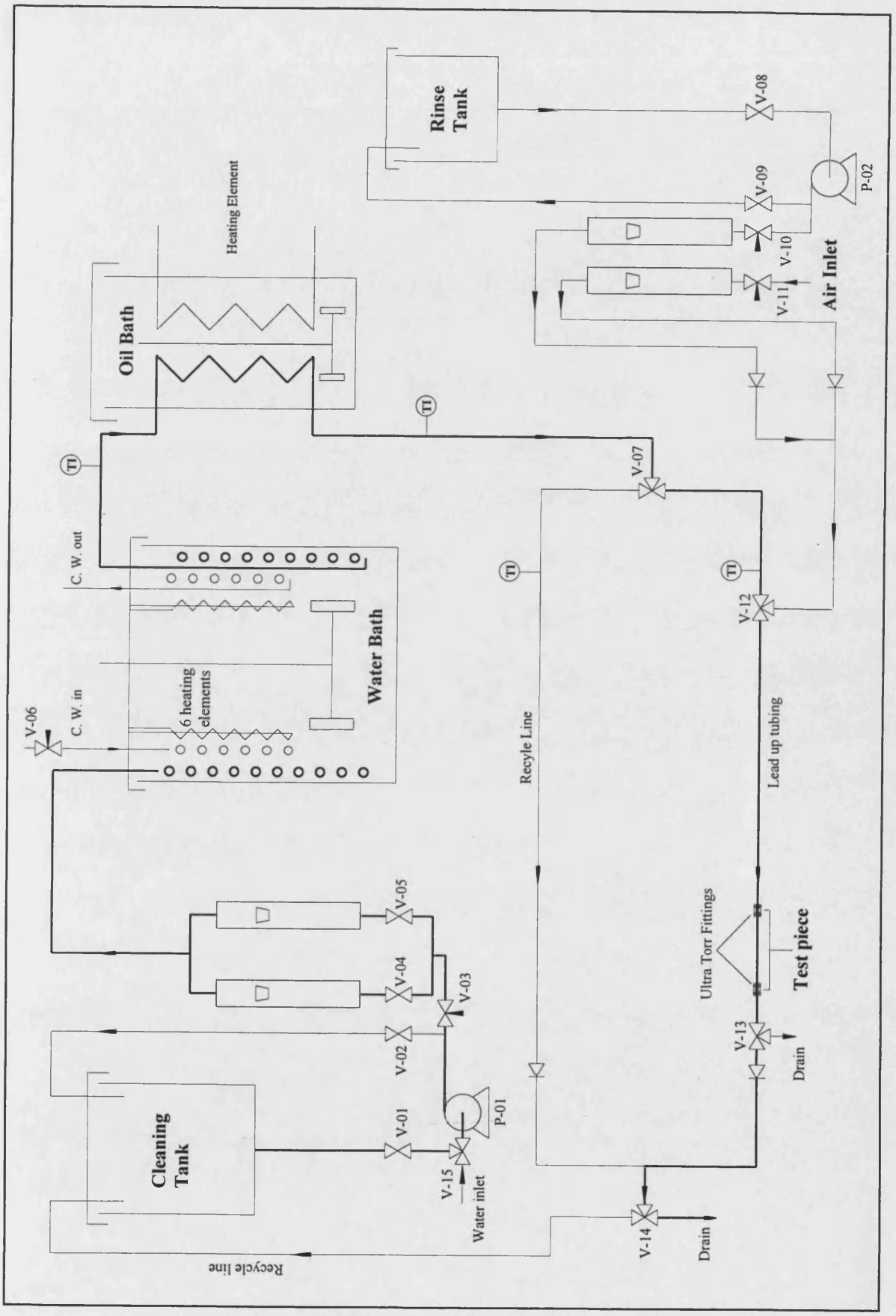

Figure 5-6 Simplified Diagram of Oil Film Cleaning Rig

The rinse tank is also connected to a centrifugal pump, P-02, providing rinse water to the test piece after cleaning. Flow is controlled in the same manner as the process stream, using V-09 and V-10 for rough and fine adjustment respectively. Rinse water is then passed to V-12 through the test piece and to drain. Air (from the laboratory supply) is subsequently introduced into the test piece, regulated through valve V-11 using the same line as the rinse water. All test pieces are rinsed with reverse osmosis water (≤17°C) for 1 minute at 1 l/min and dried for 30 seconds using 3 l/min.

After passing through the oil bath, the process line does in fact split in four. One of the extra lines is dedicated to visualisation of the cleaning process using a glass cell. The other line allows for additional test piece cleaning analysis. These lines are controlled by an additional 3-way valve and have the same setup as the test piece shown in Figure 5-6. Figure 5-7 depicts the glass cell and semi-circular test piece used to visualise the cleaning process. The glass tube has been specially drawn to be the correct inside diameter to accommodate the test piece and minimise any effect of the glass tube. Rubber tubing is used to seal the glass section to the existing tubing within the cleaning rig.

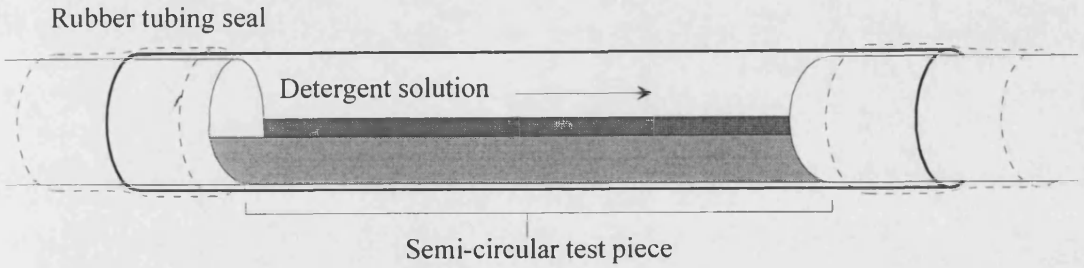

Figure 5-7 Test piece cleaning visualisation

When cleaning a test piece, the detergent effluent was passed directly to drain without recycle. Running on a once through basis is especially important when operating at very low surfactant concentrations as the cumulative effect of increased oil deposit concentration may have had a significant impact on the effectiveness of the surfactant solution, and may also lead to oil deposit redeposition.

Pump sizing details can be found in Appendix B.

5.3.5 Experimental Protocol

The overall experimental protocol is as follows- 14 test pieces are fouled and aged for 16-18 hours, under controlled conditions, to generate an oil film on the inside surface of each test piece. Test pieces are then inspected for film deposit mass and uniformity. An experimental cleaning curve can then be produced from the acceptable test pieces using the cleaning rig. The cleaning rig was operated on recycle until the desired process conditions were reached. When appropriate, cleaning agent was run through the test piece for a set period and subsequently rinsed and air dried. Finally, each test piece was analysed (section 5.3.6) to determine the amount of oil removed. Each test piece produced only one experimental point, and a batch of 8 test pieces is therefore required to construct a full cleaning curve, Figure 5-9.

5.3.6 Cleaning Analysis

The extent of cleaning is determined gravimetrically using a *Sartorius* balance accurate to ±1 mg (see section 5.2.3) . Each test piece is weighed before and after fouling. Test pieces within an acceptable deposition mass are then separately cleaned in the cleaning rig for a specific time period. After the subsequent rinsing and air drying, each test piece is withdrawn from the rig and lightly shaken to remove any loose droplets of rinse water from the internal surface of the tube. After careful drying of the external surface using a paper towel, each test piece is re-weighed. The recorded mass not only includes the test piece and any remaining oil mass, but also any rinse water which must be separately accounted for.

Each test piece is centrifuged at 2,000 rpm for 2 minutes in a dry centrifuge tube. The centrifugal force removes all the remaining rinse water and a portion of the residual oil which collect at the bottom of the centrifuge tube, see Figure 5-8.

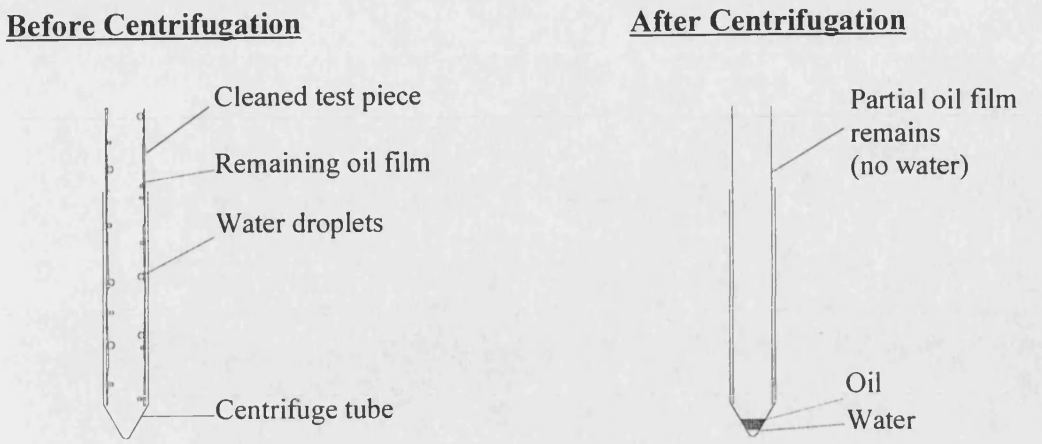

Figure 5-8 Test Piece Centrifuging

The oil and water that accumulate in the bottom of the centrifuge tube require separation. This can be accomplished through solidification. A 100 µl aliquot of chloroform is syringed into the centrifuge tube. The chloroform partitions into the oil phase, increasing the oil mobility and the oil / water interfacial forces. The centrifuge tube is then re-centrifuged at 5,000 rpm for 2 minutes and placed in a freezer at -30°C. The frozen water can then be extracted, and its mass determined. The oil removed during cleaning is then determined by a simple mass balance. Adding chloroform to determine the amount of oil remaining on a substrate is not a new technique and has been used successfully by Korestkii et al [1983]).

5.3.6.1 The Effect of the Solubility of Chloroform on the Analysis Technique

The solubility of chloroform in water was investigated to determine if it could affect the accuracy of the analysis technique. The inaccuracies are greatest when only a small amount of oil compared to water is collected in the centrifuge tube. Therefore the worst case scenario is when no oil is present, and we have only water. If 100 µl (0.15 g) of chloroform is added to 0.05 g water at 0°C only 0.0001 g of CCl_3H will dissolve in 0.05 g H_20 and only 0.0005 g H_20 will dissolve in 0.15 g CCl_3H. This represents less than a 1% detection error, which is deemed acceptable. Solubility data was obtained from Harvath [1982].

5.3.7 Experimental Error Estimate

Experimental errors are to be expected; data will always have a degree of scatter. Errors can be classified into two types: random and systematic. Random errors come

from the inability of a measuring device or operator and can be decreased by repeating the result. Alternatively, systematic readings which produce an offset from the real value can be reduced by re-calibration of a balance for example.

An estimate of the overall error associated with the experimental protocol must be determined. Three separate kinetic removal runs were performed using water at 2 l/min and 60°C (Figure 5-9). Run 1 and run 2 were performed over a range of cleaning times and in run 3 five data points were produced for five separate cleaning times; 60, 240, 360, 720 and 1500 seconds. The curve shows a degree of acceptable scatter and indicates good reproducibility.

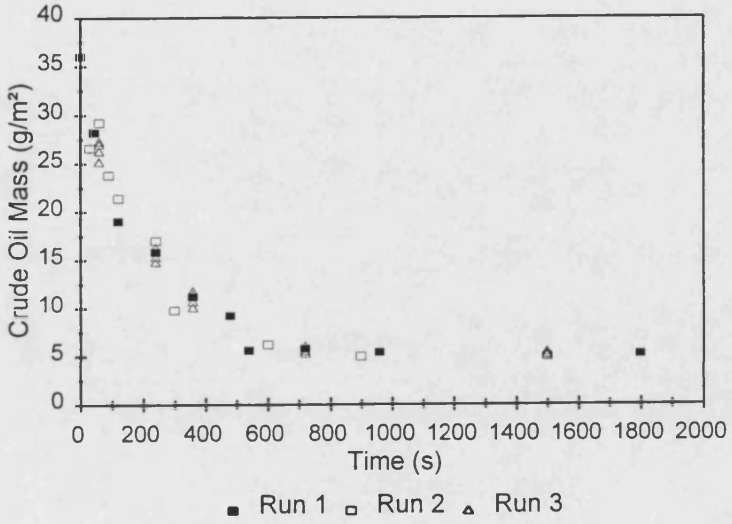

Figure 5-9 Error Assessment- Three experimental Runs, 2 l/min 60°C, Water

Utilising the experimental data determined in run 3 it is possible to determine the standard deviation at the five different cleaning times and represent it as error bars (Figure 5-10). The global error of each data point is approximately ±4.6% and is considered valid for all experimental data points presented in this thesis. The global errors can be traced to three origins- fouling experiments, cleaning experiments and cleaning analysis.

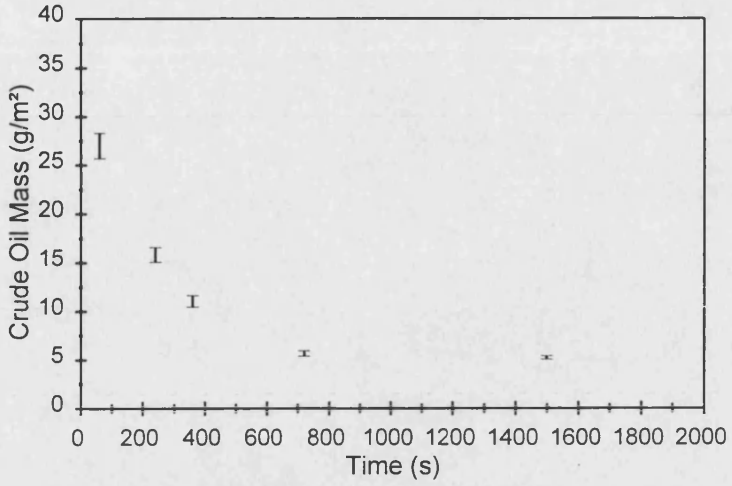

Figure 5-10 Global Error Estimate ±4.6%, 2 l/min, 60°C, Water

5.3.7.1 Fouling Experimental Errors

Fouling errors could originate from change in crude oil composition, the fouling apparatus and the conditions before cleaning. Variations have been minimised as far as possible. All crude oil used in this study was taken from one barrel only and stored in an air tight container. Fouling conditions were kept as constant as possible, and test pieces which showed any significant variation in film mass or uniformity were discarded. Test pieces were cleaned 16-18 hours after fouling. Any test pieces remaining after this period were rejected.

5.3.7.2 Cleaning Experimental Errors

The main sources of cleaning experimental error are likely to be from variation in the detergent composition, and variation in cleaning process conditions. The surfactant used in the cleaning experiments was purchased as a single batch minimising any composition variation. Concentrations were made up the evening before and allowed to age overnight to ensure even distribution of surfactant before application and low concentrations were made up through serial dilution. Cleaning solution flowrates were calibrated for each rotameter. The Pt100 resistance probes readings were checked in ice.

5.3.7.3 Cleaning Analysis Experimental Errors

An error assessment of the cleaning analysis technique has been undertaken. 10 fouled test pieces of known deposit mass were immersed in rinse water for 10

seconds, carefully shaken, the external surface dried and re-weighed. Care was taken not to remove any oil from the substrate during the process. The cleaning analysis technique discussed in section 5.3.6 was then performed on each of the test pieces. The amount of water separated from the oil was then compared to the actual amount of water remaining on the test piece after being dipped in the rinse water. The results are depicted in Table 5.1 shown below.

Table 5.1 Cleaning Error Analysis

Tube No.	Deposit Mass (g)	Water Deposited (g)	Water Recovered (g)	Result Deviation (g)
A	0.144	0.047	0.046	-0.001
B	0.141	0.040	0.041	0.001
C	0.129	0.041	0.037	-0.004
D	0.120	0.049	0.047	-0.002
E	0.120	0.048	0.047	-0.001
F	0.140	0.053	0.057	0.004
G	0.131	0.041	0.039	-0.002
H	0.120	0.060	0.058	-0.002
I	0.128	0.048	0.047	-0.001
J	0.133	0.064	0.069	0.005
Average	**0.131**	**0.049**	**0.049**	**±0.002**

The average result deviation is ±0.002g with a maximum of ±0.005g. The variation is not skew but normal. This was also undertaken early on in the results generation and as the experimenter became more experienced with the technique, the accuracy would certainly have expected to have increased.

Chapter 6

Experimental Results and Discussion

6.1 Introduction

This Chapter presents and describes the core results produced in this thesis and can be split into two sections: quantitative and qualitative analysis. The quantitative analysis makes up the majority of the cleaning results. This is in the form of kinetic removal curves which determine the effect of individual parameters upon removal: temperature, shear rate, concentration and type of detergent. Qualitative analysis supplements the quantitative data and is in the form of direct observation, videoing and subsequently photographing the removal process through a glass cell and determinating any change in crude oil composition with cleaning time using a gas chromatograph. The aim of the experimental programme was to improve the understanding of oil film mechanisms of removal with a view to modelling the process, Chapter 7.

6.2 Quantitative Analysis

In this section quantitative evaluation of the cleaning of oily films from stainless steel test pieces is studied using a variety of aqueous solutions. Kinetic curves are produced portraying the change of oily soil mass with time. The influence of temperature, flow rate cleaning solution composition and concentration is investigated. The majority of the results produced use $C_{9\text{-}11}E_6$, a nonionic surfactant, (refer to section 2.3.4.1 Chapter 2).

6.2.1 Typical Cleaning Curve

A typical cleaning curve is shown in Figure 6-1, the cleaning conditions were 40°C using 1 v/v% $C_{9\text{-}11}E_6$ and a volumetric flow of 2 l/min (linear velocity of 0.26 m/s). The y axis represents the average coverage (g/m^2) of the crude oil layer on the surface of a test piece and the x axis portrays the cleaning time (s). The average initial oil film coverage is 36 g/m^2 for each test piece at t=0. Initially, as time increases, the removal rate remains constant for 180 seconds, indicated by the linear relationship, (region A, seen in Figure 6-1). Further cleaning, and the mass of oil decreases sharply with removal becoming dependent on the amount of oil remaining, (region B). The removal curve finally reaches an asymptote with a residual layer remaining which is equivalent to 3.6 g/m^2 for the conditions investigated.

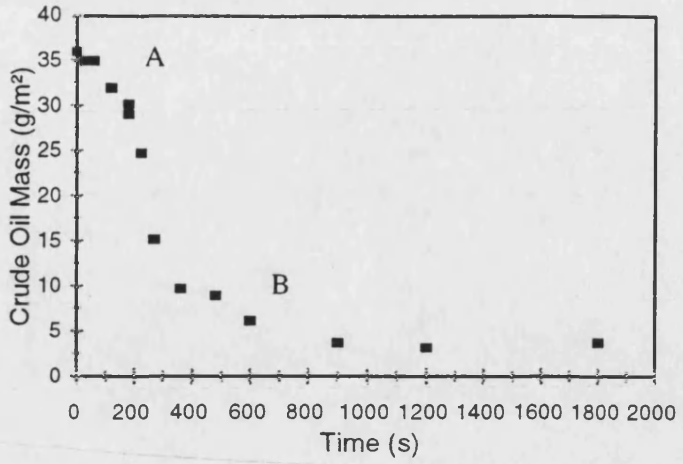

Figure 6-1 1v/v% $C_{9-11}E_6$, 2 l/min, 40°C

All removal curves follow this characteristic shape and typically can be split into two regions A and B as shown. Region A represents the removal of loose oil drops on the surface that are sheared off (and is therefore primarily a function of the fluid mechanics) and region B is dependent on the particular detergent effect. The duration of region A varies significantly. At 70 and 80°C the duration of region A is short, this increases to 300 seconds at 30°C. The transition from region A to B occurs at a distinct point, which can be clearly seen in Figure 6-1.

6.2.2 Assessing Cleaning Efficiency

The shape of the removal curves is described by simple zero and first order models in Chapter 7. Region A has been modelled as zero order and region B has been modelled as first order with respect to deposit mass. The resulting equations are shown in equations 6.1 and 6.2 respectively. Figure 6-2 portrays the fit between the model and the experimental data. Using the mathematical model developed, a graph of the rate of removal against time can be plotted, shown in Figure 6-3. This is an alternative way of presenting cleaning kinetics, where the area under the curve now equals the total amount of oil removed.

Region A:

$$m_a = m_O - a_c t \qquad 0 \leq t \leq t_{rev} \qquad 6.1$$

Region B:

$$m_b = m_a e^{-k(t-trev)} - A_{res} \qquad t_{rev} \leq t \leq \infty \qquad 6.2$$

where t = cleaning time

A_{res} = residual layer mass per unit area

k = region B removal rate constant

a_c = region A removal rate constant

t_{rev} = duration of region A

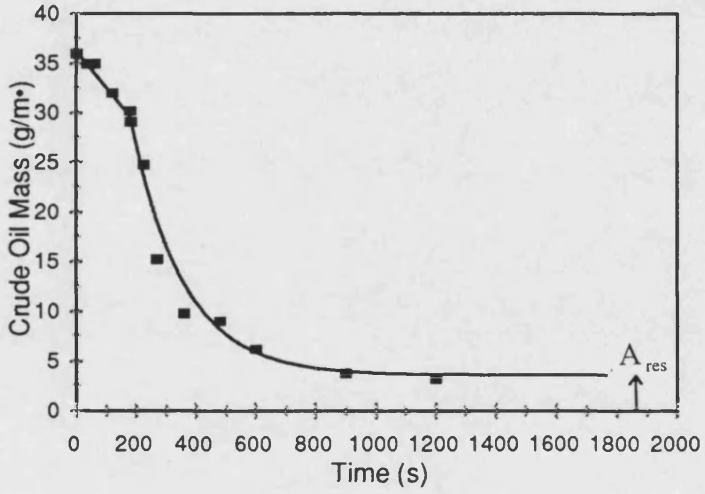

Figure 6-2 1v/v% $C_{9-11}E_6$, 2 l/min, 40°C, model presented

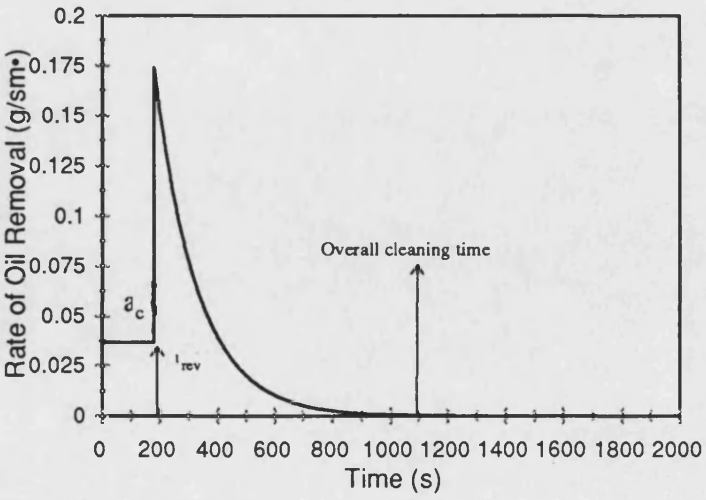

Figure 6-3 1v/v% $C_{9-11}E_6$, 2 l/min, 40°C, rate of removal

Each removal curve is individually characterised by four key parameters which define the overall removal efficiency of the process conditions: A_{res}, k, a_c and t_{rev}. The parameters are determined through semi-empirical modelling of each of the curves. Where appropriate they are labelled in Figure 6-2 and Figure 6-3. Comparing kinetic curves is difficult with this many parameters, ideally one variable needs to be specified for each removal curve. Since region A is independent of any chemical effect 't_{rev}' and 'a_c' are disregarded leaving 'A_{res}' and 'k'. Unfortunately, the relationship between 'k' and 'A_{res}' is complex. However, although not directly proportional they are closely related. As the rate of removal is increased the mass of the residual is reduced. 'k' is defined as the main parameter to evaluate removal efficiency. It value is derived from all the kinetic data points (rather than the last few: A_{res}) and unlike Ares cannot report a zero value.

6.2.3 Result Analysis

Results are grouped together in terms of the parameter under investigation. This parameter is then varied while maintaining the others. The effect of the individual parameter can then be characterised. While studying a particular variable it is important not to have other parameters dominating i.e. very high flow rates or the effects of the parameter being examined will hardly be noticeable. The removal curves are presented as the change in mass of the crude oil layer with time. The raw data is represented as symbols and the models indicated by a thin line. All the Figures within the parameter under investigation use the same scale on both the x and y axis to facilitate direct comparison of individual curves. The first Figure presented in each section is an overlay plot, each curve representing the modelled experimental data at the different conditions of the parameter under investigation. The experimental data is not shown directly on to this plot to avoid confusion. For each condition Reynolds number and surface shear stress were determined. The initial deposit thickness was 0.04 mm which gives an approximate e/d of 0.003 which will decrease on cleaning. Therefore the piping is assumed to be a smooth surface throughout removal allowing equations 6.3 and 6.4 to be applied (Coulson and Richardson [1980]).

$$\tau_w = \frac{8\rho(u^2)}{Re} \qquad \text{Streamline Flow (Re < 2000)} \qquad 6.3$$

$$\tau_w = 0.0396\rho(u^2)\mathrm{Re}^{-0.25} \qquad \text{Turbulent Flow } (2.5\times10^3 < \mathrm{Re} < 10^5) \qquad 6.4$$

Since cleaning is complex the effect of rinsing (the most fundamental form of cleaning) is assessed first followed by the supplementary effect of chemical additives.

6.2.4 Characterising Rinsing

Rinsing has no chemical effect and is an elementary form of cleaning. It has been studied in detail for various deposits (Paulsson [1989] and Plett [1985]) although studies concerning removal of oil by water by investigators such as Nagarajan and Welker [1992] are almost nonexistent (Mahé et al [1988]). Removal will only be as a result of the shear forces exerted on the deposit that occur when passing over the boundary of the test piece. The effect of temperature and flow rate of rinse water on the removal of crude oil has been determined. The consequence upon cleaning efficiency of increasing the crude oil film mass and the age of the fouled deposit have also been investigated.

6.2.4.1 The Effect of Rinse Water Temperature on Removal

Crude oil rinsing with reverse osmosis (RO) water has been studied at temperatures of 30 to 80°C at 10°C intervals at a flow rate 2 l/min, a velocity of 0.29 m/s and Reynolds numbers in the range of 4070 and 9400. The kinetic removal curves are depicted in Figures 6.4(a) to (g). Figure 6.4(a) presents an overlay plot of the modelled data at each of the rinse water temperatures. Figure 6.4(h) portrays the variation of the rate of removal constant, k, with temperature and finally Figure 6.4(i) shows the effect of temperature on the mass of the residual layer, A_{res}.

The consequence of rinsing with hard water (high calcium and magnesium ion content) has been determined at 50, 60, and 70°C, Figures 6.4(c), (d) and (e). The experimental data is depicted by the symbols with rectangular outlines.

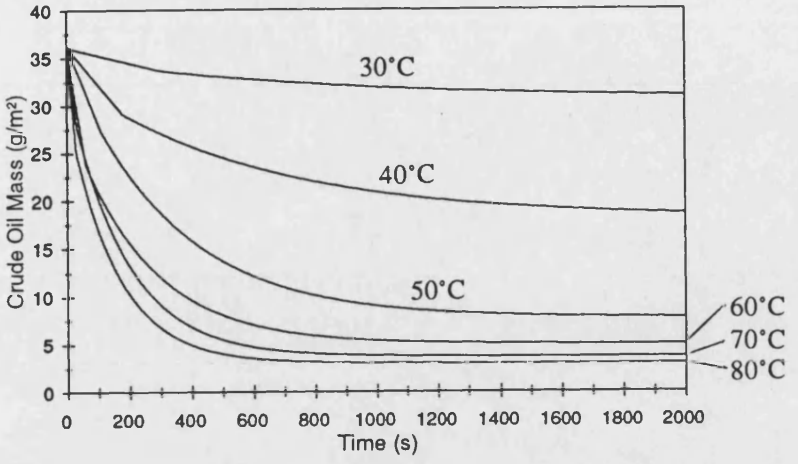

Figure 6.4 (a) Overlay plot: model curves from the individual plots Figures 6.4(b)-(g)

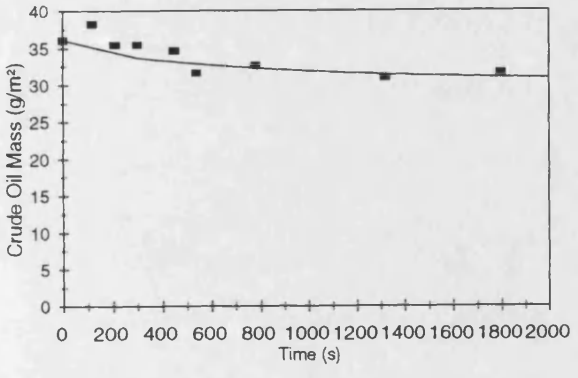

Figure 6.4(b) 30°C, Re=4070, S.S= 0.40N/m²

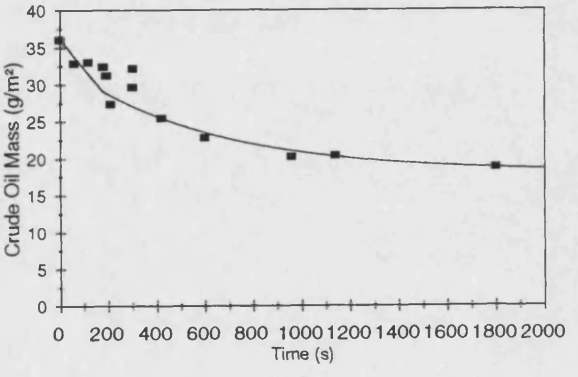

Figure 6.4(c) 40°C, Re= 4800, S.S.= 0.39N/m²

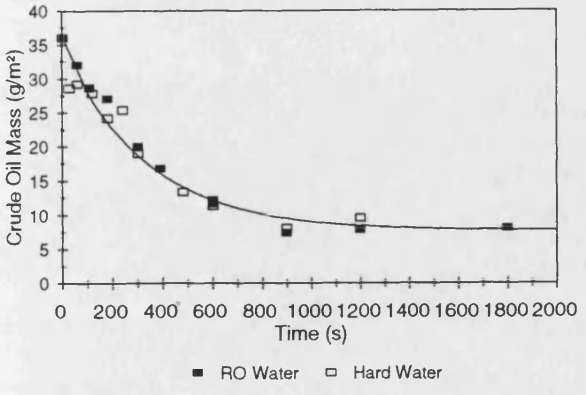

Figure 6.4(d) 50°C, Re= 5930, S.S.= 0.36N/m²

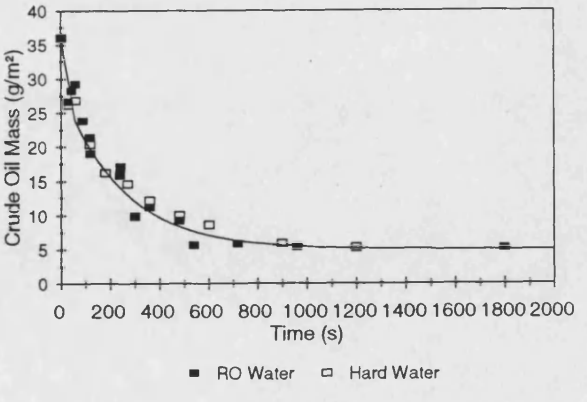

Figure 6.4(e) 60°C, Re=6840, S.S.= 0.35N/m²

Figure 6-4 The Effect of Rinse Water Temperature on Crude Oil removal, 2 l/min, 0.29 m/s (S.S.: Shear Stress)

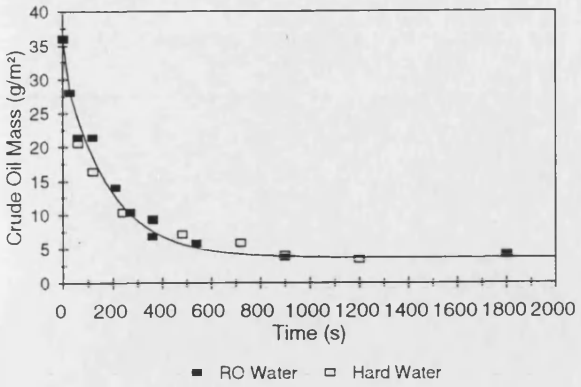

Figure 6.4(f) 70°C, Re=8110, S.S.= 0.33N/m²

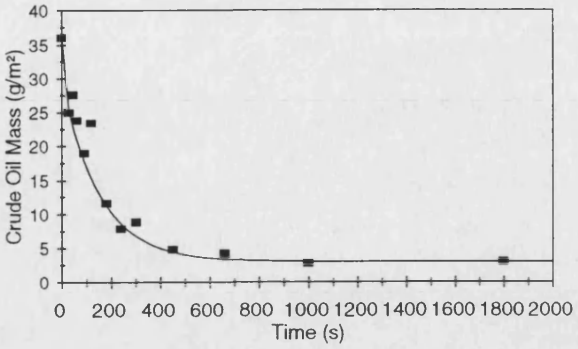

Figure 6.4(g) 80°C, Re=9400, S.S.= 0.32N/m²

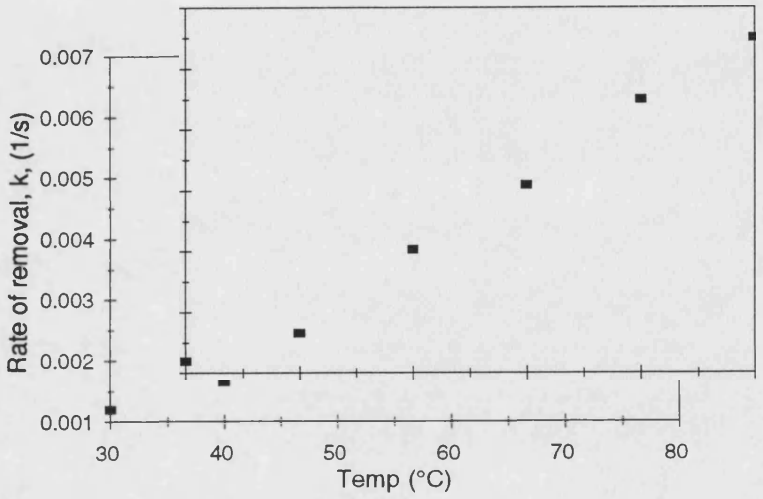

Figure 6.4(h) The Effect of Temperature of the Removal Rate Constant, k

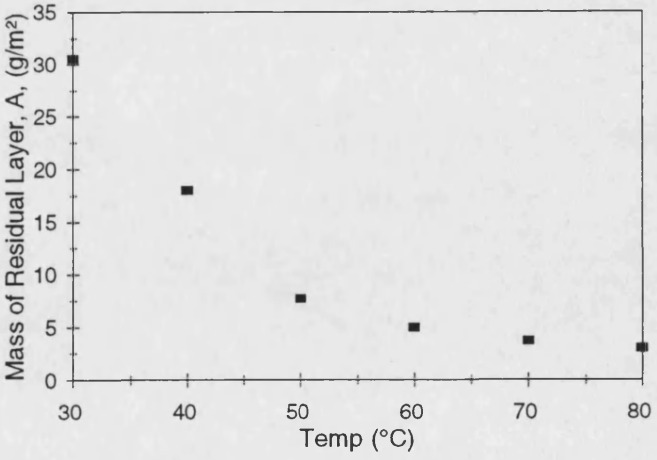

Figure 6.4(i) The Effect of Temperature on the Mass of the Residual Layer, A

Figure 6-4 The Effect of Rinse Water Temperature on Crude Oil removal, 2 l/min, 0.29 m/s (S.S.: Shear Stress)

6.2.4.1.1 Discussion of results

Each of the individual curves follow the typical removal shape forming asymptotic residual layers after a maximum of 30 minutes cleaning. In Figure 6.4(a) it can be seen that rinse water temperatures 60°C and above are crucial for effective removal. Further increases in temperature provide minimal benefits to removal. The large majority of the oil can be removed with high temperature rinse water although water alone will not completely remove the residual layer, with a minimum of 7.2 wt% of the original deposit mass remaining.

At 30°C removal is slow, (figure 6.4(b)). Initially the shear forces remove any loose deposit remaining on the surface (region A) over a period of about 300 seconds. Prolonged cleaning at 30°C provides minimal further benefit, with 84.7 wt% of the original deposit mass remaining. Subsequent 10°C increases in temperature up to 50°C dramatically reduce the mass of the residual layer and increase the rate of removal k, 21 wt% remaining after 2000 seconds at 50°C, (figures 6.4(h) and (i)). The strong dependence of k against A_{res} is clearly visible comparing Figures 6.4(h) and (i). The use of temperatures above 60°C results in little further benefit when water is used. The removal curves follow a similar path, the extra energy required to operate at a higher temperature offsetting any benefits to removal.

The effect of rinsing with hard water has not been documented in the literature. Rinsing of oil deposits with hard water at temperatures of 50, 60, 70°C has the same effect as when using reverse osmosis water. This is indicated and confirmed by Figures 6.4 (c), (d) and (e) where there is no discernible difference between the points rinsed with RO water or hard water.

6.2.4.2 The Effect of Rinse Water Velocity

The effect rinse water velocity has on the removal of the oil deposit has been characterised. A wide range of velocities has been studied (0.071 to 0.71 m/s) at 50°C primarily in the turbulent flow regime. Flow rates of 0.5, 1, 2, 3, 4, and 5 l/min with Reynolds nos of 1480, 2960, 5930, 8890, 11860, and 14820 respectively are presented. Results are depicted in the previous format, an overlay plot Figure 6.5(a) and individual curves Figures 6.5(b) to (g). Figures 6.5(h) and 6.5(i) plot the effect of Reynolds no. upon the removal rate and the mass of the residual layer respectively.

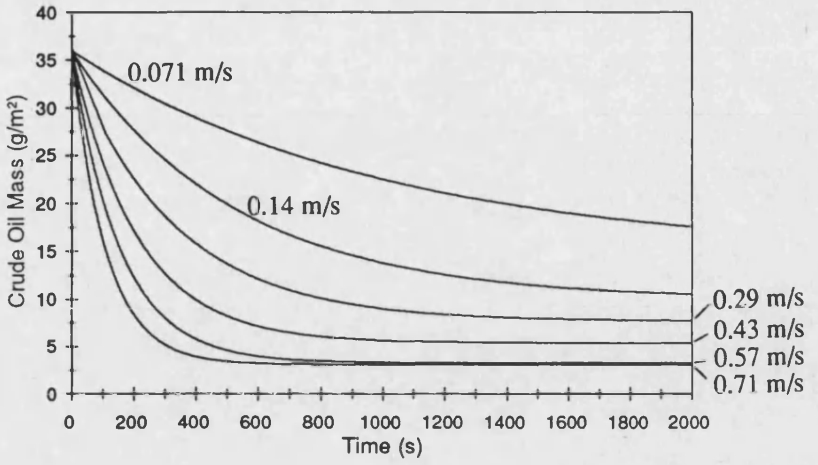

Figure 6.5(a) Overlay plot: model curves from the individual plots Figures 6.5 (b)-(g)

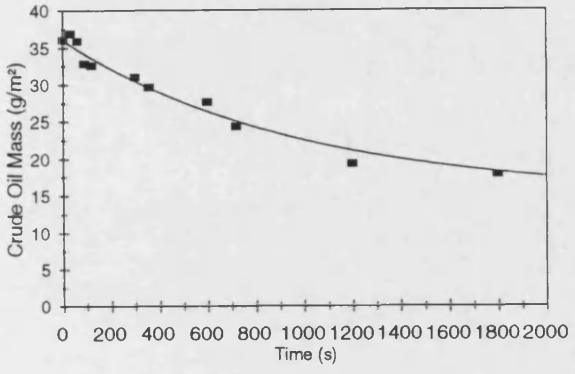

Figure 6.5(b) 0.071m/s, Re=1480, S.S.= 0.027N/m²

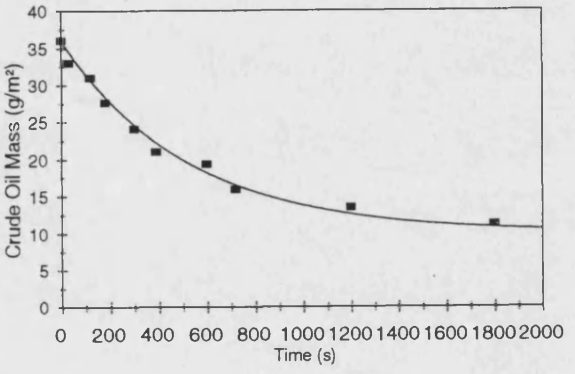

Figure 6.5(c) 0.14m/s, Re=2960, S.S.= 0.11N/m²

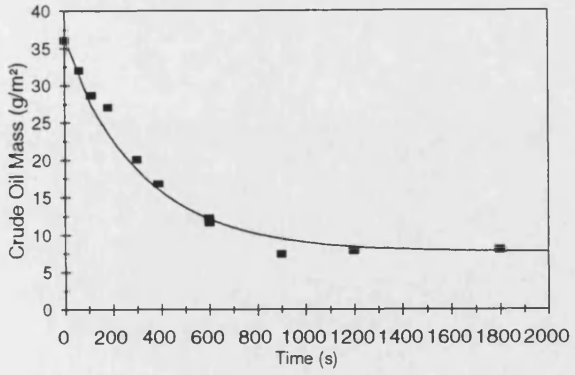

Figure 6.5(d) 0.29m/s, Re=5930, S.S.= 0.36N/m²

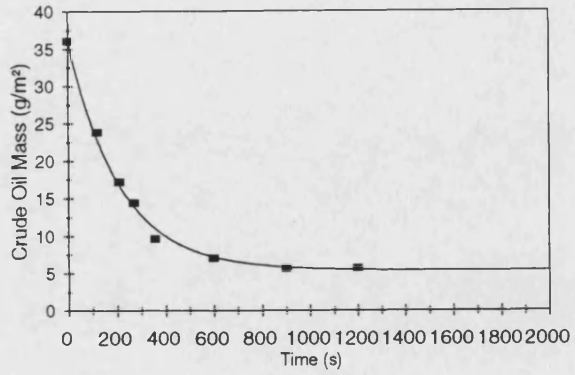

Figure 6.5(e) 0.43m/s, Re=8890, S.S.= 0.74N/m²

Figure 6-5 The Effect of Water Velocity on Removal of Crude Oil Cleaned at 50°C (S.S.: Shear Stress)

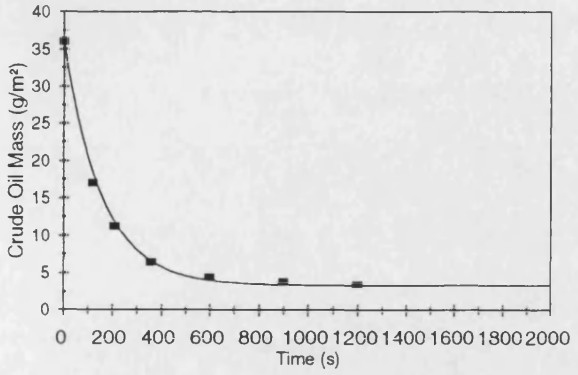

Figure 6.5(f) 0.57m/s, Re = 11860, S.S.= 1.22N/m²

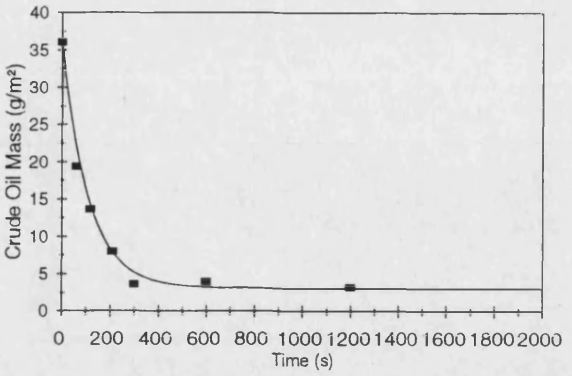

Figure 6.5(g) 0.71m/s, Re= 14820, S.S.= 1.81N/m²

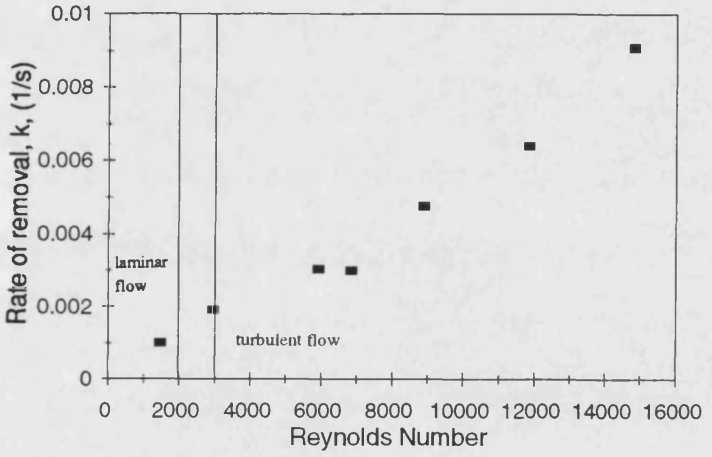

Figure 6.5(h) The Effect of Rinse Water Reynolds no. upon removal rate, k

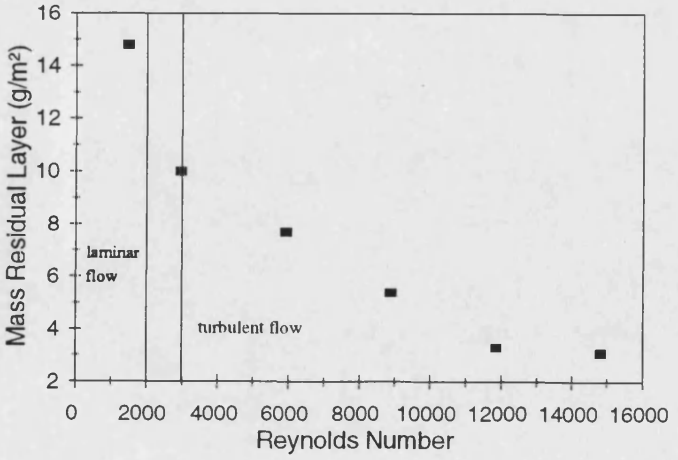

Figure 6.5(i) The Effect of Rinse Water Reynolds no. upon the Residual Layer, A

Figure 6-5 The Effect of Water Velocity on Removal of Crude Oil Cleaned at 50°C (S.S.: Shear Stress)

6.2.4.2.1 Discussion of results

Over the wide range of flowrates, increasing the velocity and hence the Reynolds number and shear stress is always beneficial to removal. The removal curves all follow the characteristic shape. As Reynolds number is increased from 1400 to 15000 there is a linear increase in the rate of removal Figure 6.5(h). Changing the flow regime from laminar, to transition and turbulent flow, Figures 6.5(b), (c) and (d) respectively, shows no fluctuation in the linear relationship. This contrasts several cleaning studies which have found a critical flow rate necessary for removal. High flow rates have less of an effect on the mass of residual layer A_{res} than the rate of removal k, Figure 6.5(i).

6.2.4.3 The Effect of Reynolds Number and Shear Stress upon Removal

Without any chemical effect, it would appear plausible to expect cleaning efficiency of rinsing to be directly proportional to the applied surface shear stress or the Reynolds number of the rinse water. Results have been produced to investigate this hypothesis. Figures 6.6(a) to (h) depict the variation of cleaning kinetics at temperatures of 30, 40, 50, 60, 70, and 80°C at constant Reynolds numbers. Rinsing kinetics produced at 60°C and 2 l/min (Re= 6850) were used as a base case.

The effect of maintaining the surface shear stress with temperature has not been investigated since the first set of data characterising the effect of water temperature on removal at 2 l/min is approximately at constant shear stress (3.6 ± 0.4 N/m^2) (Figures 6.4(a) to (h)). Further analysis is therefore unnecessary.

6.2.4.3.1 Discussion

Clearly cleaning performance cannot be characterised by either Reynolds number or surface shear stress alone, Figures 6.6(a) and 6.4(a) respectively. Both Reynolds number and shear stress have a strong dependence on temperature.

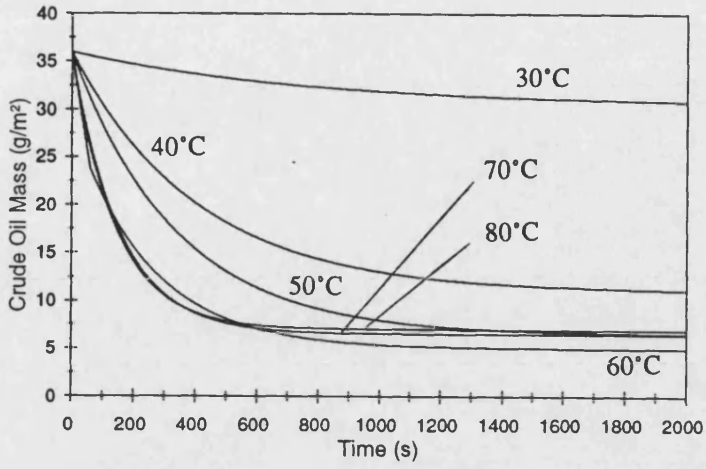

Figure 6.6(a) Overlay plot: model curves from the individual plots Figure 6.6 (b)-(g)

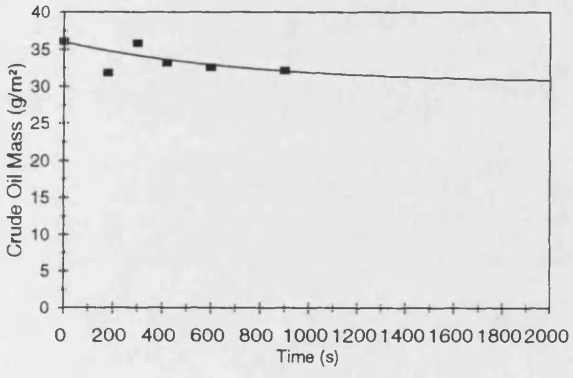

Figure 6.6(b) 30°C, 3.36l/min, S.S. 1.0N/m²

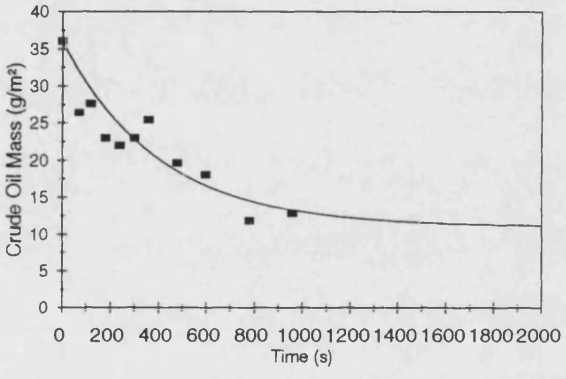

Figure 6.6(c) 40°C, 2.86l/min, S.S.= 0.72N/m²

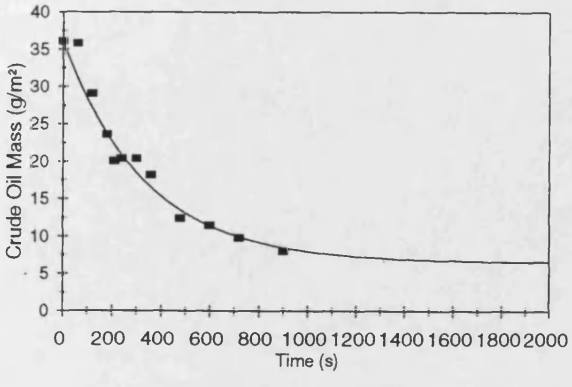

Figure 6.6(d) 50°C, 2.31l/min, S.S.= 0.47N/m²

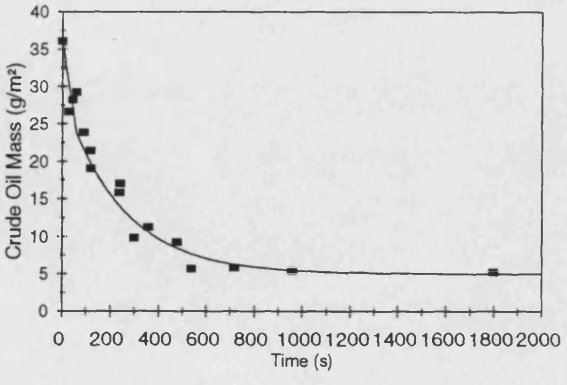

Figure 6.6(e) 60°C, 2l/min, S.S.= 0.35N/m²

Figure 6-6 Rinsing at constant Reynolds number over a range of temperatures (S.S.: Shear Stress)

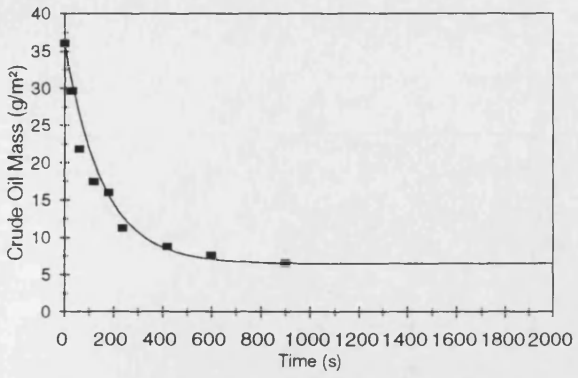

Figure 6.6(f) 70°C, 1.7l/min, S.S.= 0.25N/m²

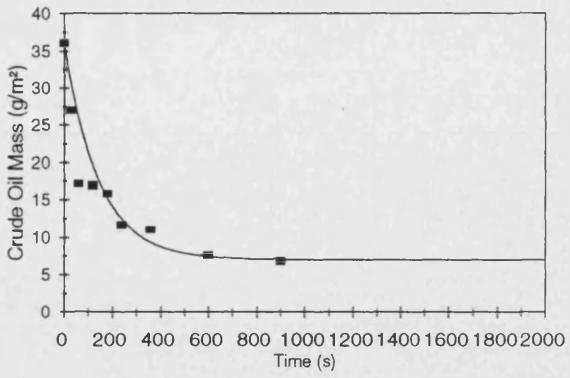

Figure 6.6(g) 80°, 1.5l/min, S.S.= 0.18N/m²

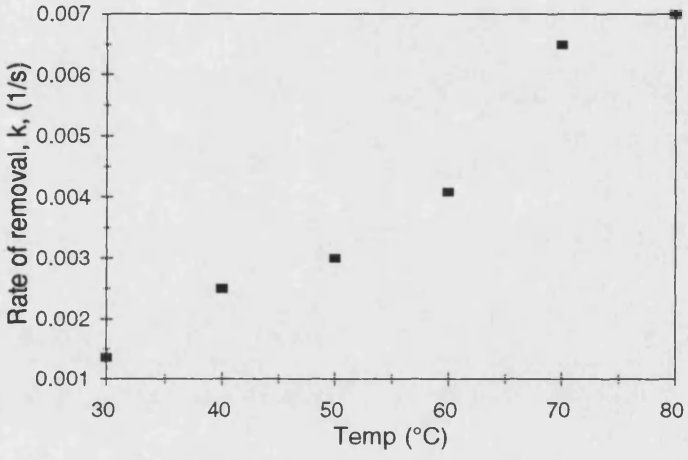

Figure 6.6(h) Temperature variation against k at constant Reynolds number

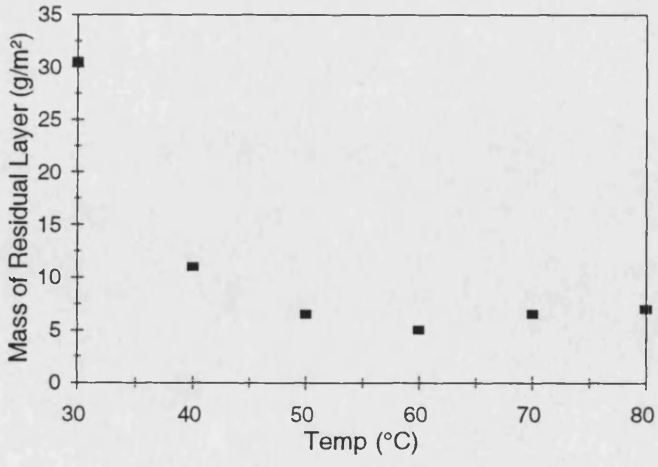

Figure 6.6(i) Temperature variation against A at constant Reynolds number

Figure 6-6 Rinsing at constant Reynolds number over a range of temperatures (S.S.: Shear Stress)

At 30°C (figure 6.6(b)) a rinse water flow rate of 3.36 l/min has a Reynolds number of 6850. If the operating temperature is increased by 10°C (figure 6.6(c)) the flow rate is reduced to 2.86 l/min to maintain the Reynolds number at 6850. The increase in temperature dramatically improves cleaning efficiency out weighing the reduction in flow rate. Further increases in temperature Figures 6.6(d) to (g) steadily improve the removal rate but have minimal effect on the mass of the residual layer (figure 6.6(i)). This suggests that above 40°C Reynolds number is proportional to the mass of the residual layer although the higher the temperature the quicker the overall cleaning time. It is therefore critical that the rinse water temperature is above 40°C for effective removal.

Shear stress does not characterise uniquely removal. Increasing the temperature and maintaining the surface shear stress, Figure 6.5(a) to (g), improves removal efficiency, even above 40°C. Removal is a far more significant function of temperature than shear stress. At low temperatures, removal is small, and increasing the velocity provides little benefit, (Figures 6.4(b) and 6.6(b)), however at high temperatures removal is significant and increasing velocity increases removal dramatically (Figures 6.6(g) and 6.4(g)).

6.2.4.4 Variation of oil film thickness

The depth of a deposit is an important parameter in cleaning. The effect of increasing the crude oil film thickness upon rinsing has been determined at 50°C, 2 l/min. Results have been produced for the standard surface coverage of 36 g/m^2 with a thickness of 0.04 mm and 51 g/m^2 with a thickness of 0.05 mm, Figures 6.7(a) to (c). In contrast to the preceding sections the overlay plot (figure 6.7(a)) depicts the raw experimental data not the fitted models.

6.2.4.4.1 Discussion

Increasing the surface coverage of crude oil to 51g/m^2 from 36 g/m^2 has no significant effect on the kinetic curves, Figure 6.7(a). Each experimental data point follows the same kinetic curve irrespective of the initial deposit mass. The only discernible difference between the two curves, Figures 6.7(c) and (d), is the initial mass at t= 0. The same model is fitted to each individual set of data. The increased mass of crude oil is simply flushed out in the first few seconds of rinsing. The oil-oil bonding forces

clearly being very weak compared to the oil / substrate bonds. Confirming van der Waals bonding as the main adhesion mechanism.

6.2.4.5 The Age of the Deposit

It is accepted that the longer the period before cleaning the more tenacious the deposit. Several authors have considered this effect but it has not been documented for crude oil deposits. The majority of the cleaning results have been produced 16-18 hours after fouling, unless otherwise stated. As the oil deposit is left in the atmosphere the light ends evaporate (nC_{14} or less) forming a reproducible oil film. The composition of the crude oil deposit has been analysed, results are found in Chapter 5.

A preliminary study of the importance of the age of the deposit on rinsing has been undertaken (figure 6.8(a)-(c)). The crude oil deposits were left in the controlled environment for an extra 24 hours (28-32 hours in total) (figure 6.8(c)). The same average surface coverage was used. The prolonged time did not have a significant effect on the final deposit mass before cleaning.

6.2.4.5.1 Discussion

The crude oil deposit is slightly more difficult to rinse after leaving the deposit an additional 24 hours (figure 6.8(a)). Not only did the mass of the residual layer increase but the time to reach the final level of cleanliness was lengthened. Cleaning after 16-18 hours is 5 wt% more effective in terms of the mass of residual layer compared to leaving it an extra 24 hours.

6.2.4.6 Summary:- The effect of rinsing

The key points are listed below:

- Water is effective at removing crude oil films but will not remove the oil completely, a residual layer always remains. The soil-substrate bonding being much stronger than the soil-soil bonds.
- For effective rinsing the temperature must be 60°C and above, however further increases do provide additional benefit.

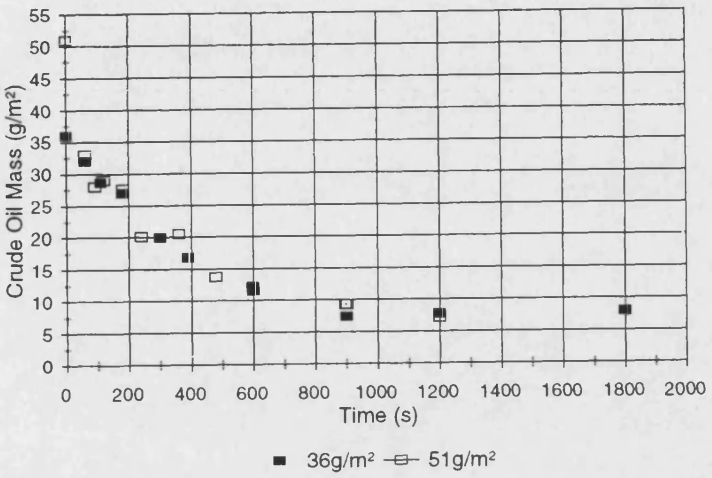

Figure 6.7(a) Overlay plot experimental data

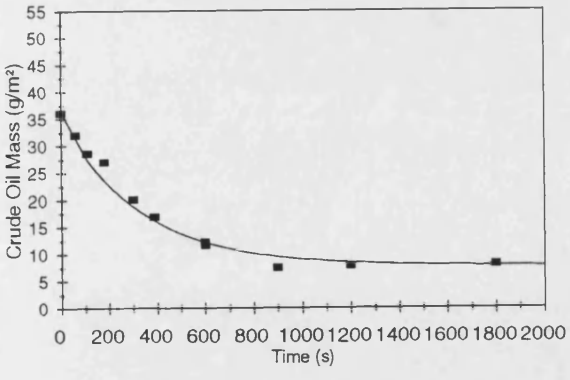

Figure 6.7(b) Coverage 36g/m², thickness 0.04mm

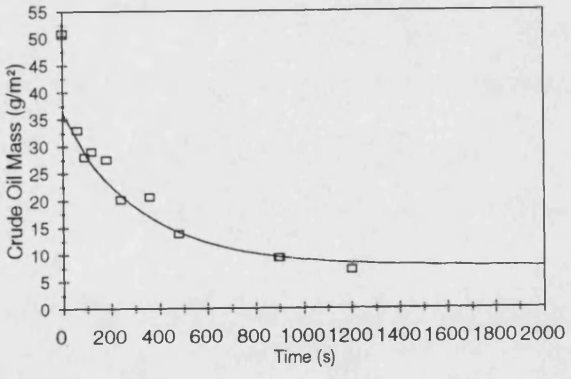

Figure 6.7(c) Coverage 51g/m², thickness 0.05mm

Figure 6-7 Variation of initial crude oil film thickness, 2 l/min, 0.29 m/s, 50°C

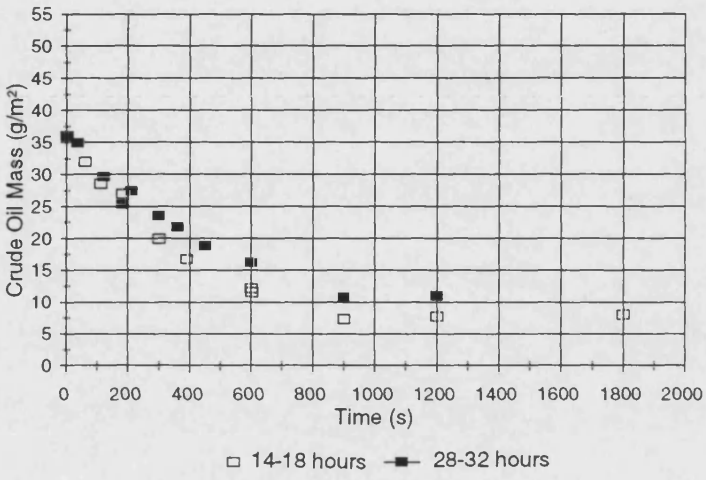

Figure 6.8 (a) Overlay plot: experimental data

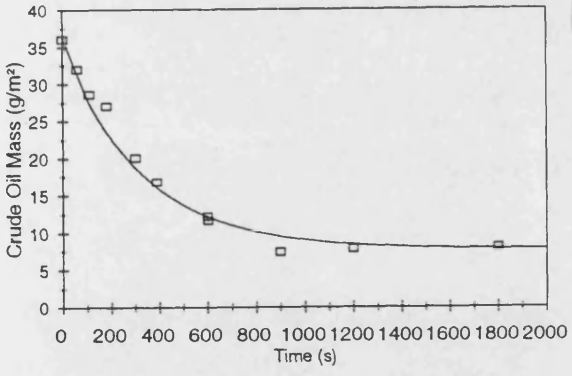

Figure 6.8(b) 14-18 hrs before cleaning

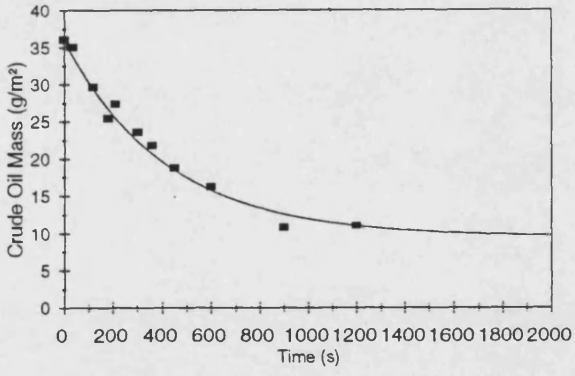

Figure 6.8(c) 28-32 hrs before cleaning

Figure 6-8 The Age of the deposit before cleaning at 2 l/min, 0.29 m/s, 50°C

- No difference was found between the rinsing performance of hard water (600 μS/cm) or reverse osmosis water (20 μS/cm).
- The rate of removal was directly proportional to the flow rate and hence the Reynolds number. During the transition from laminar to turbulent flow, no fluctuations in the linear relationship were apparent.
- Cleaning performance was not proportional to the Reynolds number or the surface shear rate. These parameters cannot be used to uniquely characterise the mechanical effect. Although, above 40°C the mass of the residual oil layer remained constant with constant Reynolds number.
- Removal is a strong function of temperature. The effect of velocity at low temperatures is small and significant at high temperatures.
- Increasing the depth of the oil film by 20% (from 0.04 mm to 0.05 mm) had no significant effect on the removal kinetics. The additional mass was simply flushed out within a few seconds of rinsing. Confirming van der Waals adhesion as the dominant mechanism.
- Increasing the period before cleaning the oil deposit from approximately 16 hours to 24 hours made the deposit slightly more tenacious. The residual layer mass was reduced by 5 wt%.

6.2.5 The Addition of Chemical Additives

Removing a deposit is energy intensive. Energy can be supplied in either thermal, kinetic or chemical forms. The analysis of rinsing has only considered the first two components. Detergents complicate matters by the addition of chemical effects. In the case of oils detergents provide energy in the form of deposit reaction, reduction of interfacial forces or deposit break down. This increases the cleaning power and will therefore reduce the requirement for thermal or kinetic energy or improve the amount and rate of removal.

The additional chemical effect of a nonionic surfactant is complicated, Chapter 4. Firstly, its monomer structure which defines its properties is a function of temperature. Secondly, it exhibits reverse solubility with temperature and finally the applied

concentration will also effect the packing and shape of the micelles formed. Unlike previous surfactant studies the results have investigated these effects over a wide range of temperatures and concentrations on the removal of oily films.

6.2.5.1 The effect of $C_{9\text{-}11}E_6$ concentration and temperature upon removal

The effect of the concentration of the selected surfactant, $C_{9\text{-}11}E_6$, with temperature has been studied in detail at a flow rate of 2 l/min, 0.29 m/s. Analysis has been performed at temperatures of 30, 40, 50, 60, 70, and 80°C over concentrations of 0 (water), 0.001, 0.01, 0.1, 1 to 5 v/v%. Results are presented in numerical temperature order beginning at 30°C in the same format as before with an overlay plot of the modelled data followed by the raw experimental data. The cloud point temperature of the $C_{9\text{-}11}E_6$ is 57°C and the critical micelle concentration is between 0.018 to 0.015 v/v% at 30 to 80°C respectively (Chapter 4).

6.2.5.1.1 Discussion of effect of $C_{9\text{-}11}E_6$ concentration upon removal at 30°C

Figures 6.9(a)-(g) display the change in removal kinetics upon the addition $C_{9\text{-}11}E_6$ at 30°C. Irrespective of concentration, typical removal curves are produced, Figures 6.9(b) to (g). Typically, they can be split up into two regions A and B as discussed earlier in section 6.2.1. Region A depends solely on the fluid dynamics of the cleaning solution and therefore is independent of concentration. Region A removes any loose oil deposits, lasts 300 seconds and removes 6.5 wt% of the deposit at 30°C and 2 l/min. Region B is a function of the applied chemical effect of the solution. On the overlay plot, region A is described by a single line and region B is described by the subsequent division of the line into six separate lines. An immediate saving in detergent volume could be obtained by applying an initial rinse lasting 300 seconds for region A followed by the application of the detergent solution.

Compared to water (figure 6.9(b)) the additional chemical effect always enhances removal (figures 6.9(c)-(g)). Even at concentrations of 0.001 v/v% there is a noticeable improvement in cleaning efficiency. Further increases enhance removal up to 0.1 v/v% whereupon additional surfactant reduces cleaning effectiveness. This reduction in removal with surfactant concentration continues to 5 v/v%, where 5 v/v% is equivalent to a surfactant concentration of between 0.01 and 0.1 v/v%. A surfactant removal optimum has not been published before and for 30°C lies just above the

surfactant cmc of 0.018 v/v% which indicates reduction of interfacial forces plays the key role in removal. Removal occurring below the cmc confirms roll up as the likely removal mechanism.

6.2.5.1.2 Discussion of effect of $C_{9-11}E_6$ concentration upon removal at 40°C

Figures 6.10(a)-(g) display the change in removal kinetics upon the addition $C_{9-11}E_6$ at 40°C. The same phenomena found at 30°C is repeated at 40°C. A concentration optimum exists at 0.1 v/v% lying just above the surfactant cmc of 0.017 v/v%. The effect of $C_{9-11}E_6$ at 40°C is much more pronounced than at 30°C which corresponds to the effect with water alone (Figures 6.4(a)-(g)). The mass of the residual layer compares to 1.8 g/m^2 at 0.1 v/v% and 18 g/m^2 with water (0 v/v%), the dramatic improvement is depicted in Figure 6.10(a). Region A plays a minor part, lasting only 180 seconds and removing 17.8 wt% of the deposit. Cleaning above 0.1 v/v% at 1 and 5 v/v% $C_{9-11}E_6$ does not show such a large decrease in removal but the optimum is still present well defined outside the bounds of experimental error.

6.2.5.1.3 Discussion of effect of $C_{9-11}E_6$ concentration upon removal at 50°C

Figures 6.11(a)-(g) display the change in removal kinetics upon the addition $C_{9-11}E_6$ at 50°C. A concentration optimum also exists although, operating at the higher temperature, 50°C, has shifted the point of maximum removal away from 0.1 v/v% to 1 v/v% $C_{9-11}E_6$ whereupon removal is total. At 50°C the chemical contribution to removal is beginning to become overpowered by the increasing significance of the thermal effect and is therefore less pronounced.

When removal is total, further increases in cleaning efficiency are indicated by a reduction in the overall cleaning time.

6.2.5.1.4 Discussion of effect of $C_{9-11}E_6$ concentration upon removal at 60°C

Figures 6.12(a)-(g) display the change in removal kinetics upon the addition $C_{9-11}E_6$ at 60°C. At concentrations above 0.1 v/v% the surfactant is above its cloud point curve (Chapter 4). Cleaning above the cloud point does not appear to effect the previous trends in removal shown at 30-50°C. The effects of concentration are very similar to those at 50°C, the optimum in removal is still at 1 v/v% $C_{9-11}E_6$ whereupon removal is total. The chemical effect is less significant at the higher temperature with the lines more closely bunched together. 5 v/v% is equivalent to 0.01 v/v% $C_{9-11}E_6$ following

almost the same kinetic curve. 0.01, 0.1, and 5 v/v% kinetic curves produce the same mass of residual layer ($0.8 g/m^2$) however the cleaning time is much shorter at 0.1 v/v% compared to 0.01 and 5 v/v% which are 400 and 750 seconds respectively.

6.2.5.1.5 Discussion of effect of $C_{9\text{-}11}E_6$ concentration upon removal at 70°C

Figures 6.13(a)-(g) display the change in removal kinetics upon the addition $C_{9\text{-}11}E_6$ at 70°C. Applied solutions above a concentration of 0.01 v/v% $C_{9\text{-}11}E_6$ are now above the cloud point curve. No removal optimum is found but whether this is due to the increased significance of temperature shielding the effect or the cloud point curve is not discernible. Increasing concentration to 0.01 v/v% $C_{9\text{-}11}E_6$ completely removes the oil film after 610 seconds. Cleaning at 0.1 v/v% reduces the overall cleaning time to 300 seconds for total removal. Further increases up to 5 v/v% have provided no benefit following the same kinetic curve.

6.2.5.1.6 Discussion of effect of $C_{9\text{-}11}E_6$ concentration upon removal at 80°C

Figures 6.14(a)-(g) display the change in removal kinetics upon the addition $C_{9\text{-}11}E_6$ at 80°C. Applied solutions above a concentration of 0.01 v/v% are now above the cloud point curve and the surfactant and oil system is approaching the phase inversion temperature (PIT). A similar phenomena occurs at 80°C compared to 70°C. Total removal occurs after 570 seconds at 0.01 v/v% and after 300 seconds at 0.1, 1, and 5 v/v%. No concentration optimum exists. Increasing the concentration improves cleaning efficiency up to 0.1 v/v% $C_{9\text{-}11}E_6$ where subsequent increases provide no further benefit.

6.2.5.1.7 Variation of removal rate and residual layer with concentration (30 to 80°C)

The effect on the rate of removal, k, and the mass of the residual layer, A_{res}, with concentration over temperatures of 30, 40, 50, 60, 70 and 80°C is described in Figures 6.15(a) and (b) respectively. In both Figures water is portrayed as a concentration of 0.0001 v/v% to allow direct comparison with the other concentrations. Clearly k and A_{res} are related: as k increases A_{res} decreases.

Operating well below the cmc provides clear improvements in removal over the complete temperature range (30-80°C). Even increasing the concentration from water (0.0001 v/v%) to 0.001 v/v% provides a minimal benefit in removal, at all temperatures (Figure 6.15(a)). The effect upon k on further increases in concentration

is a function of the applied temperature. At 30°C the value of k is maintained whatever the concentration. At 40°C increasing the concentration increases k up to a maximum at 1 v/v% where at 5 v/v% k is reduced. This trend continues with increasing temperature up to 60°C, each maximum more prominent than the last, between 0.1 and 1 v/v%. At 70 and 80°C the maximum in k plateaus with increasing concentration. Operating at 80°C provides only a small benefit in k. The optimum must be due to micelles at low concentrations acting as monomer reservoirs and at higher concentrations hindering removal.

The mass of residual layer, A_{res}, (Figure 6.15(b)) is strongly temperature dependent. The chemical effect becoming more insignificant with each temperature rise from 30°C. Each line becoming more horizontal with each increase in temperature. Dramatic increases in A_{res} are obtained when removing crude oil at 40°C compared to 30°C. Further increases benefit A_{res} but at a reducing rate. The chemical effect is more significant at the lower temperatures with concentration over 30 to 80°C. Removal is strongly dependent on temperature.

As with the rate of removal k, increasing the concentration of the cleaning solution decreases the mass of residual layer, A_{res}, up to 0.1 to 1.0 v/v%. Whereupon subsequent increases in concentration increase A_{res} reduce the mass of the residual layer, confirming the concentration optimum.

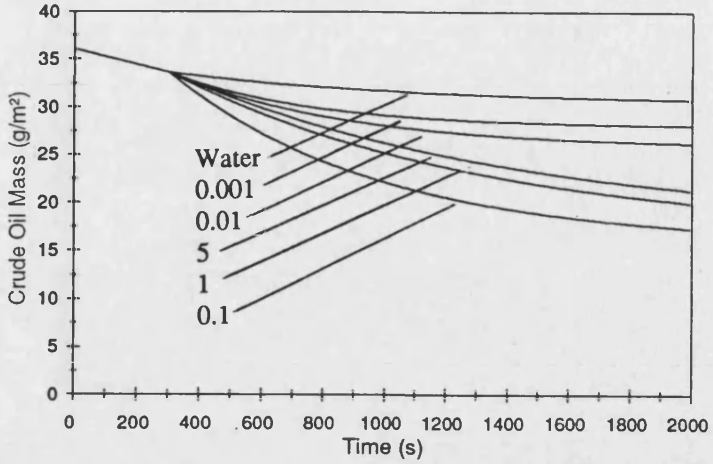

Figure 6.9(a) Overlay plot: model curves from the individual plots Figures 6.9(b)-(g)

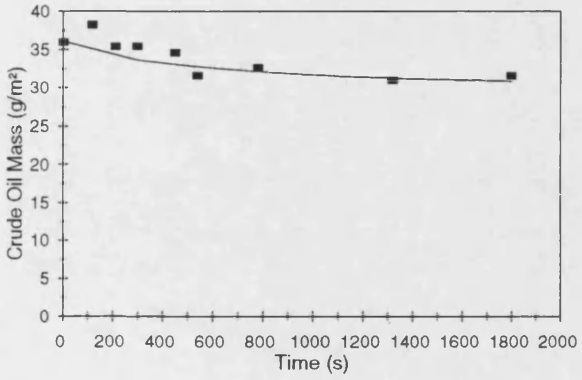

Figure 6.9(b) Water

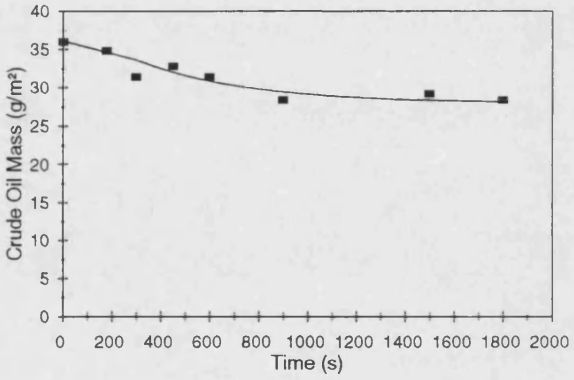

Figure 6.9(c) 0.001v/v%

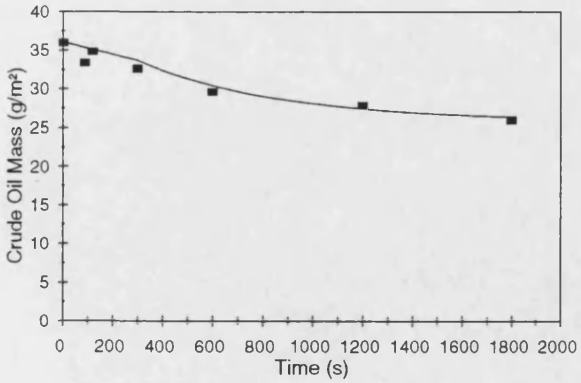

Figure 6.9(d) 0.01v/v%

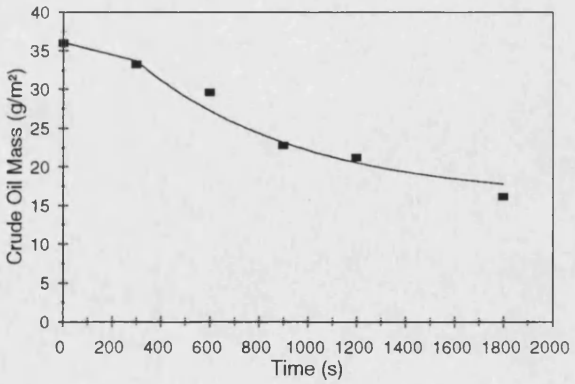

Figure 6.9(e) 0.1v/v%

Figure 6-9 The Effect of $C_{9-11}E_6$ on removal of Crude Oil cleaned at 2 l/min, 0.29 m/s, 30°C

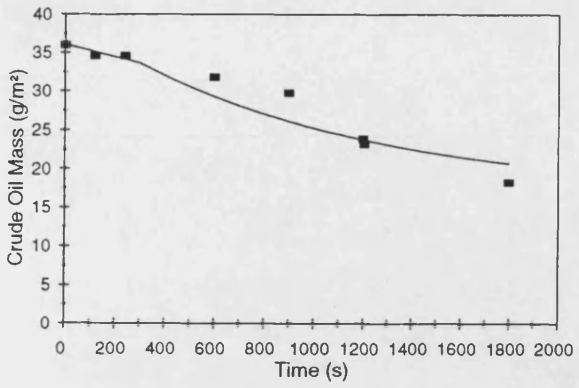

Figure 6.9(f) 1v/v%

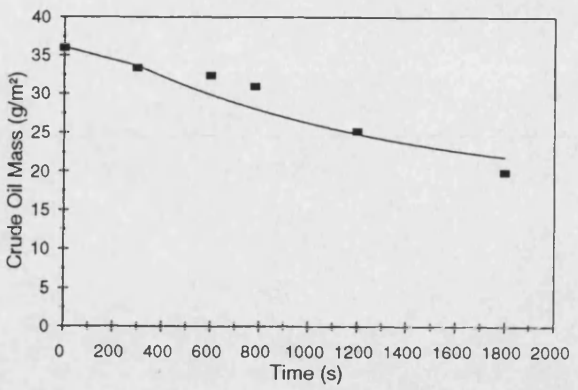

Figure 6.10(g) 5v/v%

Figure 6-9 The Effect of $C_{9-11}E_6$ on removal of Crude Oil cleaned at 2 l/min, 0.29 m/s, 30°C

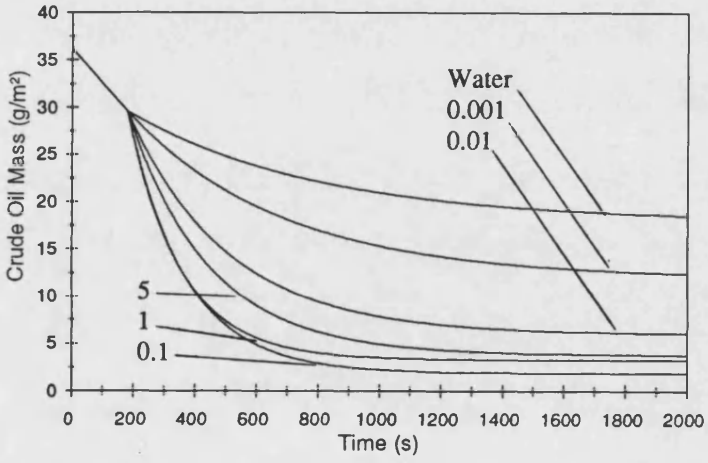

Figure 6.10(a) Overlay plot: model curves from the individual plots Figures 6.10(b)-(g)

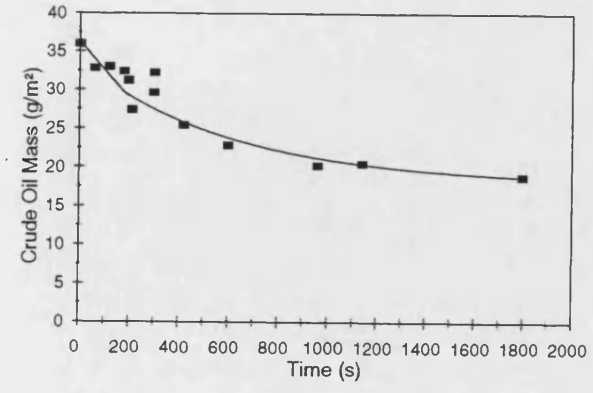

Figure 6.10(b) Water

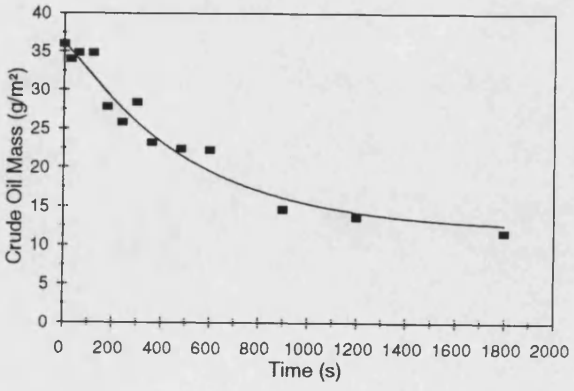

Figure 6.10(c) 0.001v/v%

Figure 6-10 The Effect of $C_{9-11}E_6$ on removal of Crude Oil cleaned at 2 l/min, 0.29 m/s, 40°C

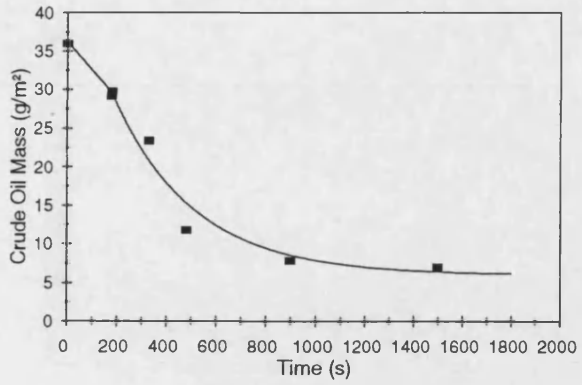

Figure 6.10(d) 0.01v/v%

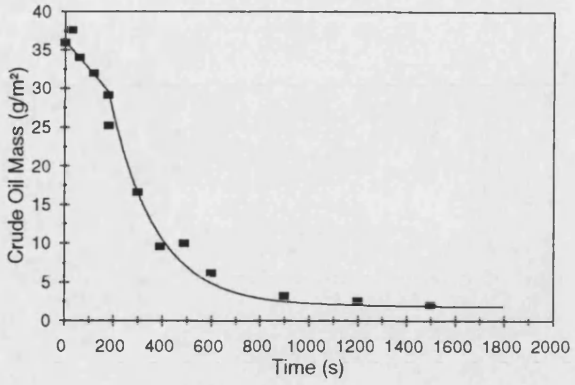

Figure 6.10(e) 0.1v/v%

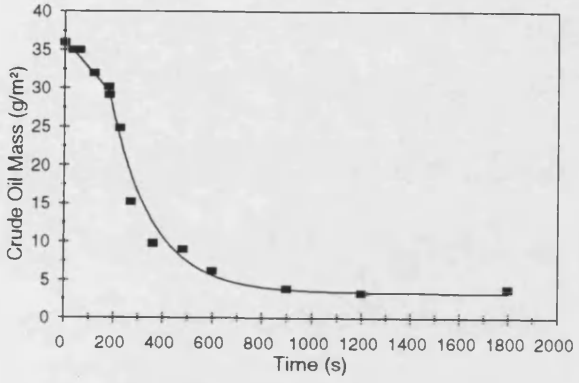

Figure 6.10(f) 1v/v%

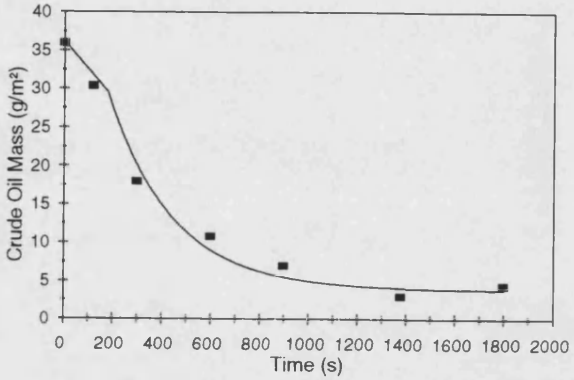

Figure 6.10(g) 5v/v%

Figure 6-10 The Effect of $C_{9\text{-}11}E_6$ on removal of Crude Oil cleaned at 2 l/min, 0.29 m/s, 40°C

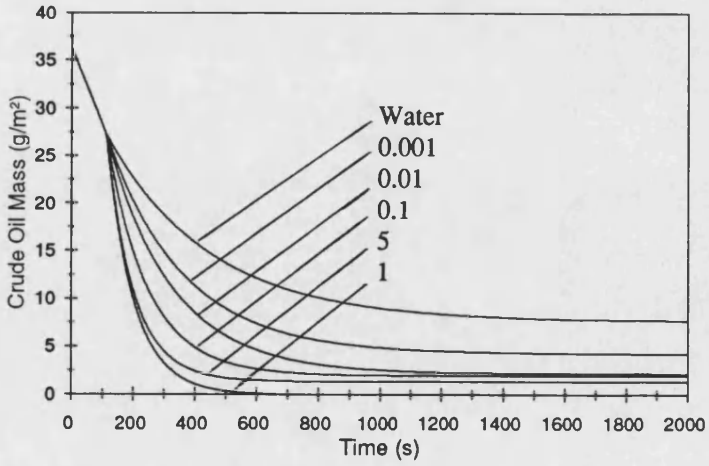

Figure 6.11(a) Overlay plot: model curves from the individual plots Figures 6.11(b)-(g)

Figure 6-11 The Effect of $C_{9\text{-}11}E_6$ on removal of Crude Oil cleaned at 2 l/min, 0.29 m/s, 50°C

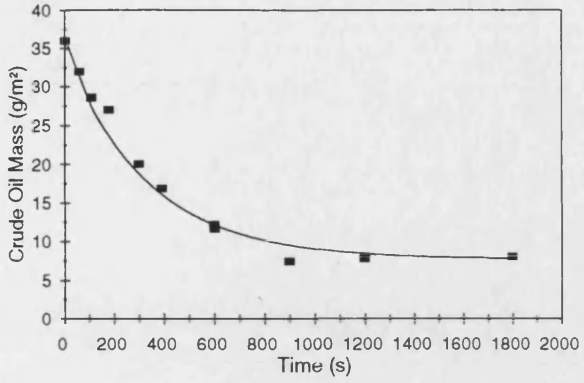

Figure 6.11(b) Water

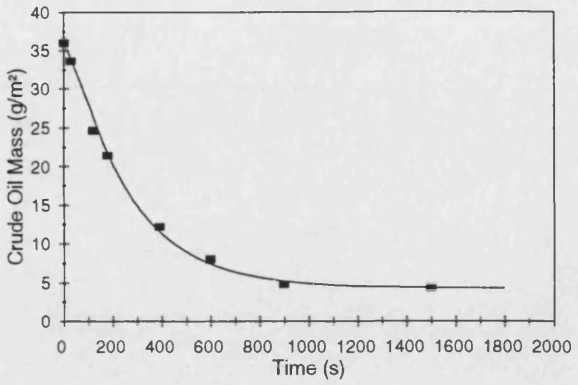

Figure 6.11(c) 0.001v/v%

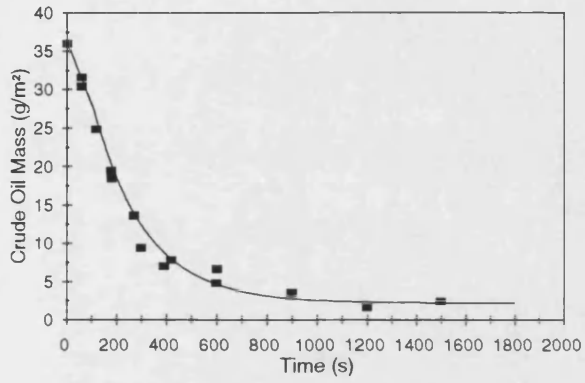

Figure 6.11(d) 0.01v/v%

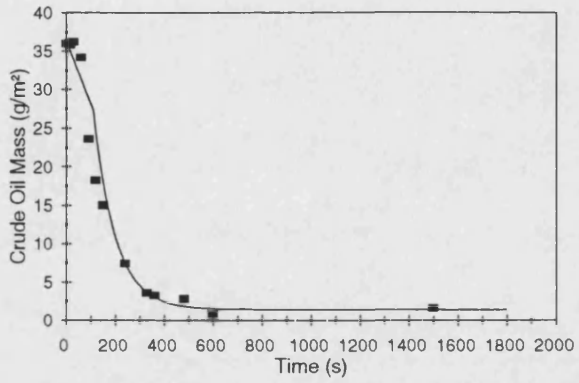

Figure 6.11(e) 0.1v/v%

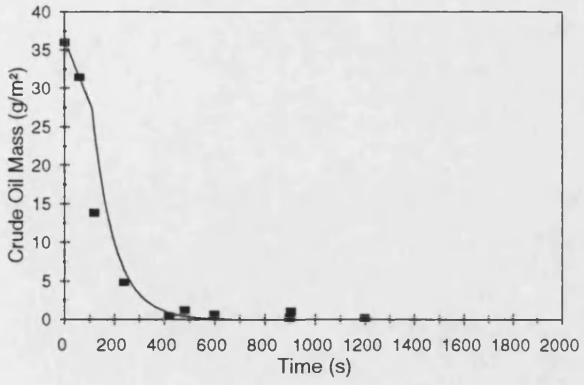

Figure 6.11(f) 1v/v%

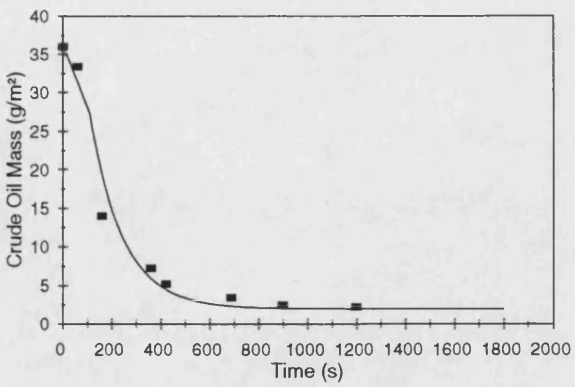

Figure 6.11(g) 5v/v%

Figure 6-11 The Effect of $C_{9-11}E_6$ on removal of Crude Oil cleaned at 2 l/min, 0.29 m/s, 50°C

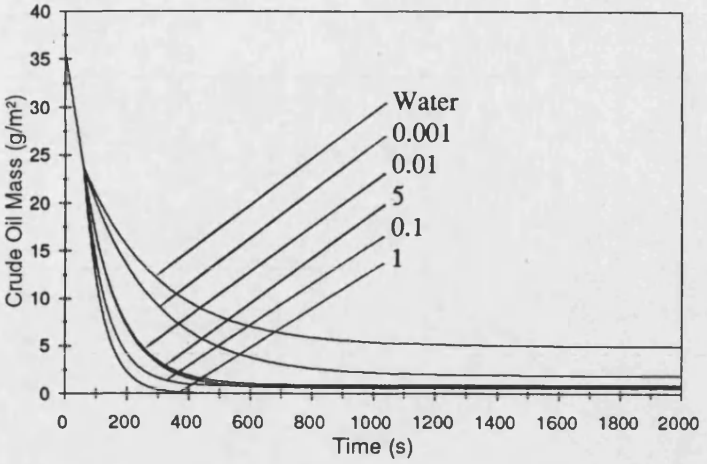

Figure 6.12(a) Overlay plot: model curves from the individual plots Figures 6.12(b)-(g)

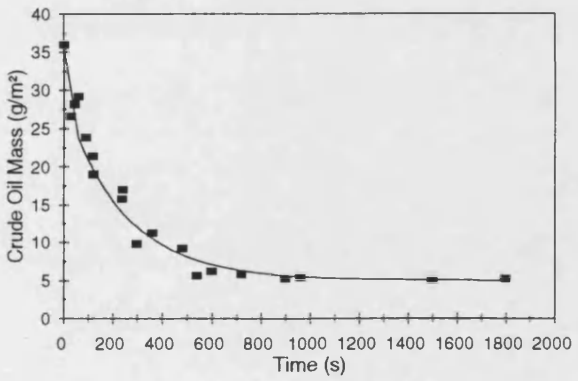

Figure 6.12(b) Water

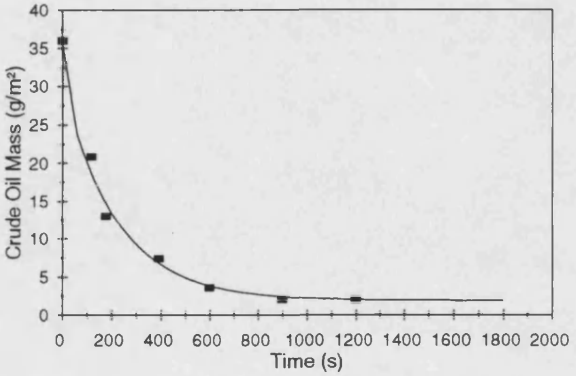

Figure 6.12(c) 0.001v/v%

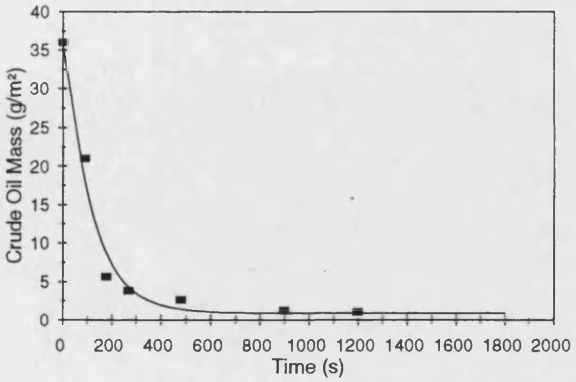

Figure 6.12(d) 0.01v/v%

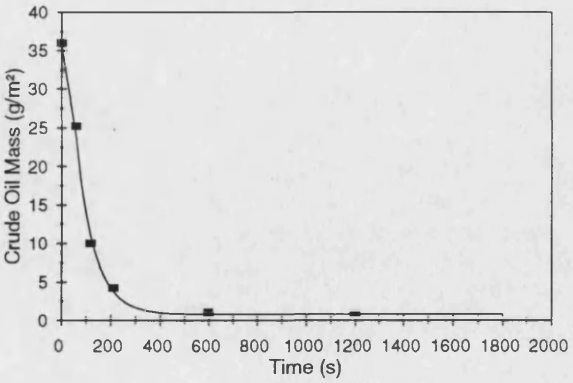

Figure 6.12(e) 0.1v/v%

Figure 6-12 The Effect of $C_{9\text{-}11}E_6$ on removal of Crude Oil cleaned at 2 l/min, 0.29 m/s, 60°C

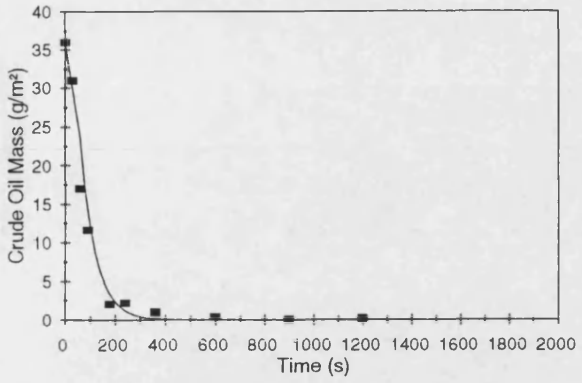

Figure 6.12(f) 1v/v%

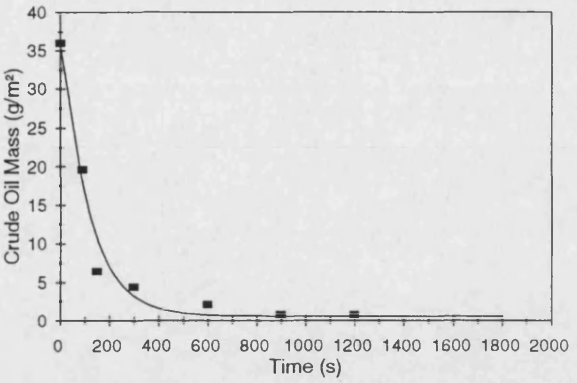

Figure 6.12(g) 5v/v%

Figure 6-12 The Effect of $C_{9-11}E_6$ on removal of Crude Oil cleaned at 2 l/min, 0.29 m/s, 60°C

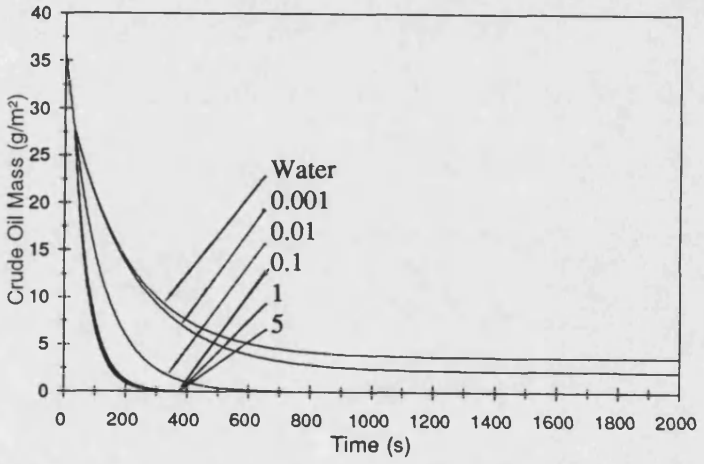

Figure 6.13(a) Overlay plot: model curves from the individual plots Figures 6.13(b)-(g)

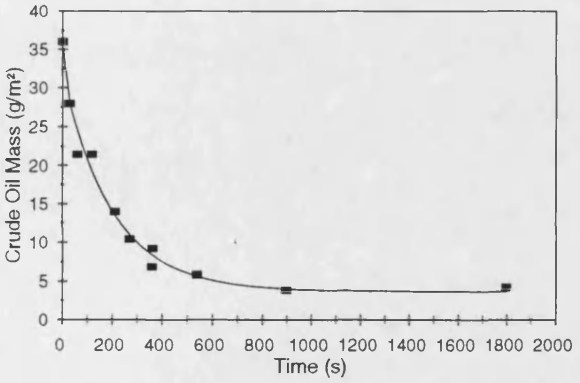

Figure 6.13(b) Water

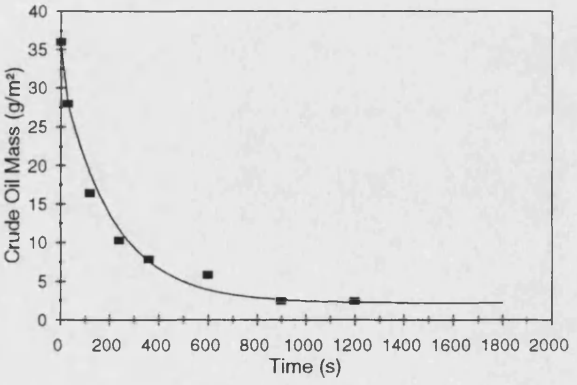

Figure 6.13(c) 0.001v/v%

Figure 6-13 The Effect of $C_{9-11}E_6$ on removal of Crude Oil cleaned at 2 l/min, 0.29 m/s, 70°C

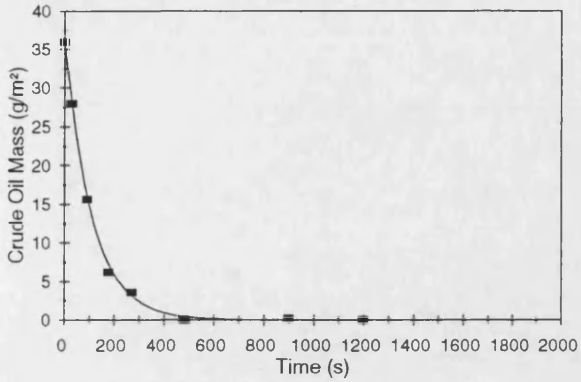

Figure 6.13(d) 0.01v/v%

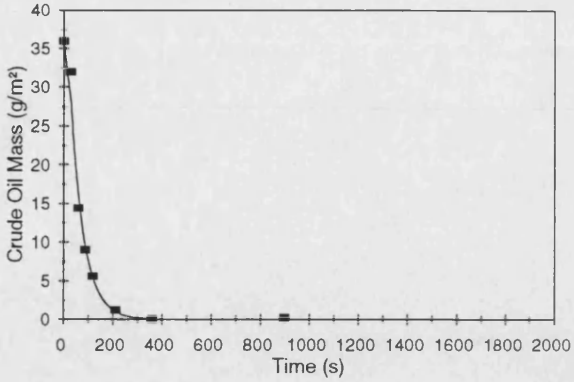

Figure 6.13(e) 0.1v/v%

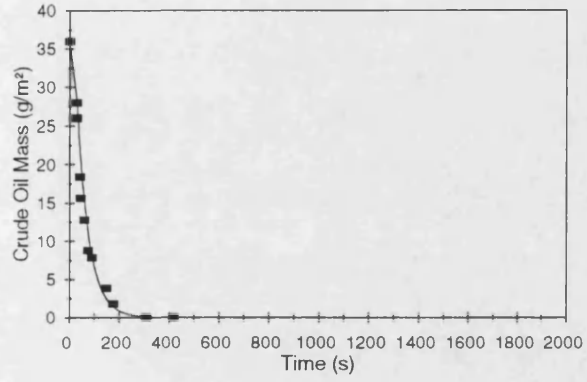

Figure 6.13(f) 1v/v%

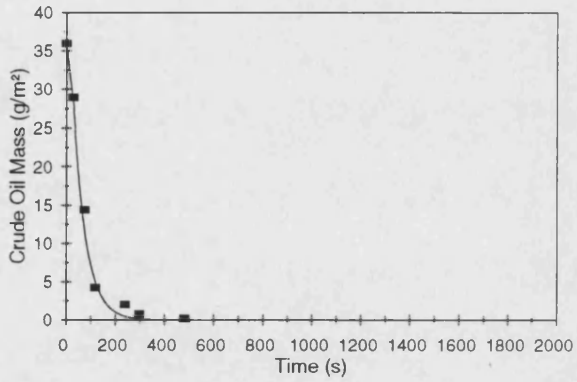

Figure 6.13(g) 5v/v%

Figure 6-13 The Effect of $C_{9\text{-}11}E_6$ on removal of Crude Oil cleaned at 2 l/min, 0.29 m/s, 70°C

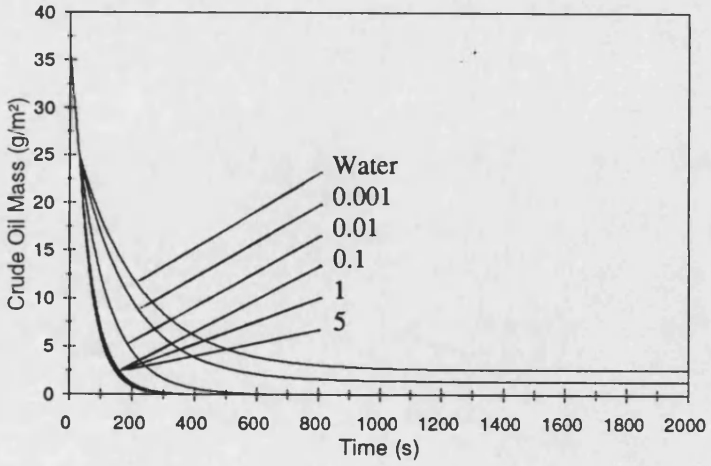

Figure 6.14(a) Overlay plot: model curves from the individual plots Figures 6.14(b)-(g)

Figure 6-14 The Effect of $C_{9\text{-}11}E_6$ on removal of Crude Oil cleaned at 2 l/min, 0.29 m/s, 80°C

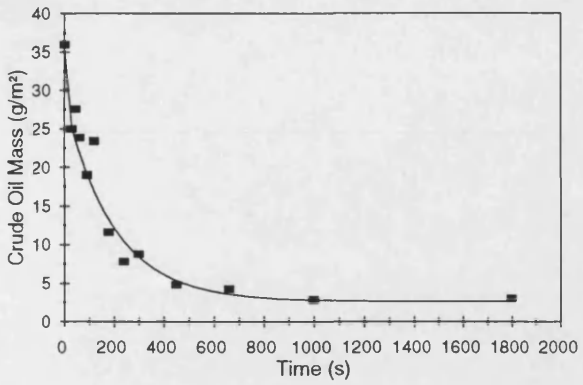

Figure 6.14(b) Water

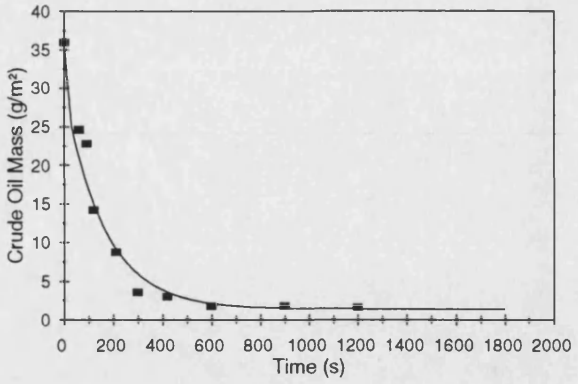

Figure 6.14(c) 0.001v/v%

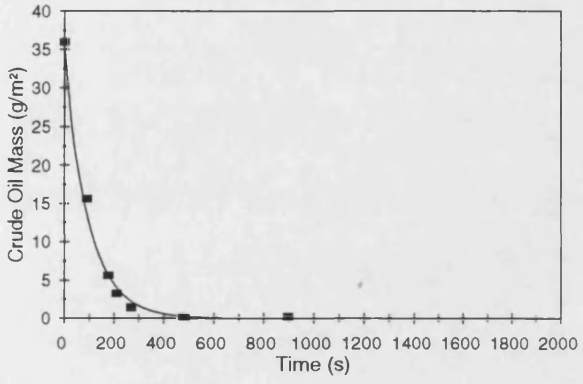

Figure 6.14(d) 0.01v/v%

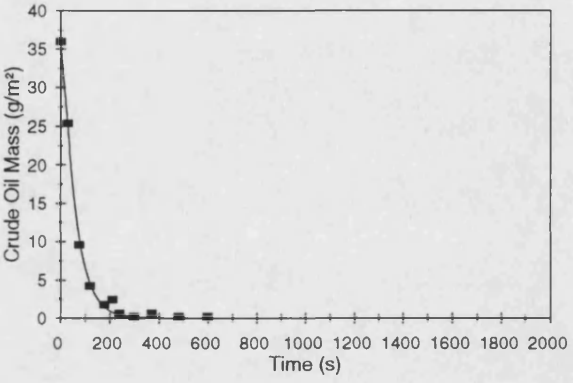

Figure 6.14(e) 0.1v/v%

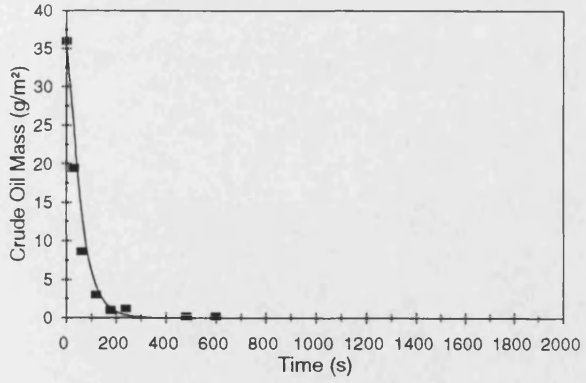

Figure 6.14(f) 1v/v%

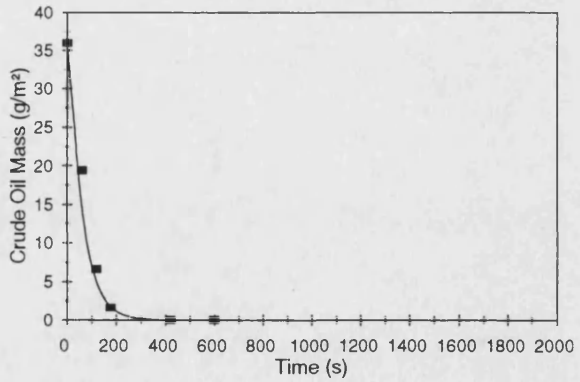

Figure 6.14(g) 5v/v%

Figure 6-14 The Effect of $C_{9-11}E_6$ on removal of Crude Oil cleaned at 2 l/min, 0.29 m/s, 80°C

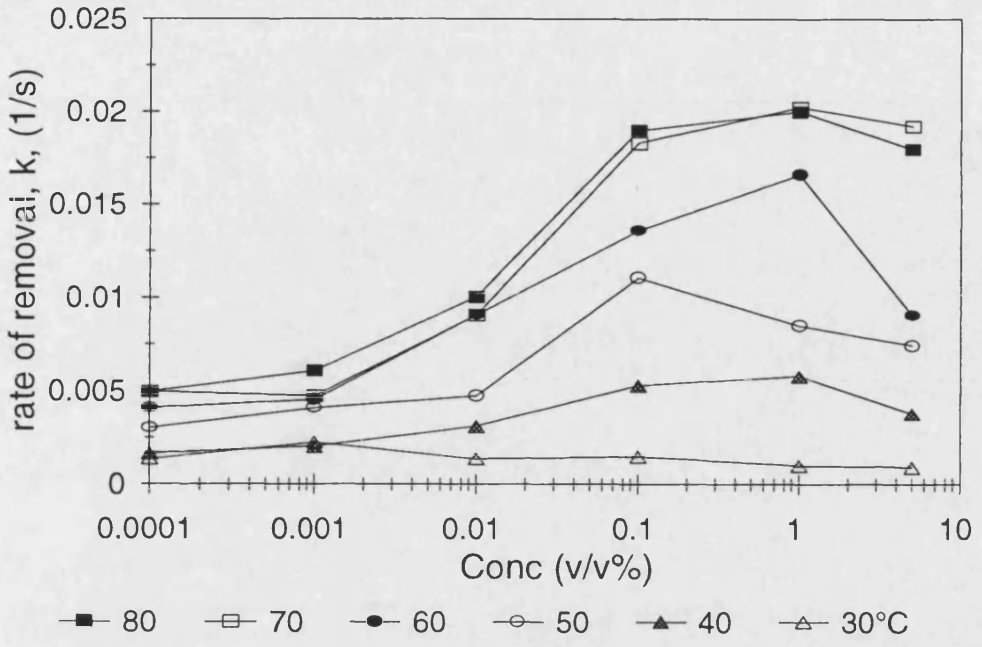

Figure 6.15(a) The variation of removal constant, k, with concentration over 30 to 80°C

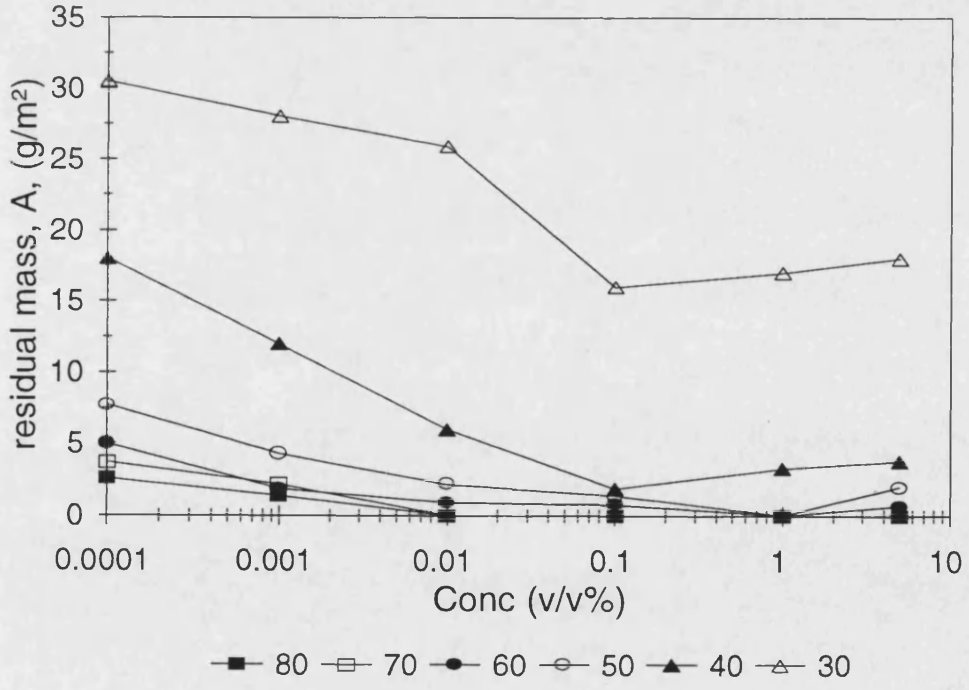

Figure 6.15(b) The variation of mass of residual layer, A, with concentration over 30 to 80°C

Figure 6-15 The variation of k and A_{res} with $C_{9\text{-}11}E_6$ concentration and temperature.

6.2.5.2 The effect of $C_{9-11}E_6$ Velocity upon removal

The importance of surfactant velocity has been investigated. A wide range of velocities has been studied (0.071 to 0.57 m/s) at 50°C and 1 v/v% $C_{9-11}E_6$. Flow rates of 0.5, 1, 2, 3 and 4 l/min with Reynolds numbers of 1440, 2790, 5590, 8380 and 11200 respectively are presented. Results are depicted as an overlay plot Figure 6.16(a) and as individual curves Figures 6.16(a) to (f). Figure 6.16(g) shows the variation of the rate of removal with change in Reynolds number.

6.2.5.2.1 Discussion of results

Increasing the velocity steadily decreases the time to clean. Although increases above 0.57 m/s have minimal effect. At 0.071 m/s the deposit is clean in 1400 seconds, double the flow and the time is reduced by 350 seconds to 1050 seconds.

As with rinsing, the type of flow regime is not significant, a linear relationship between Reynolds number and the rate of removal exists up to 0.57 m/s. Compared to rinsing at 50°C (Figure 6.5), Reynolds number has a more significant effect on the rate of removal, indicated by the steeper gradient (Figure 6.16(g)). Shear forces clearly more significant on the deposit when applying a surfactant solution as opposed to pure water.

6.2.5.3 Summary:- The effect of concentration with temperature

The key points are listed below:

- $C_{9-11}E_6$ was able to completely remove the crude oil deposit giving a 100% clean surface.
- The addition of $C_{9-11}E_6$ was always beneficial to removal irrespective of temperature, compared to rinsing. However, the surfactants effect was much more pronounced at lower temperatures.
- Increasing the temperature consistently improved removal efficiency, the higher the temperature the faster the rate of removal.

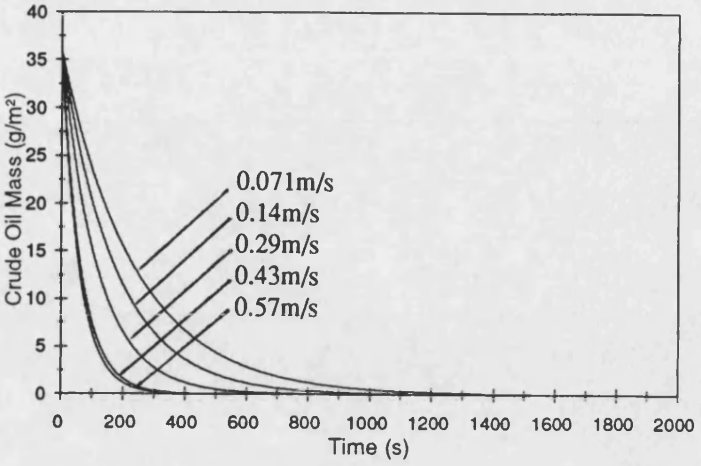

Figure 6.16(a) Overlay plot: model curves from the individual plots Figures 6.16 (b)-(f)

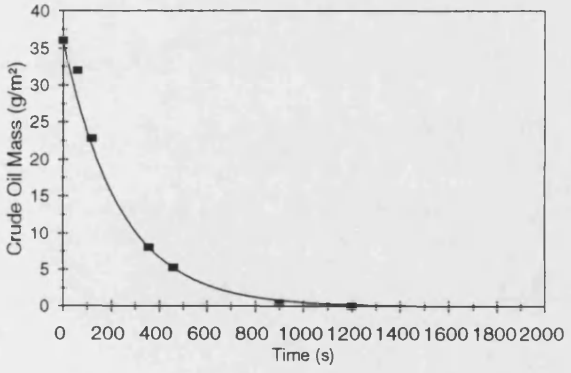

Figure 6.16(b) 0.071m/s, Re=1440, S.S.= 0.029N/m²

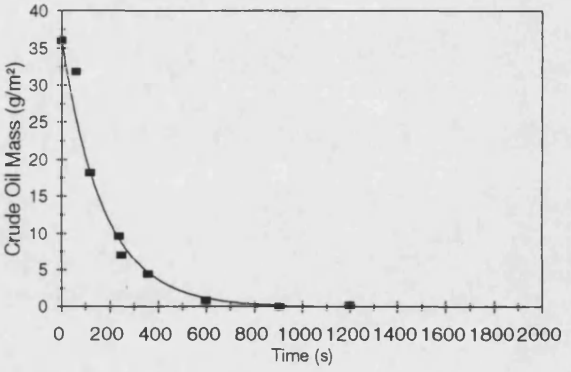

Figure 6.16(c) 0.14m/s, Re=2790, S.S.= 0.11N/m²

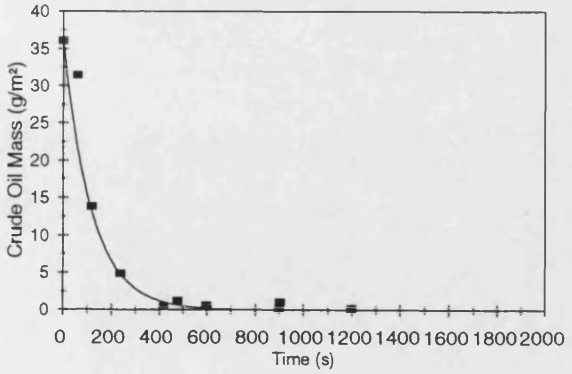

Figure 6.16(d) 0.29m/s, Re=5590, S.S.= 0.37N/m²

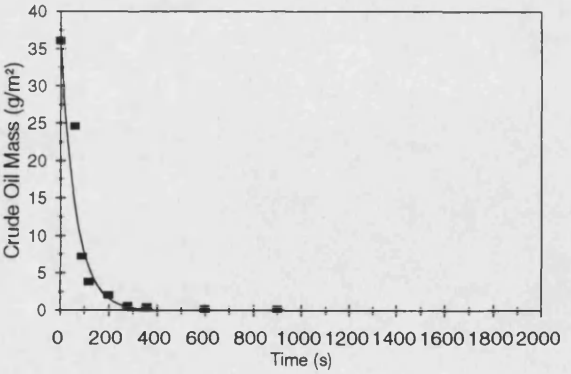

Figure 6.16(e) 0.43m/s, Re=8380, S.S.= 0.75N/m²

Figure 6-16 The Effect $C_{9-11}E_6$ velocity on removal of crude oil cleaned at 50°C

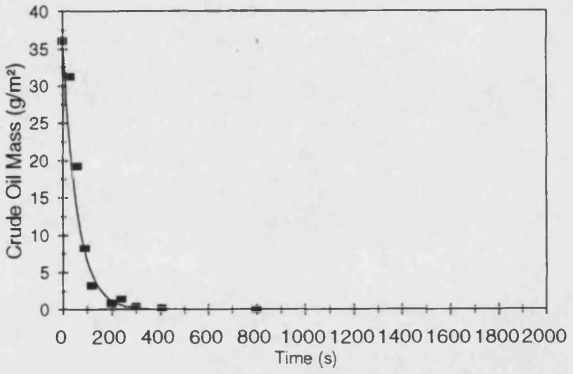

Figure 6.16(f) 0.57m/s, Re = 11200, S.S.= 1.24N/m²

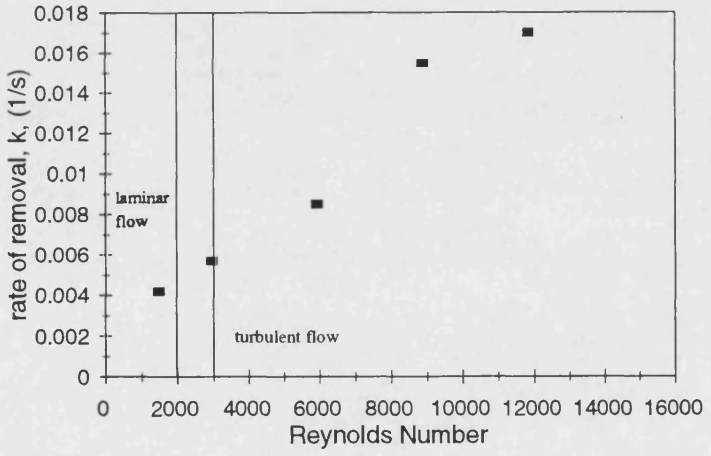

Figure 6.16(g) The Effect of Rinse Water Reynolds no. upon removal rate, k

Figure 6-16 The Effect $C_{9-11}E_6$ velocity on removal of crude oil cleaned at 50°C

- Concentration optima exist at 30, 40, 50, 60°C at 0.1, 0.1, 1.0 and 1.0 v/v% $C_{9-11}E_6$ respectively coinciding with the cmc at temperatures of 30 and 40°C Above 50°C at 1.0 v/v % the crude oil removal was total. At the optimum concentrations a maximum removal rate and minimum residual layers was produced.
- At 70 and 80°C, increases in concentration improved removal efficiency up to 0.1 v/v% $C_{9-11}E_6$ whereupon further increases had no beneficial effect on removal.
- For all temperatures, an initial pre-rinse is recommended to shear off the top layer and provide savings in cleaning chemicals.
- The cloud point curve of the surfactant had no significant effect on removal.
- At 1 v/v% $C_{9-11}E_6$ increasing the velocity steadily decreases the time to clean up to 0.57 m/s and the type of flow regime is not significant.
- Reynolds number and shear forces of 1 v/v% $C_{9-11}E_6$ have a more influential effect on the rate of removal than water alone.

6.2.6 Anionic, Alkali and Commercial Formulations

Commonly available chemical additives and detergents considered effective at oil residual removal have been analysed. The effect of anionic surfactant, an alkali salt and a commercial formulation have been determined. Concentrations similar to those used in industry have been chosen. Sodium lauryl sulphate, the anionic surfactant, was used at 1, 2, and 5 wt% (figure 6.17(d)). Sodium hydroxide (alkali), was used at 3 wt% (figure 6.17(e)) and *Micro* (commercial formulation), was used at 1 and 2 v/v% (figure 6.17(f)). All experiments were performed at a temperature of 50°C and a flow rate of 2 l/min allowing direct comparison with earlier results. Results are portrayed in Figure 6.17(a) - (f) in the same format used previously.

6.2.6.1 The Effect of Chemical Additives

Increasing the concentration of sodium lauryl sulphate from 1 through to 5 wt% has no appreciable effect upon cleaning efficiency (figure 6.17(d)). All the experimental data points produced at the different concentrations lie on the same kinetic modelled curve. The anionic surfactant being only marginally more proficient than rinsing with water alone, Figure 6.16(a). A similar effect was produced using sodium hydroxide

(figure 6.16(e)) although the alkali was even closer in performance to that of water. Sodium hydroxide left a residual layer of 7.5 g/m^2 compared to 7.7 g/m^2 for water and 6 g/m^2 for the anionic cleaner. The commercial formulation (figure 6.16(f)) was dramatically more effective reducing the residual layer mass to 2 g/m^2 and decreasing the overall cleaning time by half of that when rinsing with water. Using *Micro* at 1 v/v% compared to 2 v/v% had no effect on removal kinetics. The non-ionic surfactant (figure 16.6(c)) completely removes the oil film and is clearly the best performer. Although some of the detergents proved similar in performance to rinsing, further the removal mechanisms may prove to be quite different. Further analysis is required using different tube lengths and visual techniques to identify their true performance (Chapter 8).

6.2.6.2 Summary:- The effect of chemical additives

The key points are listed below:

- The non-ionic surfactant $C_{9\text{-}11}E_6$ was the best chemical additive.
- The anionic and alkali cleaners only marginally out performed water rinsing.
- The concentration optima found when using the non-ionic surfactant were not repeated for the anionic or commercial cleaners. Increases in concentration providing no further improvement in removal in these cases.
- The commercial formulation was effective. This could primarily be due to a non ionic surfactant component.

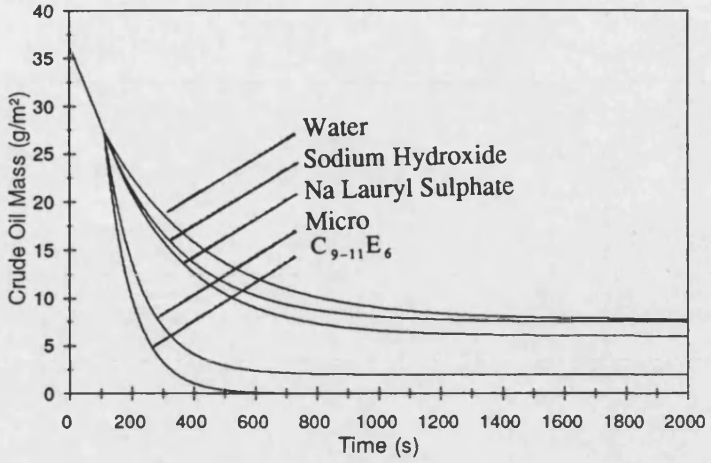

Figure 6.17(a) Overlay plot: model curves from the individual plots Figures 6.17(b)-(f)

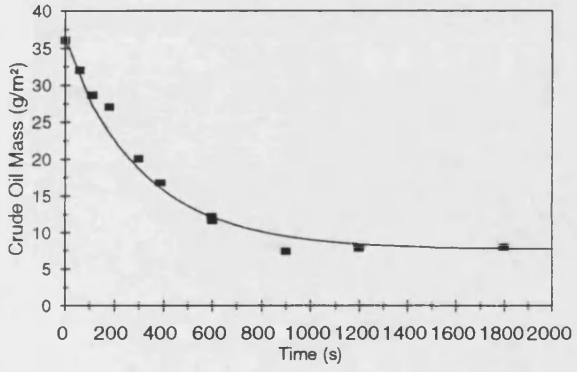

Figure 6.17 (b) Water

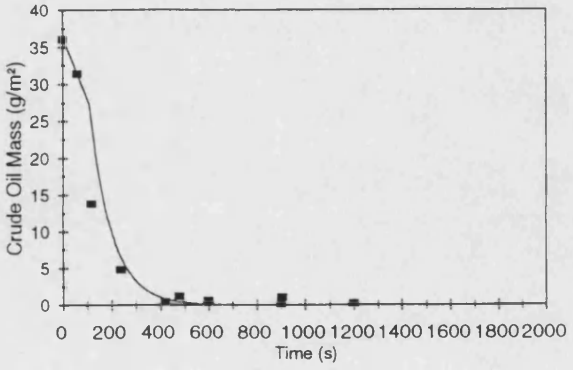

Figure 6.17(c) Non-ionic Surfactant 1v/v%

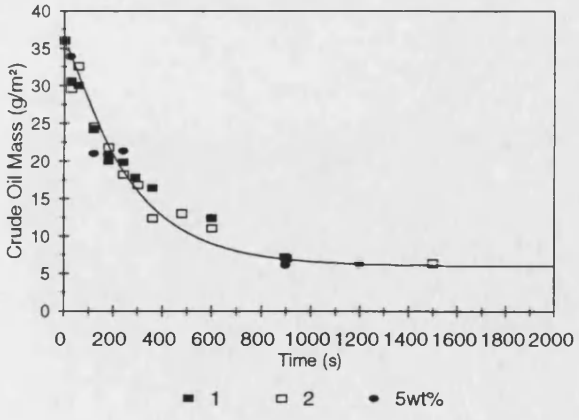

Figure 6.17 (d) Sodium Lauryl Sulphate

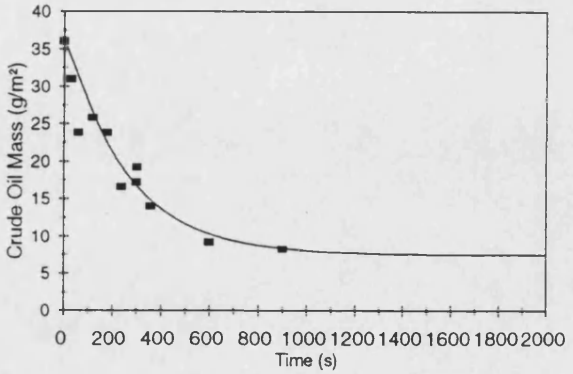

Figure 6.17 (e) Sodium Hydroxide 3wt%

Figure 6-17 The addition of Chemical Additives at 2l/min, 0.29m/s, 50°C

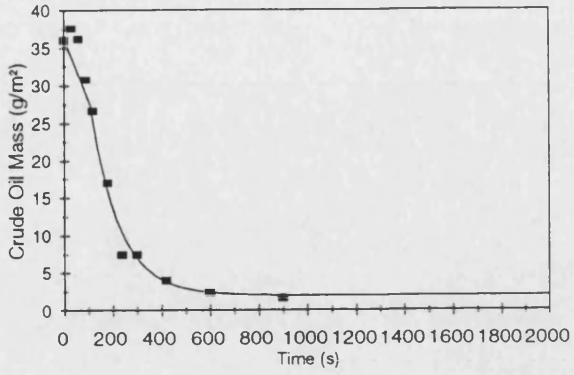

Figure 6.17(f) Commercial formulation- Micro

Figure 6-17 The addition of Chemical Additives at 2 l/min, 0.29 m/s, 50°C

6.3 Qualitative Analysis

Qualitative analysis provides valuable information on the removal mechanisms supplementing the main kinetic quantitative data. Observations involve gas chromatograph (GC) analysis of the oil film deposit during cleaning to investigate the possibility of selective component removal and cleaning process visualisation through advanced video photography to determine any change in deposit structure with cleaning time.

6.3.1 Gas Chromatography Analysis

Since crude oil is a complex mixture of hydrocarbons, application of a cleaning solution is likely to induce selective component removal. The fouled deposit comprises of mainly hydrocarbons with a minimum boiling point equivalent to nC_{14} to boiling points above nC_{44}. Adhesion of each component to the substrate and soil will be different and they will have contrasting solubilities in the applied solution. Selective solubilisation of crude oil has also been reported before but not in cleaning applications.

Using the same cleaning analysis procedure (described in Chapter 5, section 5.3.6) except rotating the centrifuge tube containing the test piece at 5,000 rpm for 5 minutes, samples of oily deposit after cleaning are obtained. The oil can then be diluted to a 90% solution of hydrogen disulphide and injected in the GC (Chapter 4).

The unedited chromatograms and their calculated percentage residue are depicted to compare for any crude oil composition change since boiling point distribution curves (ASTM D5307 [1992]) could hide small differences in composition. The analysis technique determines the overall composition of any oil remaining on the surface of a test piece after cleaning rather than the composition of the top surface of the oil (Chapter 4 and Appendix A).

Analysis has concentrated on the composition of the residual layer which remains when rinsing and under certain conditions of surfactant application. The composition of the residual layer was examined at 50, 60, 70 and 80°C at 2 l/min rinse water and 40, 50 and 60°C 0.1 v/v% $C_{9\text{-}11}E_6$ at 2 l/min. Two example chromatograms are presented: Figure 6-18 was determined after rinsing for 45 minutes at 2 l/min 80°C and Figure 6-19 was produced after 20 minutes cleaning with 0.1 v/v% $C_{9\text{-}11}E_6$ at 2 l/min at 50°C. A chromatogram of the crude oil before cleaning is depicted in Figure 5.4, Chapter 5. Results show no discernible change in deposit composition with cleaning time. Not only do the chromatograms appear identical to the chromatogram produced before cleaning but the calculated percentage column residues are also of the same magnitude.

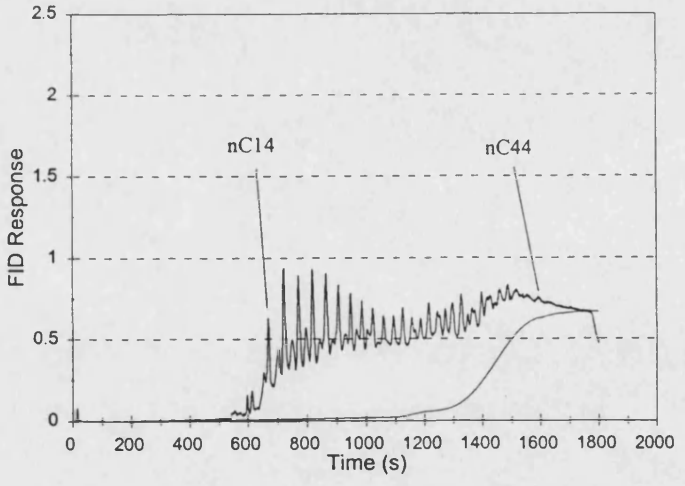

Figure 6-18 Gas Chromatogram of residual layer, rinsed for 45 mins at 2 l/min

Crude Oil Residue = 45%

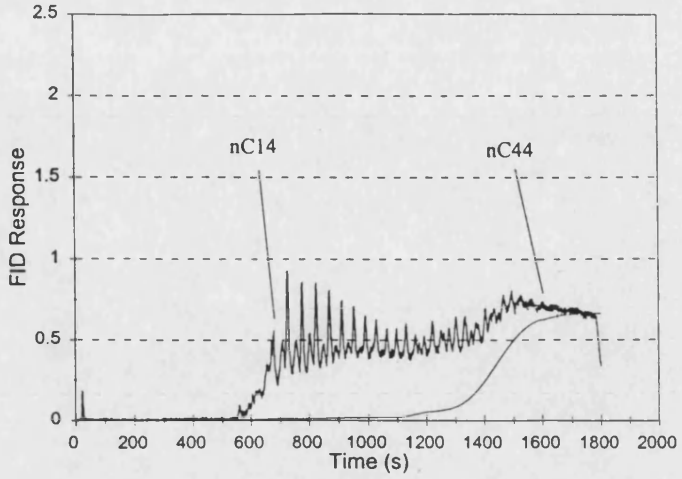

Figure 6-19 GC of residual layer, cleaned with $C_{9-11}E_6$ 0.1 v/v% for 20 mins at 2 l/min

Crude Oil Residue = 48%

6.3.2 Process Visualisation

There is little published work on direct visualisation of the cleaning process. The experimental apparatus developed allows advanced video photography of the cleaning process to take place using a glass cell (figure 5.6, Chapter 5). As described in Chapter 5, semi-circular test pieces are fouled with crude oil and left for 16 to 18 hours. Smooth films with a surface coverage of between 33.6 and 38.4 g/m^2 are accepted and ready for positioning in the glass cell. Cleaning is then observed over a wide range of conditions. The process was examined using water, $C_{9-11}E_6$ and *micro* at 50°C and 2 l/min. $C_{9-11}E_6$ was investigated at concentrations of 0.001, 0.01, 1, and 5 v/v% and micro at a concentration of 2 v/v%. Difficulty was found in providing conditions of minimal reflection especially from the glass cell and an even light distribution.

Removal was recorded using a betamax video recorder, enabling high quality stills to be photographed at specific periods of the cleaning process. Figure 6-20 shows a photograph of the smooth stainless steel surface of the test piece. Figure 6-21 portrays the surface fouled with crude oil (36 g/m^2). For an idea of scale the test piece width is 0.5 inch. The fouling is uniform but the lefthand side is lit more strongly than the right. The evenly spread white dots are small droplets of oil which reflect in the strong light.

Figure 6-20 Clean Test Piece

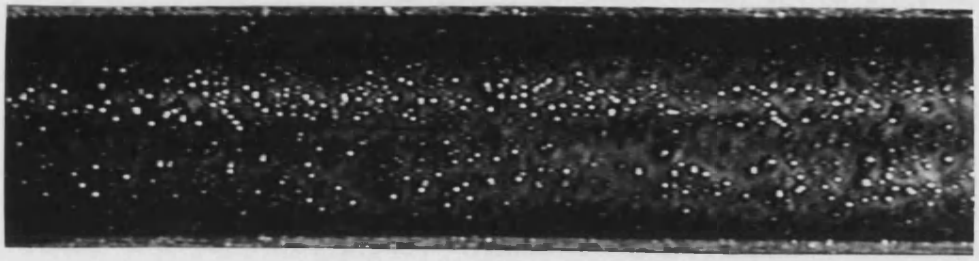

Figure 6-21 Crude Oil Fouled Test Piece

6.3.2.1 Water Removal

Figures 6-23(a) to (d) depict the effect of water on the crude oil film. Water is applied at 50°C and 2l/min and points where the photographs were taken are represented as black squares on the removal curve in Figure 6-22. Initially a small amount of loose material is flushed from the film this is seen as small droplets sheared from the surface.

Figures 6-23(a). The deposit then begins to open up and thin longitudinal streaks which cover the complete length of the test piece appear along the surface of the deposit,

Figures 6-23(b). The oil film, although uniform, has an uneven surface and the streaks tend to originate from areas of plentiful crude. The areas in between the streaks still have a thin oil film which is indicated by a light brown colouration

As cleaning progresses, after 400 seconds (Figure 6-23 (c)), the strands become thicker and it becomes clear that the oil is rolling along the surface of the test piece. The direction of the flow is from right to left. The strands follow channels of oil that remain from previous strands. The process is analogous to rain water driven along the side window of a car by turbulent air currents, following the previous trails of water. There is no droplet removal and the surfaces in between the strands remain discoloured. Removal is non-uniform, areas to the right having less oil deposit.

The rate of oil progression reduces at a decreasing rate. After 1000 seconds (Figure 6-23 (d)) movement is minimal and a thin residual layer remains. The trails can still be made out but only a small thickness of oil remains.

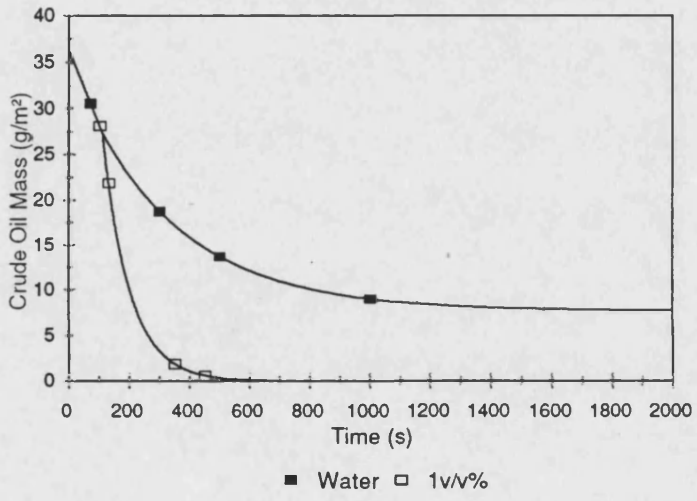

Figure 6-22 Points along Removal Curve where Pictures were taken, 50°C, 2 l/min

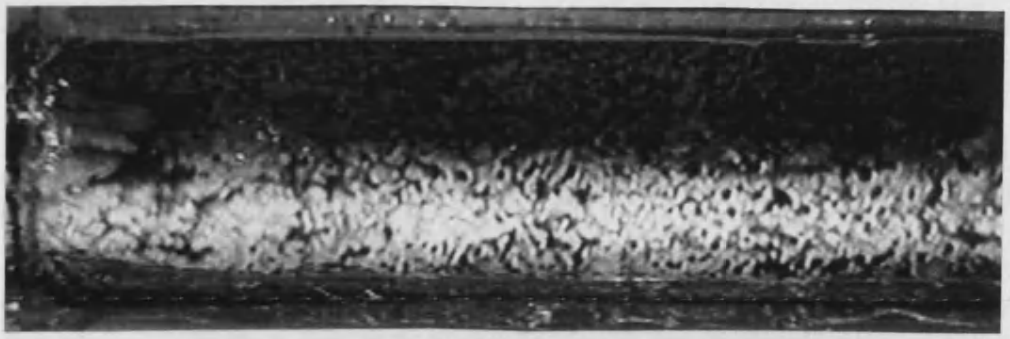

Figure 6-23(a) Crude oil removal by water after 70 seconds

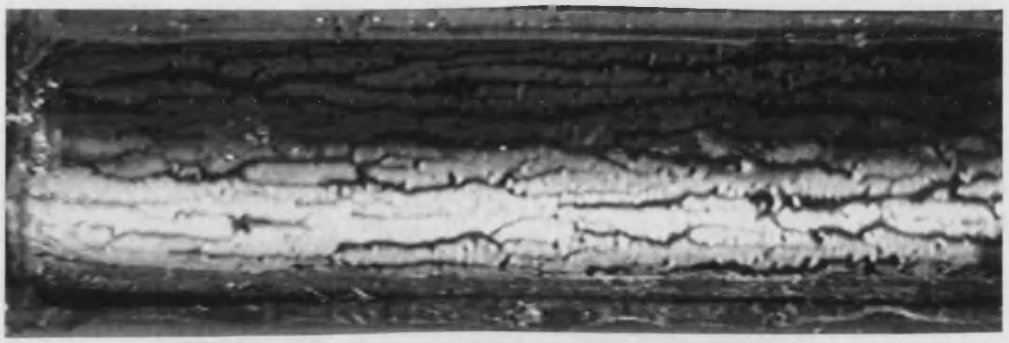

Figure 6-23(b) Crude oil removal by water after 300 seconds

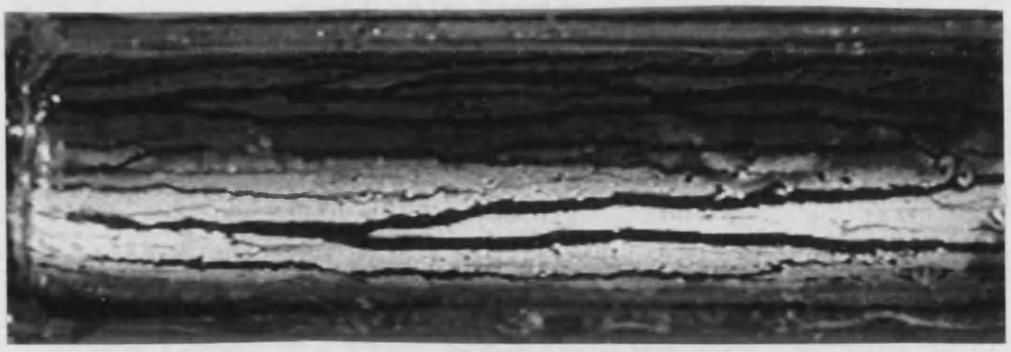

Figure 6-23(c) Crude oil removal by water after 500 seconds

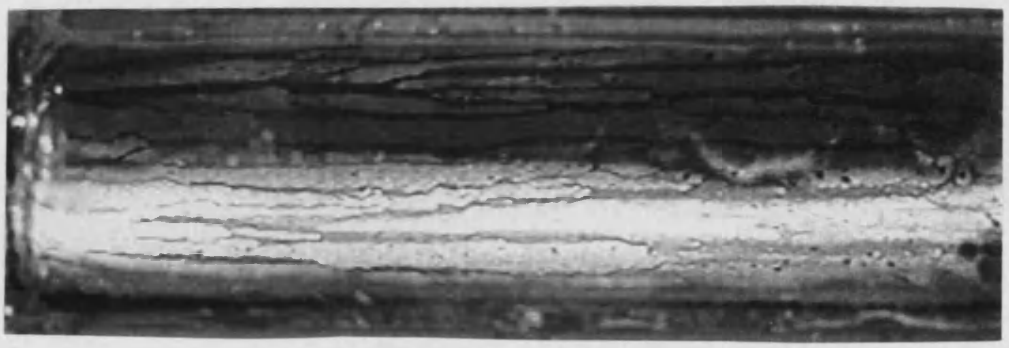

Figure 6-23 (d) Crude oil removal by water after 1000 seconds

Figures 6-23(a) -(d) Photographs of crude oil removal by water, 2 l/min, 50°C

6.3.2.2 Surfactant Removal

The addition of a surfactant has a dramatic effect on the removal mechanisms. Figure 6-24(a) to (d) display photographs of the oil film taken during cleaning with 1 v/v% $C_{9\text{-}11}E_6$ at 2 l/min at 50°C. The points at which the photographs were taken are represented as rectangular outlines on the removal curve in Figure 6-22. After 100 seconds of surfactant cleaning an immediate difference to rinsing mechanisms is apparent, (Figure 6-24(a)), the oil film forms a cobweb like structure. Strands appear as before, but they are much shorter and follow a variety of directions instead of solely following the direction of flow. At the extreme, strands are even at right angles to the direction of flow. As with rinsing the strands originate in area of high oil coverage. They tend to twist and turn as opposed to being straight in nature. The oil still rolls along the short strands but at the corners and ends of the strands droplets are removed which are approximately 0.1 mm in diameter. The size of droplet removed is proportional to the strand thickness. The thicker the strand the larger the droplet diameter. Unlike rinsing, the strands do not progress along the length of the tube. The difference in strand structure compared to rinsing explains why when using a surfactant the rate of removal is more sensitive to shear forces. When using a surfactant the deposit structure becomes much more open and exposed to the fluid flow.

After 170 seconds of further cleaning (400 seconds in total, Figure 6-24(c)) a significant proportion of oil has been removed. Remaining strands are much thinner and more longitudinal in nature. Strands pointing at right angles to the direction of flow having are removed first. Removal is uniform, and unlike rinsing the areas between the strands are shiny and clean indicating the absence of oil.

After 450 seconds of cleaning, the substrate is almost free from oil. Only a further 150 seconds is required for complete removal.

Figure 6-24(a) Crude oil removal by 1v/v% $C_{9-11}E_6$ after 100 seconds

Figure 6-24(b) Crude oil removal by 1 v/v% $C_{9-11}E_6$ after 130 seconds

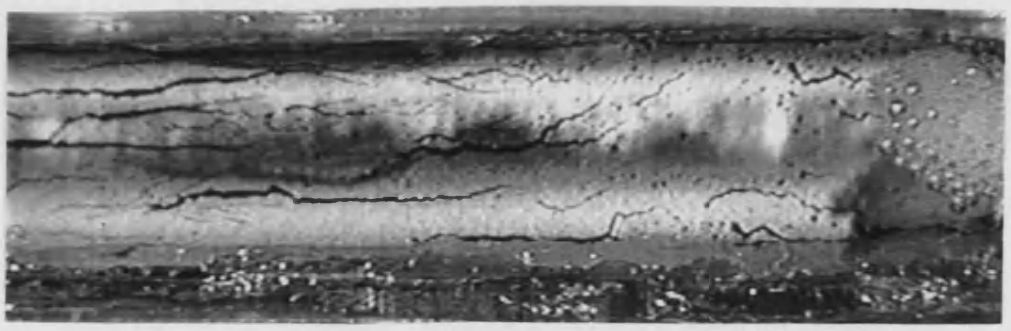

Figure 6-24(c) Crude oil removal by 1 v/v% $C_{9-11}E_6$ after 400 seconds

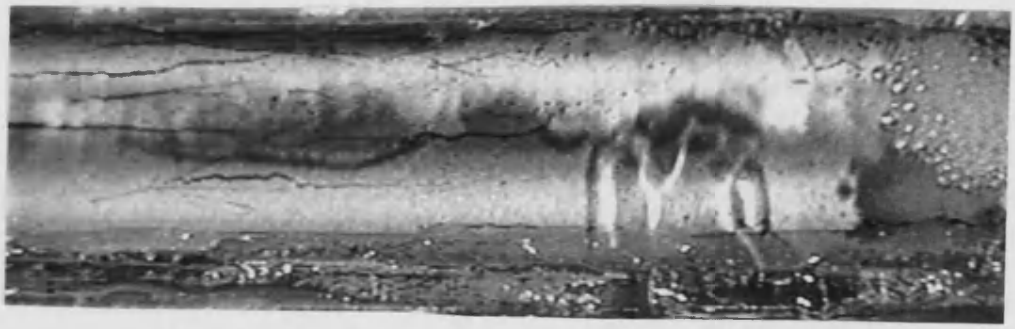

Figure 6-24(d) Crude oil removal by 1 v/v% $C_{9-11}E_6$ after 450 seconds

Figures 6-24(a) to (d) Photographs of crude oil removal by 1 v/v% $C_{9-11}E_6$, 2 l/min, 50°C

Increasing the surfactant concentration above 5 v/v% $C_{9-11}E_6$ has little additional visible effect upon removal. The oil film strands into cobwebs like those similar to those seen when cleaning at 1 v/v% $C_{9-11}E_6$. Removal is through droplets. Yet, after prolonged cleaning thin residual strands remain. Decreasing the concentration to 0.1 v/v% $C_{9-11}E_6$ has the same effect as cleaning at 5 v/v%. However, cleaning at 0.01 and 0.001 v/v% $C_{9-11}E_6$ has a more pronounced effect. The cleaning transitions from the observed removal pattern seen at 1 v/v% $C_{9-11}E_6$ to that seen when cleaning with water. The strands become longer and thicker with decreasing concentration and increasingly they are in the direction of the flow. The strands progress along the substrate surface and a decreasing portion of the oil can be seen to be removed by droplets. The portion of oil removed through droplets as opposed to rolling along the surface is very difficult to determine.

6.3.2.3 Removal Mechanisms

Clearly solubilisation does not play an important role in the removal process, removal occurring below the cmc and through droplets, leaving roll-up and emulsification as likely alternatives. In the presence of surfactants removal is through roll-up. The difference between the water and surfactant is its effectiveness as a wetting agent. Since the surfactant prefers the wet substrate more than the oil, the oil cannot roll along the surface and is therefore removed. In the case of water, the oil prefers to wet the substrate rather than the water and the oil will progress along the substrate with no tendency to be removed as a droplet. Removal is sensitive to shear forces and in their absence removal will be zero. The optimum surfactant will be one that is the most effective wetter of the surface.

6.4 Experimental Discussion

Visualisation of the cleaning process is paramount. From the kinetic data, water appears to be fairly effective at removing the bulk of the crude oil film. However, in reality oil is simply pushed along the surface of the substrate by the applied shear force of the solution. The addition of a good wetting agent changes the mechanism and rolls up the oily soil enabling droplet removal in the bulk flow. Longer test pieces would enhance this difference in removal mechanisms and efficiency. The surfactant would maintain the same rate of removal and the rinsing would exhibit a much reduced

removal rate compared to the shorter tubing. Roll up of oily soils has been shown many times before (Thompson [1994], Kao et al [1989], Otani et al [1985], Saito et al [1985], Aronson et al [1983] and Dillan et al [1979]).

Results show optimum surfactant removal in the region and above the cmc and linked to the reduction of interfacial forces. The presence of micelles acting as monomer reservoirs. Relationships between interfacial tensions, removal and droplet contact angle have been reported many times before. But unfortunately these cannot be generalised and depend on the surfactant system (Thompson [1994]). This work agrees with the that of Prieto et al [1996] who related the optimum spray cleaning of oven baked oily soils from stainless steel to a minimum in dynamic surface tension. No mechanisms were proposed but roll up would appear likely. The wetting of the oil to the substrate is the key parameter but it is dependent on the electrostatic, van de Waals and structural forces. The electrostatic forces are in turn a function of the oil composition and the type of substrate (Hirasaki [1988]).

Very few authors have considered the effect of surfactant concentration upon cleaning performance. The effect of temperature has generally been considered, often the effects are much more pronounced. There is also little information published on cleaning below the cmc especially with nonionic surfactants. Cleaning studies carried out below the cmc can give important mechanistic information as to the significance of solubilisation. Beaudoin et al [1995] found effective removal of flux residues from rotating disks using nonmicellar solutions but the concentration was very close to the cmc and could be due to monomer dimer and trimer formation. The authors found that increasing the concentration well above the cmc improved the rate of removal still further but reported no optimum. These findings can be contrasted with the kinetic data produced when using $C_{9\text{-}11}E_6$ in this thesis. However, Koretskii et al [1984] studied five nonionic surfactants over a wide range of concentrations for the removal of oily soils from steel plates. For four of the surfactants removal increased with increasing concentration above the cmc but for the remaining surfactant removal increased up to the cmc, with no additional benefit resulting from further concentration increases. Performances could be related to the greatest lowering of interfacial tensions and micellar shape. The remaining surfactant also exhibited the

greatest lowering of interfacial tension at the cmc. Unfortunately no visual study of the mechanisms of removal was undertaken.

Explaining the low temperature optimum in surfactant concentration found at the cmc is difficult. First thoughts are that the removal at high concentrations could be diffusion limited by the presence of a large proportions of micelles. However, the rate limiting step has been identified (see Chapter 7) and even at conditions of high flux, diffusion is not the limiting step. It is also unlikely to be due to the monomer/micelle equilibrium relationship shown in Figure 6-25 because the concentration optimum was reported above the cmc and micelles contribute to removal. The optimum must be due to a high concentration of micelles hindering the kinetics of roll up at the interface.

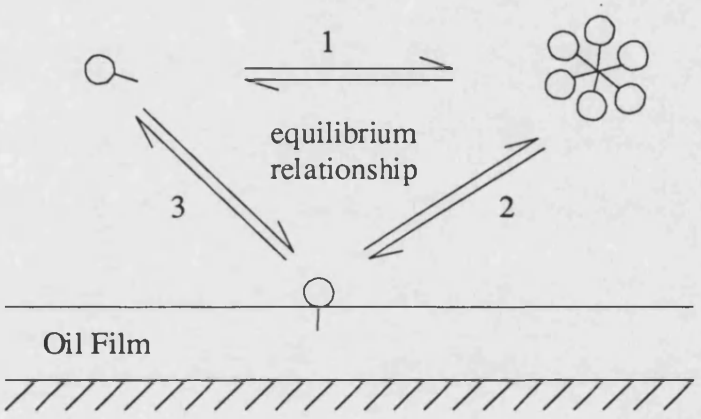

Figure 6-25 Monomer/Micelle Equilibrium Relationship

The effect of temperature upon removal is well documented. Recent authors agree that optimum removal occurs at the phase inversion temperature (PIT) rather than the cloud point. Unfortunately the PIT cannot be calculated for the crude oil $C_{9\text{-}11}E_6$ system but it is often found to be 20°C above the cloud point which would make it approximately 80°C. The results in this thesis agree with the PIT optimum but further evidence is required such as cleaning at 90°C. Given the current experimental setup, this is not possible. Preito et al [1996] undertook an interesting study finding that for the majority of nonionic surfactants temperature optimum occurred at the cloud point. However, in common with the results found in this thesis several surfactants showed no optimum at the cloud point suggesting that it could possibly occur at the PIT.

Miller and Raney [1993] suggest that roll up is promoted on hydrophilic surfaces like cotton due to the low contact angle. The authors suggest that oil is removed from

surfaces having high polyester (hydrophobic) by a solubilisation-emulsification mechanism. However, the results show that roll up is the main mechanism of removal of the crude oil from stainless steel which is partially hydrophilic. This suggests that the although the oil effectively wets the surface of the substrate the surfactant is a much more effective wetter of the surface and therefore roll up occurs. Ogino and Agui [1976] found roll up was soil specific observing roll up with all soils except oleyl alcohol and liquid paraffin.

Solubilisation generally occurs with nonionic surfactants and roll up with anionic surfactants. Since the primary mechanism of removal with $C_{9\text{-}11}E_6$ has been shown to be roll up the difference between $C_{9\text{-}11}E_6$ and other nonionic and anionic surfactants has been investigated. The micelle structure, which has been modelled in Chapter 4 appears to be the connection. At low temperatures the micelle structure in solution is globular similar to that found in anionic solutions. Nonionic surfactants often have large polydispersed micelles which promote solubilisation. This indicates why solubilisation is not important to removal with $C_{9\text{-}11}E_6$ but does not explain why it aids roll up.

GC analysis found that the crude oil deposit acted as a single component showing no evidence of any selective removal or solubilisation. This contrasts with the investigation undertaken by Chui and Huang [1993], who suggest that the crude is selectively solubilised when surfactant solutions are applied. Saito et al [1985] found that longer chain foulants were more difficult to remove. Nagarajan and Ruckenstein [1984] found that selective solubilisation occurred for binary hydrocarbon mixtures. The extent of solubilisation was found to differ for different solubilisates and was also dependent upon the temperature, concentration and composition of the surfactant. The absence of any selective removal is probably due to the oil being removed primarily through roll up and in a dynamic rather than a static system.

Water has proved effective at loosening tar like deposits from the shorelines of beaches (Pasquet and Denis [1983]). This is unlikely be due to oil deposit detachment rather movement from one surface to another, as shown by the visual analysis reported in this thesis. Removal either by surfactant or water was strongly shear dependent, increasing shear increased removal. These findings contrast with the work of Mahé et

al [1988] who deposited alcane droplets onto glass and found that a critical water shear stress was needed for removal. This is not surprising as droplets will behave quite differently to oil films. The rinsing of fluorescein-Na undertaken by Plett [1985] is much more analogous. Four removal periods were proposed, two of which were comparable to the regions found in the removal of crude oil films.

In summary it is a difficult area to study with so many parameters effecting removal: surface composition and charge, soil-soil and soil-substrate bonding, surfactant concentration and composition, the applied temperature, interfacial forces, contact angles and micelle shape. Surfactant removal cannot be generalised, mechanisms that occur are specific to particular surfactant systems. The optimum removal conditions subsequently rely on the type of removal mechanism. Visualisation is useful to identify the mechanism present. Roll-up and emulsification are closely linked requiring liquid soils, minimum in interfacial forces and maximum in contact angles with high temperatures promoting their removal. Solubilisation can only occur in micellar solutions and the type of micelles present play a significant role in removal. Cloud point optima appears with solubilisation, roll up optimum occurring at the PIT.

Chapter Seven

Modelling Oil Film Removal

7.1 Introduction

The removal of oil films from stainless steel is clearly a complex process. Results and observations of the cleaning process produced in Chapter 6 have identified roll up as the primary mechanism when cleaning with a surfactant, and rolling of the oil along the substrate as a primary mechanism when rinsing. Minimal information has been presented in the literature on modelling in this area and this has been reviewed in Chapter 2. The mathematical modelling described in this Chapter is novel and a series of equations describing removal have been developed. The key mechanistic steps in removal have also been identified. The models predict the effect of different parameters on the cleaning process and aid in the optimisation of oil film removal by water and $C_{9\text{-}11}E_6$.

In developing the models to describe cleaning it was important to maintain a balance between simplification and sophistication. The removal of oil films is complicated. Initially simple zero and first order models were used to describe removal. Theoretical analysis was then used to identify the rate determining step to removal and finally empirical models were developed to predict removal. The effect of water and surfactant were treated independently.

7.2 Simple Zero and First Order Models

Many workers have greatly simplified removal by expressing the kinetics in terms of the amount of deposit remaining. The models describe removal in terms of reaction kinetics of zero, first, second, etc. order.

A detailed matrix of kinetic cleaning curves has been produced for the removal of crude oil by nonionic surfactant, $C_{9\text{-}11}E_6$ (Chapter 6). Data has been produced at 30, 40, 50, 60, 70 and 80°C over a concentration range of water, 0.001, 0.01, 0.1, 1, 5 v/v%. Figure 7-1 depicts typical removal kinetics at 40°C using 1 v/v% $C_{9\text{-}11}E_6$ at volumetric flow of 2 l/min.

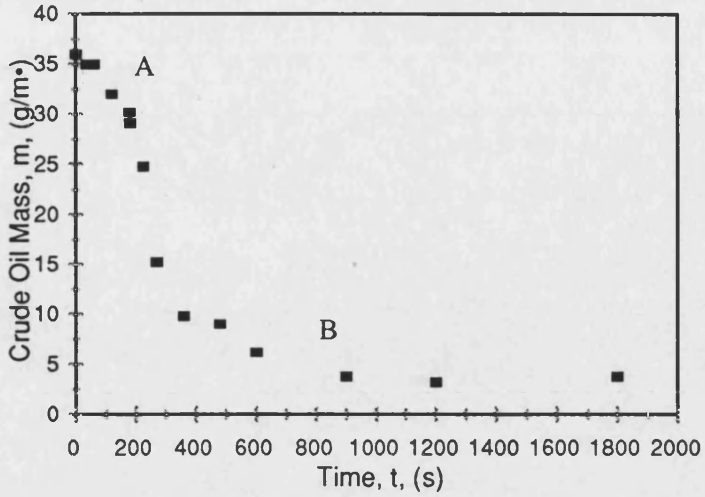

Figure 7-1 1 v/v% $C_{9-11}E_6$, 2 l/min, 40°C

All removal curves have been found to follow this characteristic shape. In region A, the rate of removal is constant, this is indicated by the linear slope. The gradient of the slope is independent of concentration. In region B, the removal is asymptotic and the rate is strongly dependent on the detergent effect. In Figure 7-1, a residual layer remains which under more severe conditions can be removed. The transition from region A to B is fast and can be clearly seen. Treating each region independently, region A can be described by a zero order model with respect to deposit mass, equation 7.1:

$$-\frac{dm}{dt} = a_c \qquad 7.1$$

Subsequently, region B, removal decreases asymptotically leaving a clean surface or a residual layer depending on process conditions and the rate of removal can be described by equation 7.2:

$$-\frac{dm}{dt} = km^n \qquad 7.2$$

Where n is the order of removal and k is the removal rate constant (1/s). Taking natural logarithms of both sides the following is obtained (7.3):

$$ln\left(-\frac{dm}{dt}\right) = lnk + n\ lnm \qquad 7.3$$

which is in the form of y=mx+c where the slope of a plot of *ln*(-dm/dt) as a function of *ln*m represents the order of removal, n, with the intercept equal to *ln*k.

For region A, the value of constant 'a_c' is determined by plotting all the data produced at constant thermo hydraulic conditions on the same graph and using linear regression to calculate the gradient of the points. An example is shown in Figure 7-2, using the data produced using $C_{9\text{-}11}E_6$ at 40°C and 2 l/min at concentrations of 0, 0.001, 0.01, 0.1, 1, 3 and 5 v/v%. All the data for each concentration is represented as squares and is not differentiated.

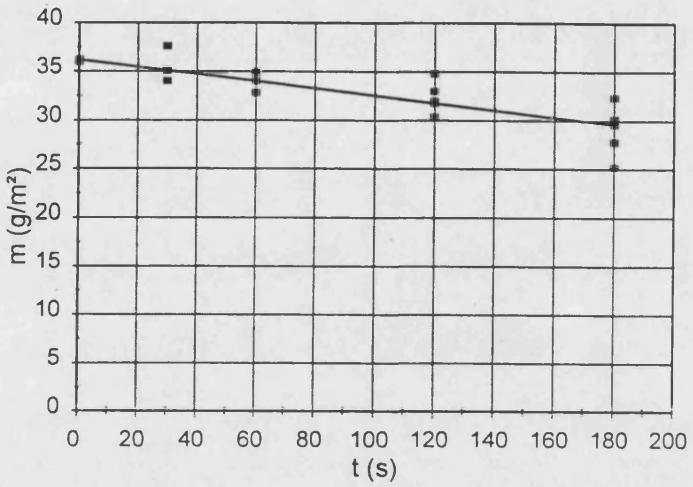

Figure 7-2 Region A of Removal Curves 40°C, 2 l/min, 0, 0.001, 0.01, 0.1, 1, 3 and 5 v/v% $C_{9\text{-}11}E_6$

For region B the procedure is more complicated. Firstly the data points within region A are removed, then the axis on each curve is set to start at t=0 and finish at m=0, by subtracting A_{res} and t_{rev} from m and t respectively Figure 7-3. A smooth freehand curve is then drawn through the points. No function is 'fitted' to the points because it is important not to specify any relationship between the points before any model is applied. Finally, at each of the points the gradient and hence the differential (dm/dt) is calculated.

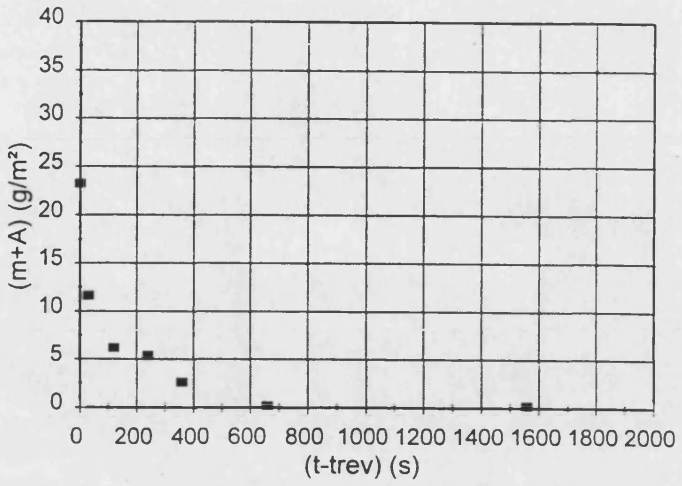

Figure 7-3 Region B of removal curve, 40°C, 2 l/min, 1 v/v% $C_{9\text{-}11}E_6$

A graph of *ln*(-dm/dt) against *ln*(m) is plotted in Figure 7-4(a). Through linear regression the line of best fit can then be determined allowing the variables k and n to be determined. Figure 7-4(b) portrays both the modelling of region A and B compared to the experimental data, a good fit is obtained.

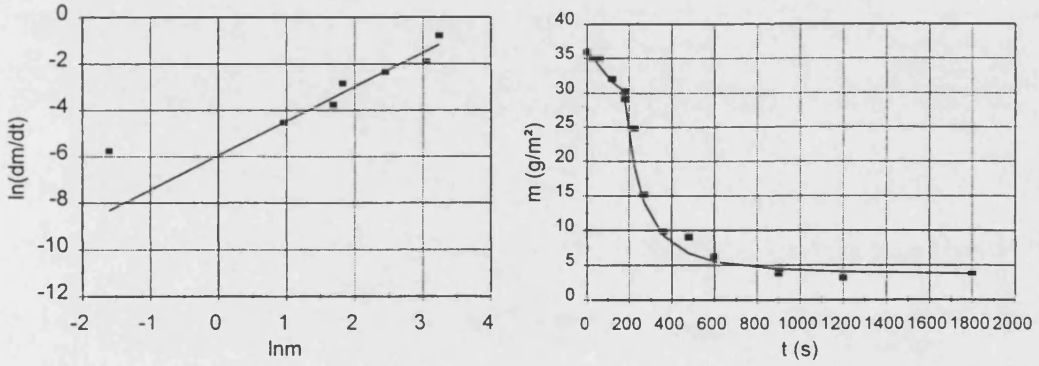

Figure 7-4(a) and (b) Modelled Removal Curves

The equations that describe removal are as follows:

Region A:

$$m_a = m_O - a_c\, t \qquad 0 \le t \le t_{rev} \qquad 7.4$$

Region B:

$$m_b = \left[m_a^{(1-n)} - (1-n)k\left(t - t_{rev}\right)\right]^{1/(1-n)} - A_{res} \qquad t_{rev} \le t \le \infty \qquad 7.5$$

For the example (40°C 2 l/min 1 v/v% syn) $a_c = 0.0368$ g/s m^3

k	=	0.00261	1/s
n	=	1.48	dimensionless
t_{rev}	=	180	s
m_0	=	36	g/m^2
A_{res}	=	3.6	g/m^2

This procedure was then repeated for every kinetic removal curve at each concentration and temperature, determining all the above parameters. Graphs of the determined reaction orders (n) and removal rate constants (k) against concentration are portrayed in Figure 7-5(a) and (b) respectively. (As before water is represented by 0.0001 v/v%.).

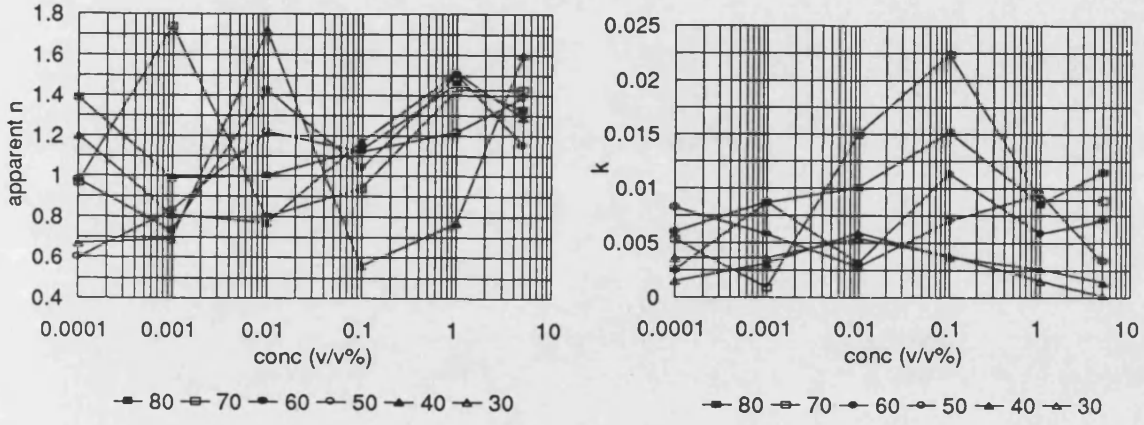

Figure 7-5(a) and (b) Removal rate vs Conc, ($C_{9\text{-}11}E_6$)

The reaction order and rate constant vary significantly with concentration and temperature and there is no discernible trend. From the visualisation technique (Chapter 6) it is likely the same mechanism of removal (rolling along the strands and subsequent roll up) occurs at all the different conditions of concentration and temperature. Therefore a single order of reaction should be applied to all the kinetic data. Since the reaction order lies between 0.55 and 1.7, a value of 1.0 would appear appropriate (there is no evidence to suggest otherwise). Using this revised reaction order of 1 the removal rate was recalculated. Even at the extremes where reaction order was 0.55 or 1.7 the linear relationship of *ln*(dm/dt) versus *ln*(m) was still maintained.

Therefore the revised equations that describe region B removal are as follows:

Section B:

$$m_b = m_a e^{-k(t-trev)} - A \qquad t_{rev} \leq t \leq \infty \qquad 7.6$$

For the example (40°C 2 l/min 1 v/v% syn)

$a = 0.0368$ g/s m^3

$k = 0.0674$ 1/s

$n = 1.00$

$trev = 180$ s

$m_0 = 36$ g/m^2

$A_{res} = 3.6$ g/m^2

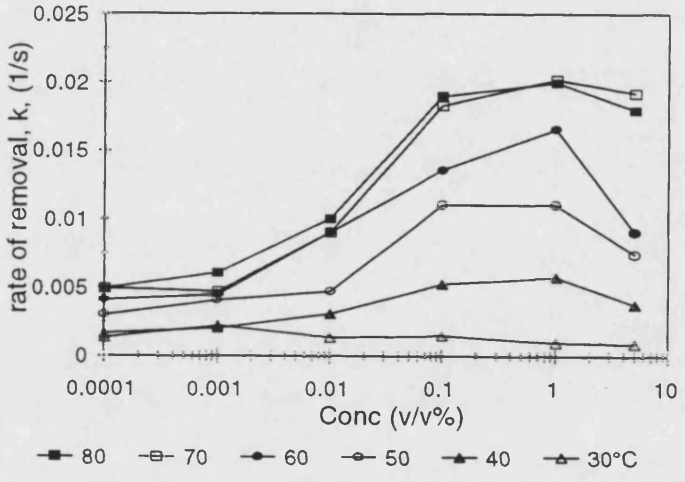

Figure 7-6 Rate of removal with conc $C_{9-11}E_6$ over 30 to 80°C

Specifying the removal as first order shows much more clearly the effect concentration and temperature have upon the rate of removal (Figure 7-6). Applying a first order model to the kinetic data is a simple technique but assumes the removal is not diffusion limiting, this assumption is investigated later in section 7.4.1. The simple models provide a good fit to the data and are represented as the smooth curves in all the figures presented in Chapter 6.

7.3 Arrhenius Kinetics?

As discussed in Chapter 2 the oil removal mechanisms involve a surface modification step. The process is purely physical, the surfactant breaking the bonds between molecules, rather than a chemical process where the oil molecular bonds would be broken and reformed to form a new compound. This has been confirmed by observing

the removal mechanism (Chapter 6). By assuming the deposit acts as a single compound (Chapter 6) and drawing a similarity to reaction kinetics, the Arrhenius equation 7.7 can be used to determine the apparent activation energies for removal.

$$k = Ae^{-E_{act}/RT} \qquad 7.7$$

where k = reaction rate constant

A = pre-exponential factor

E_{act} = apparent activation energy, J/mol

R = gas constant, (8.314 J/mol K)

T = absolute temperature, K

The apparent activation energy has been equated with a minimum energy that must be possessed by reacting molecules before reaction will occur (Fogler [1992]). If the value is small < 20 kJ/mol then the process is said to be physically (diffusion) controlled and >120 kJ/mol then chemically (reaction) controlled (Bird [1993]). Taking natural logarithms the equation yields the equation of a straight line, y = mx + c (7.8).

$$\ln k = \ln A - \frac{E_{act}}{R}\left(\frac{1}{T}\right) \qquad 7.8$$

Using the removal constants k, determined for the main proportion of the cleaning curves, *ln*k is plotted against (1/T). The apparent activation energy at each concentration can then be determined from the gradient which is equal to ($-E_{act}/R$), Figure 7-7. The heavy black lines show the extremes of apparent activation energy, the gentle gradient representing purely a physically controlled process (E_{act} = 20 kJ/mol) and the steep gradient representing a chemical reaction controlled process (E_{act} = 120 kJ/mol).

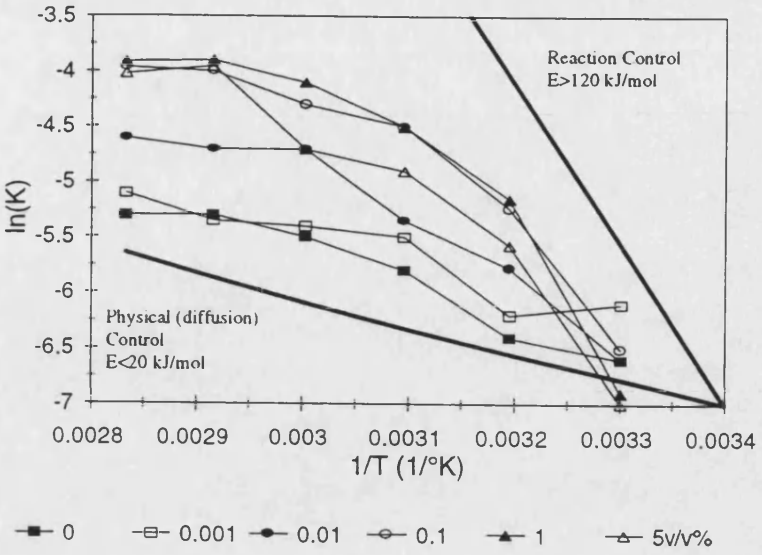

Figure 7-7 Arrhenius Plot for $C_{9\text{-}11}E_{6}$ (

When removal is through water alone a linear relationship is produced indicating that rinsing follows Arrhenius kinetics. As expected the calculated apparent activation energy is equal to 26 kJ/mol indicating removal is purely through physical shear forces.

The addition of the nonionic surfactant has a pronounced effect even at low concentrations, sharply deviating the data from Arrhenius kinetics. If the effect of the surfactant was purely to speed up the same physical process of removal by rinse water then a series of parallel lines would be expected. The greater the removal the further up the y axis. However, this is clearly not the case. At high detergent concentrations a smooth curve is produced which appears to be physically controlled at high temperatures and a combination of chemically and diffusion controlled process at low temperatures. However the action of a surfactant can only be physical. The higher than average apparent activation energies at low temperatures must be due to the reduction of interfacial tensions which will involve the breaking of strong hydrogen bonds in water. The limiting physical process at high temperatures could be due to a number of steps, referred to in the following section.

7.4 Removal Steps

Determining the limiting step will help identify the origin of the removal optimum. Since removal must be physically limiting, removal could be limited through either

diffusional processes or surface modification steps. The raw experimental data can be described by a first order reaction indicating the process is unlikely to be diffusion limited, although two diffusion processes could produce the characteristic removal curve shape. However, the results find cleaning efficiency proportional to log of surfactant concentration up to the cmc, indicating that, concentration of monomers at the substrate surface (and hence monomer diffusion) could play an important role in removal. Investigation is required to identify the limiting removal step. Five physical steps have been proposed to describe the removal process:

7.4.1 Proposed Steps

1. Diffusion of surfactant monomers across boundary, from bulk to oil interface
2. Adsorption of surfactant monomers at the oil surface.
3. Modification of the oil film, by roll-up / emulsification.
4. Desorption of oil droplets and surfactant monomers from the surface to the interface.
5. Diffusion of oil droplets and surfactant monomers into bulk.

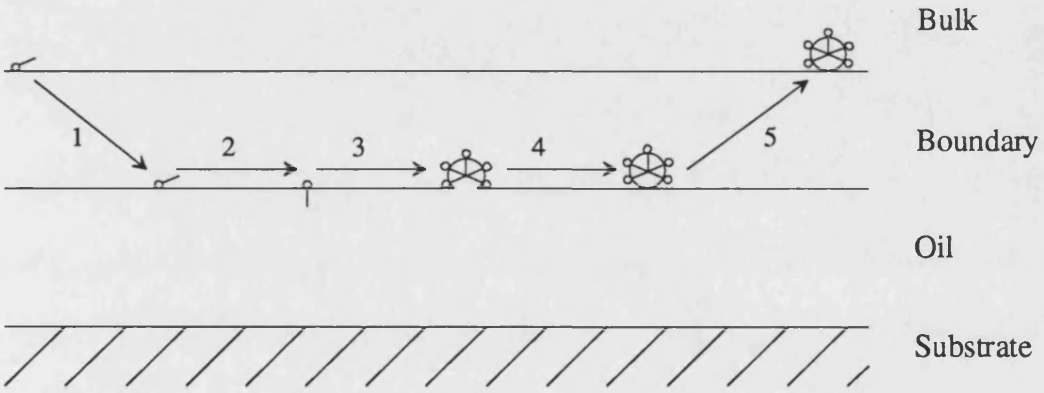

Figure 7-8 Diagram of the proposed removal steps

The proposed removal steps are expressed diagramatically in Figure 7-8. It is important to note the aggregated monomers around the oil droplets (steps 3, 4 and 5) are not micelles solubilising the oil droplet, but reducing the interfacial forces between the oil and surfactant and the surfactant and substrate.

From the Arrhenius analysis it was found that there are likely to be at least two physical processes limiting removal. Step 5 will be fast and can be ignored because the concentration of surfactant in the oil phase is high, developing a large concentration gradient. This is confirmed numerically at the end of this section. Steps 2-4 can be

combined to form an overall surface modification step; this results in two plausible limiting physical processes remaining: one of diffusion of surfactant monomer to the substrate and one of surface modification. Each of these two steps becoming limiting under specific conditions. No published information is available on the kinetics of roll up (steps 2-4), however, the rate of diffusion of monomers to the surface, (step 1), can be estimated. Cleaning is a strong function of the concentration of monomers in the water phase at the interface, (C_i).

Assuming that after a short time interval the boundary layer will have formed and removal will have reached steady state, (the flux of monomers leaving the substrate ($J_{d\,out}$) will equal the flux arriving ($J_{d\,in}$), accumulation $monomers_{interface}$=0), equation 7.9:

$$J_{d\,in} = J_{d\,out} \qquad 7.9$$

It is extremely difficult to determine the size of droplets removed during cleaning because they are unstable and tend to coalesce quickly. It is assumed that for particular cleaning conditions the oil droplets removed are spherical and of a constant diameter, d_r and that once the monomers diffuse across the interface they are adsorbed and removed directly. It is also assumed that there is no redeposition of oil droplets that have been removed. $J_{d\,in}$ can be calculated from Ficks first law and $J_{d\,out}$ can be estimated from the experimental data (dm/dt), determining the overall surface area of oil removed. A simple surfactant monomer mass balance results in equation 7.10. The equation is expressed diagramatically in Figure 7-9:

$$\left(\frac{D^{o}_{AB}(c_b - c_i)}{l\,b}\right) = \frac{dm}{dt}\frac{c_{io}(\pi d_r^{\,2})}{\rho_o(\pi d_r^{\,3}/6)} = \frac{dm}{dt}\frac{6\,c_{io}}{\rho_o\,d_r} \quad (mol/dm^3\,s) \qquad 7.10$$

where $D_{AB}^{\,0}$ = Diffusivity of surfactant monomer through water (m^2/s)

d_r = diameter of oil drop (m)

b = thickness of boundary layer (m)

c_i = conc. of monomers at the interface, water phase (mol/dm^3)

c_b = conc. of monomers in the bulk (mol/dm^3)

c_{io} = conc. of monomers at the interface in the oil phase (mol/dm^3)

ρ_o = density oil droplet (g/m^3)

l	=	length of test piece	(m)
m	=	mass of oil remaining on the test piece	(g/m•)

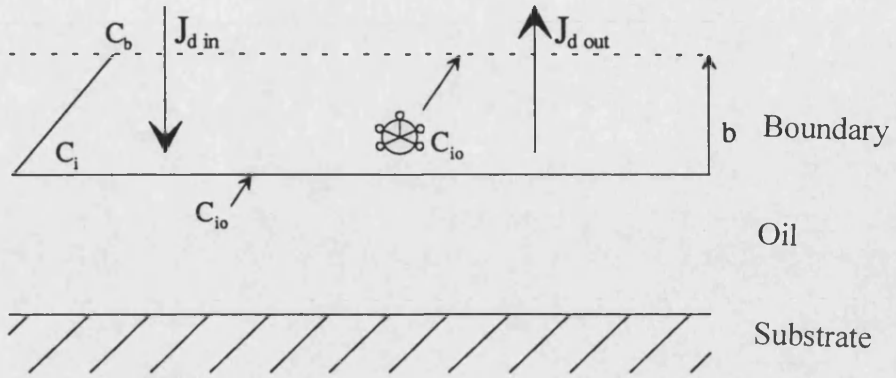

Figure 7-9 Surfactant monomer mass balance

Experimental measurement of the concentration of monomers in the oil phase at the interface of a removed oil droplet, c_{io}, is very difficult. The partition coefficient cannot be assumed to equal 1 ($c_{io}=c_i$) because a monomer in the oil phase will be in a much more thermodynamically favourable position with it's hydrophobic tail absorbed in the oil than the monomer in the water phase ($c_{io}>c_i$). However, this equilibrium relationship can be estimated by determining the free energy difference, ΔG, between monomers in the oil phase and water phase and using the following equation (7.11) which relates ΔG to the equilibrium constant (Smith and Van Ness [1987]).

$$\Delta G = -R\,T\,lnK \qquad 7.11$$

$$K = \frac{c_{io}}{c_i} \qquad 7.12$$

An estimate of ΔG has been determined using the same procedure as in Chapter 4 assuming a monomer aggregated within a micelle can be approximated to a monomer adsorbed, in a preferential state, onto the surface of the oil interface. The same four semi-empirical correlations were used to calculate the overall contribution ΔG. The values of ΔG do not vary significantly over the temperature range studied, at 30°C $\Delta G/R\,T$ = -9.6 and at 50°C $\Delta G/R\,T$ = -9.9. Taking an average of ΔG at 40°C an equilibrium coefficient of 20,000 is reported verifying the initial assumption that step 5 is fast.

The size of droplet removed during cleaning is a strong function of the oil viscosity and is difficult to estimate. Without droplet size information the model cannot be progressed further. However rough parameter estimates can be made to determine the rate limiting step. If the cleaning process is mass transfer limited then c_b will effectively equal c_b-c_i (equation 7.10). Assuming a value of $c_i = 0.01c_b$, dm/dt = 0.35 g/m^2 s (which is the highest reported value at 80°C and the most likely condition of diffusion limitation) the average droplet size of 1×10^{-3} m, (probably an under estimate since the size of the droplets removed are proportional to the strand thickness). The process is not mass transfer limited. This indicates the key process in removal is the surface modification step, since as m approaches zero mass transfer becomes less important. The correlations to estimate the parameters are found in Appendix C.

7.5 Empirical Modelling of Removal

In the previous section, simple first and second order models were used to follow removal. Theoretical relationships were derived to describe the roll up mechanism occurring when using a surfactant. Unfortunately, the theoretical model could not be fully developed without further details on the size of droplets removed during cleaning. Empirical models have therefore been constructed to simplify the process in terms of dimensionless groups which can be used for predictive purposes. The rate of removal (k) was selected to describe the removal process.

Visualisation has shown that removal occurs by two separate mechanisms: (i) rolling of the oil along the substrate (when water is used to clean) and (ii) roll up and subsequent droplet removal into the bulk solution (when surfactant is used to clean). Two empirical models have therefore been developed to describe each situation. In each case the parameters that affect removal were identified and the Buckingham Π method was used to establish all the dimensionless groups that could be formed.

7.5.1 Modelling Rinsing

The variables that effected removal were postulated as follows:

$$k = f(\gamma_l, \tau_l, \mu_o, \mu_l, u_l, \rho_o, \rho_l, d, l) \qquad 7.13$$

Since water removal is through rolling of the oil along the substrate dimensionless constants involving a Reynolds number of the oil were initially examined, such as

equation 7.14 but this relationship did not satisfactorily describe removal. Since results have shown the oil does not change composition with cleaning, the oil properties determined in the laboratory have been used (Chapter 4).

$$Re_l = f(Re_o)^{C_6} = \left(\left(\frac{\rho_l u_l d}{\mu_l}\right) = f\left(\frac{\rho_o k d^2}{\mu_o}\right)^c\right) \qquad 7.14$$

Replacing the rinse water Reynolds number with shear stress group or adding $(\mu_o/\mu_l)^{C_6}$ provided no better fit. Equation 7.14 has several flaws, the relationship should have a tube length term, if the oil is rolling along the substrate, doubling the tube length is likely to half the removal and the power of diameter squared also has no basis and therefore the equation was revised (7.15).

$$\frac{k\,l}{u_l} = f\left(Re_l^{C_6}\left(\frac{\gamma_l}{u_1(\mu_o)}\right)\right) \qquad 7.15$$

With a proportional constant of 7.1×10^{-7} and constant 'C_6' equal to 0.75 the above relationship provided a significant improvement with an R squared of 0.91 (determined from least squares regression). The model is compared to the experimental data in Figure 7-10, the black dots represent the experimental data and the straight line the model.

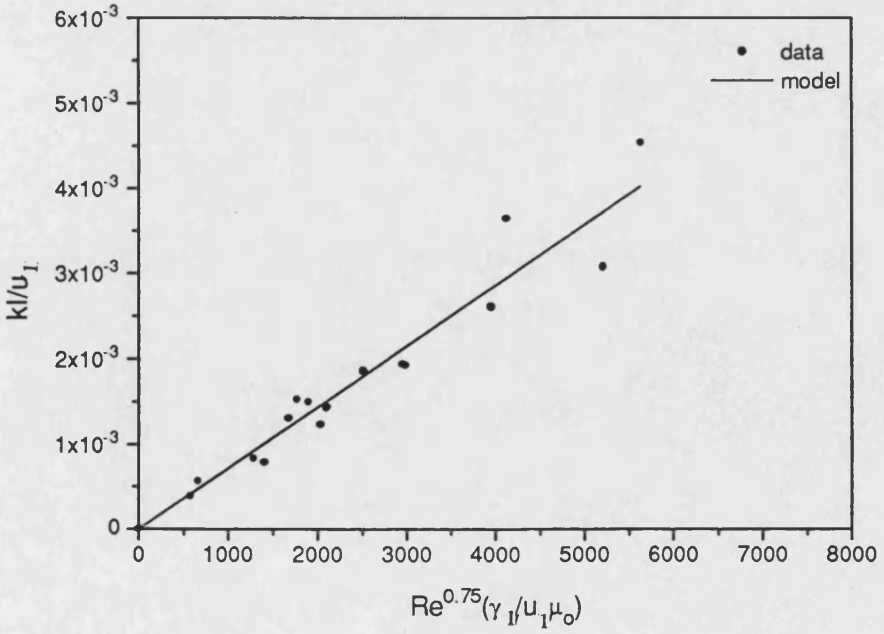

Figure 7-10 Empirical Rinsing Model

Therefore when rinsing, the rate of removal is proportional to the following parameters (7.16):

$$k \propto (u_l^{0.75}, \rho_l^{0.75}, d^{0.75}, \mu_l^{-0.75}, \mu_o^{-1}, \gamma_l, l^{-1}) \qquad 7.16$$

The correlation is limited to rinsing. It is analogous to the Chilton and Colborn mass transfer model with a Nusselt number proportional to Reynold's number to the power 0.8 (Coulson and Richardson [1980]). Unexpectedly, if the surface tension (γ_l) is decreased the rate of removal is reduced. However, the effect of altering the surface tension will also impact upon other parameters such as the viscosity of the cleaning solution. Further work is required considering the dependence of diameter and length but the dependencies expressed in the equation are not unreasonable.

7.5.2 Modelling Surfactant Removal

During the transitional period (below the cmc) removal has been shown to occur through both rinse water and the surfactant removal mechanisms. Without supplementary data on what proportion of the oil is removed through which mechanism, modelling this period is not possible only results only determined above the cmc have therefore been used to describe the surfactant removal mechanisms.

As before dimensionless groups were identified as affecting removal (7.17), with the length of the test piece omitted because with the surfactant there is no progression of the oil along the substrate.

$$k = f(\gamma_l, \tau_l, \mu_o, \mu_l, u_l, u_o, \rho_o, \rho_l, d, c_s,) \qquad 7.17$$

Equation 7.18 was found to best describe removal, with proportional constant = 7.5×10^{-8}, $C_7 = 0.8$ and $C_8 = 0.045$ R squared = 0.89. The model is compared to the experimental data in Figure 7-11, as before the black squares represent the experimental data and the straight line the model.

$$\frac{k\,h}{u_l} = f\left\{ \mathrm{Re}_l^{C_7} \left(\frac{\gamma_l}{u_l(\mu_o)} \right) \left(\frac{c_s}{c_{cmc}} \exp\left(-0.035 \frac{c_s}{c_{cmc}} \right) \right)^{C_8} \right\} \qquad 7.18$$

Unfortunately the above equation (7.18) is only limited to concentrations above the cmc and below 5 v/v%. Surprisingly, although the removal mechanisms for water and surfactant are quite different, the parameters that effect removal are quite similar. The

main differences are the replacement of tube length with h (the deposit depth), Reynolds number to the power 0.82 as opposed to 0.75 and the additional concentration relationship. As found previously (Chapter 6), velocity shows a stronger dependence upon removal when a surfactant is applied compared to rinsing (shown by the higher power of velocity). Above the cmc, the effect of concentration is small, indicated by the power of 0.045 in equation 7.18. An optimum between 0.1 and 1 v/v% is reported, but the viscosity of the oil has the most significant effect.

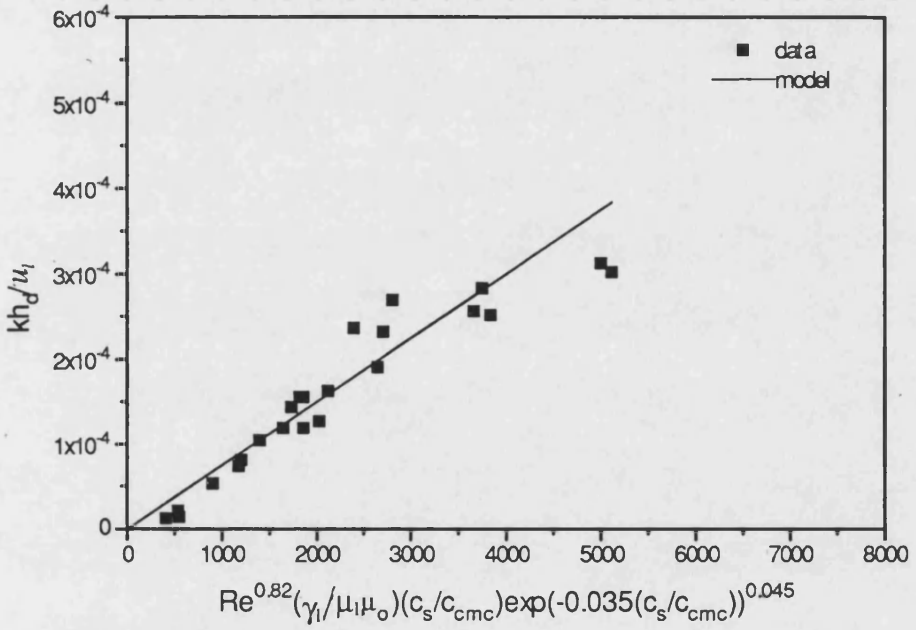

Figure 7-11 Empirical Surfactant Model

With data over the transitional period the models could be combined and used to predict removal over the complete range of concentrations. There are unfortunately several problems in obtaining this data. These are discussed in the future work section of the next Chapter.

Chapter Eight

Conclusions and Future Work

8.1 Conclusions

The removal of oil films from hard surfaces is complex and there has been little research in this area. A novel experimental protocol has been developed to produce qualitative and quantitative cleaning kinetics of the removal of crude oil films from stainless steel piping using aqueous detergent solutions. Results have found roll up to be the primary mechanism of removal and a concentration optimum for $C_{9\text{-}11}E_6$. Theoretical and empirical models have been developed to describe the process.

8.1.1 Experimental Protocol

Two experimental rigs have been designed and constructed:

Fouling Rig- Produces smooth uniform oil films on the inside surface of thin walled stainless steel tubing.

Cleaning rig- The fouled tubes can then be cleaned under controlled conditions of cleaning agent composition, concentration, temperature and flow rate.

Quantitative analysis is determined gravimetrically: weighing the tubing before and after cleaning. Any remaining detergent within the tubing is then accounted for through centrifugation and subsequent separation through solidification (Chapter 5). The technique is quick and accurate. Qualitative analysis is through direct visualisation of the cleaning process through a betamax video recorder. The tubing has a cut away cross section and is observed through a test cell. GC analysis enables examination of the deposit composition during cleaning.

8.1.2 Cleaning Results

1. Experiments have been performed using a wide range of detergents (alkali, nonionic, anionic and commercial formulations). The effect of concentration, temperature and flow rate has been determined over a wide range of values.
2. Of the detergents examined, the nonionic surfactant $C_{9\text{-}11}E_6$ proved the most effective and has therefore formed the bulk of the cleaning studies.
3. Visualisation techniques have proved invaluable in determining the true effect of the solutions applied.

4. When contacted with rinse water, the oil film forms thick strands which follow the direction of flow. The applied shear simply rolling the oil along the surface of the substrate.

5. When contacted with a surfactant above its cmc, the oil film rolls up and thin strands are formed which point in a variety of directions. There is no oil progression along the substrate and removal is uniform through droplets into the bulk solution.

6. As the surfactant concentration is reduced below the cmc, the cleaning mechanism gradually changes to that of rinsing.

7. GC experimentation has shown that when rinsing or cleaning with the nonionic surfactant $C_{9\text{-}11}E_6$ there is no selective component removal, contrary to the findings of several previous authors (Chapter 6). This is probably due to the predominance of the roll-up mechanism.

8. Irrespective of the applied solution increasing the temperature or velocity was always beneficial to removal (Re=18,000 and 80°C).

9. Surprisingly no temperature optimum was reported for $C_{9\text{-}11}E_6$ at the cloud although evidence suggests the existence of an optimum at the PIT but further analysis is required at higher temperatures (>80°C).

10. For the nonionic surfactant, a concentration optimum exists in the region of the cmc and above depending on the temperature. At low temperatures operating above the optimum was even detrimental to removal.

11. The addition of the nonionic surfactant even below the cmc substantially improved removal in comparison to rinsing.

12. In contrast to several studies roll up was observed as the main mechanism of removal for the nonionic surfactant. Unexpectedly, solubilisation played no role in removal. It is hypothesised that this is related to the structure of the micelles in solution.

13. Irrespective of the cleaning agent used, no dramatic improvement in cleaning was produced when moving from laminar to transition to turbulent flow regimes.

14. For both $C_{9\text{-}11}E_6$ and water a linear relationship of flow rate to removal efficiency was determined. The surfactant was more strongly shear dependent than water. This was due to the structure of the film becoming much more open and vulnerable to shear upon application of the surfactant.

8.1.3 Mathematical Modelling

1. Irrespective of the detergent used, simple first and second order models can be used to describe removal .

2. A theoretical model has been developed describing the flux of surfactant monomers to and from the oil film interface. The surface modification of the oil has been identified as the rate limiting step with diffusion of the surfactant monomer to or from the interface offering little resistance to removal.

3. Applying Arrhenius kinetics and calculating the activation energies for removal indicated the existence of two physical processes controlling removal. One was limiting at high temperature and the other at low temperatures. The physically limiting process at low temperatures was probably due to the reduction of interfacial forces which involve the breaking of strong hydrogen bonds within the water.

4. Dimensionless relationships have been developed to describe removal by water and the nonionic surfactant, $C_{9\text{-}11}E_6$. Similar dependencies were found for both mechanisms dispite their visual differences.

8.2 Future Work

An experimental apparatus and protocol has been developed for evaluating aqueous cleaning performance on removing oily films from stainless steel. The apparatus has opened up a wide range of opportunities for future work and the results have raised several questions which should be answered.

8.2.1 Comparative testing of detergent composition

The protocol developed could be used to explore the effect of differing cleaning agent compositions. Initially, similar surfactants to $C_{9\text{-}11}E_6$ could be used varying the chain

length. Of more interest, could be an investigation of the synergy between individual components. Synergy between detergent constituents has received only minimal attention in the literature. Results are likely to be interesting, formulations are often found to be less effective than a carefully selected single component.

8.2.2 Visualisation

Visualisation has proved an invaluable technique, which could be further extended. The visual effect of each detergent class, (anionic, cationic, nonionic, amphoteric, alkali etc) could be investigated. The still frame analysis provides important mechanistic information, although is unfortunately limited to examination below the surfactant cloud point.

8.2.3 The contribution of fluid dynamics and the detergent effect to removal.

Cleaning test pieces with a variety of lengths would allow separation of the relative contributions of the chemical effect and dynamic effect to removal. This would be particularly useful in the transitional period (below the cmc). Results produced over a range of tube lengths would allow determination of the proportion of oil removed by rolling along the surface of the substrate to be compared to the amount removed through droplets into the bulk.

Increasing the test piece length would be an effective way to determine the relative importance of water and the surfactant mechanisms. Problems in oil film reproducibility and this would need to be overcome to make this a more effective method.

8.2.4 Fouling

The experimental technique is multi-purpose and will allow the testing of various oils (> 0.02 Ns/m @ 30°C). The effect of deposit age, thickness and composition could also be determined. Testing of major components within the crude would provide useful information on the adhesion properties. Stainless steel has been used throughout this study but the test piece surface could be varied in terms of surface roughness and / or material. The technique is however, limited to light substrates, covering the majority of metals.

8.2.5 Novel cleaning approaches

Since the rate of the first phase of cleaning is irrespective of the detergent composition, the effect of an initial pre-rinse could also be investigated. This could be further extended by pulsing of the detergent concentration, temperature or flow rate. This would however, increasingly complicate the removal mechanisms and present even greater difficulties in modelling removal.

Appendices

Appendix A

Solution Property Measurement

$C_{9\text{-}11}E_6$ Density measurement

Density was measured using a 25 ml Gay-Lussac pyknometer taken from BS 733 [1987]. The bottle's precise capacity was calculated at 30°C using a constant temperature water bath (± 0.5°C) and reverse osmosis water. The density of the water was assumed to be 996 kg/m^3 (Perry [1984]) and the mass of the bottle and solution was determined using a *Sartorius* balance accurate to ±1 mg. It was necessary to leave the surfactant solution in the water bath for over one hour to ensure all bubbles were removed. Assuming the effects of buoyancy are negligible, the density of pure $C_{9\text{-}11}E_6$ was calculated to be 992 kg/m^3 at 20°C. This value is close to that of water (998 kg/m^3) therefore for 0.1 v/v% surfactant solutions and below the densities were assumed to follow that of water. Since surfactant molecules may pack differently around water molecules this assumption is not valid for higher concentrations. The densities of $C_{9\text{-}11}E_6$ with temperature at 5 v/v% are reported in Table A.1.

Table A.1 Surfactant and Crude Oil Densities

Temp (°C)	Water (kg/m^3)	$C_{9\text{-}11}E_6$ (5 v/v%) (kg/m^3)	Crude Oil (kg/m^3)
30	996	997	917
40	992	994	911
50	988	991	904
60	983	986	898
70	978	982	891
80	972	976	885

$C_{9\text{-}11}E_6$ Viscosity Determination

The viscosity of the nonionic surfactant $C_{9\text{-}11}E_6$ has been determined in accordance to BS 188 [1977]. A glass capillary U-tube viscometer (type BS/U) for direct flow measurements was used (*Fisons Scientific Equipment, Loughborough*). The viscometer was submerged in a thermostatic bath and temperature control was to ± 0.5°C. The time for a reproducible volume of liquid to flow through a glass capillary

was determined. Since only viscosities up to 5 v/v% surfactant were required the detergent solution can be assumed to be Newtonian (Porter, [1994]).

Kinematic viscosity was calculated from the mean of measured flow using the following formula, A.1

$$v = C_5\, t\ (mm^2/s) \qquad A.1$$

Where C_5 = 0.0007982 mm^2/s^2 calibrated with the conditions of the National Measurement Accreditation Service (NAMAS). Viscosities from 30 to 80°C over a concentration range of 0-5 v/v% have been determined the results are displayed in Table A.2.

Table A.2 $C_{9\text{-}11}E_6$ Kinematic viscosity variation with concentration from 30-80°C

Temps	30	40	50	60	70	80
Conc, v/v%	Kinematic Viscosities (m^2/s)					
0	0.813	0.663	0.560	0.485	0.422	0.374
0.3	0.813	0.680	0.572	0.487	0.421	0.374
0.5	0.833	0.690	0.583	0.493	0.427	0.382
0.7	0.845	0.702	0.604	0.500	0.437	0.385
1	0.875	0.716	0.623	0.519	0.440	0.394
2	0.916	0.794	0.726	0.561	0.445	0.409
3	0.979	0.901	0.872	0.611	0.470	0.427
5	1.225	1.170	1.352	0.681	0.491	0.489

Whilhelmy Plate Procedure

The Whilhelmy Plate procedure is frequently used to determine surface tension. A thin platinum ring is attached to a tensiometer (*White Elect Inst Co Ltd.*) and the solution to be tested is raised until the ring just touches the surface and is just pulled down into the liquid. The liquid is then slowly drawn away from the Pt ring until the ring breaks away from the liquid. The surface tension is given by equation A.2.

$$\gamma_l \cos\theta = \Delta M_w / p \qquad A.2$$

where ΔM_w is the change in weight (force) observed resulting from the formation of the liquid meniscus at the contact of the ring (perimeter p) and liquid. The ring must be horizontal and is roughened to give zero contact angle, θ, ($\cos 0 = 1$). Equilibrium values are obtained after approximately 5 minutes. Surface tension is dynamic as opposed to instantaneous in the case of the equilibrium relationship between monomers in solution and in micelles because, when using a platinium loop the water is raised requiring replenishment of the monomers and micelles by diffusion and convection to the surface.

Glassware was rigorously cleaned with *micro*, rinsed with RO water and subsequently dried with filter paper between readings. The Pt loop was also flamed to remove contamination. Temperature was controlled to ±1°C externally through a small water bath. A thermostatically controlled copper coil maintained the water bath's temperature. To ensure accuracy, the surface tension measurements were checked against an internal standard, reverse osmosis water. Readings were found to be reproducible and triplicated averages compare well with literature values (Lide, [1990]), Table A.3.

Table A.3 Surface Tension of Water (γ_l)

Temp	Surface Tension	
	Literature Values	Experimental Values
(°C)	(mN/m)	(mN/m)
20	72.75	71.6
30	71.20	71.0
40	69.60	69.2
50	67.94	68.2
60	66.24	67.4

Micelle Aggregation

1) Free Energy Transfer of hydrocarbon chain in to core of aggregate.

Estimated from experimental data produced for solubility of hydrocarbons in water as a function of temperature.

For CH_2 group

$$\frac{\left(\Delta\mu_g^0\right)_{tr}}{k_b\,\mathrm{T}} = 5.85\,lnT + \frac{896}{T} - 36.15 - 0.0056\,T \qquad \textit{A.3}$$

For CH_3 group

$$\frac{\left(\Delta\mu_g^0\right)_{tr}}{k_b\,\mathrm{T}} = 3.38\,lnT + \frac{4064}{T} - 44.13 + 0.02595\,\mathrm{T} \qquad \textit{A.4}$$

2) Free Energy of Deformation

For spherical micelles or globular

$$\frac{\left(\Delta\mu_g^0\right)_{defr}}{k_b\,\mathrm{T}} = \frac{9\,\mathrm{P}\,\pi^2\,\mathrm{R_s}^2}{80\,\mathrm{N}\,\mathrm{L}^2} \qquad \textit{A.5}$$

$$N = \frac{(n_c+1)}{3.6} \qquad \textit{A.6}$$

3) Free Energy of Formation of micelle hydrophobic / water interface

The free energy is accounted for as the product of the area of the interface and the macroscopic interfacial tension of the aggregate core-water interface.

$$\frac{\left(\Delta\mu_g^0\right)_{\mathrm{int}}}{k_b\,\mathrm{T}} = \left(\frac{\gamma_{agg}}{\mathrm{k\,T}}\right)(a - a_0) \qquad \textit{A.7}$$

$$\gamma_{agg} = \gamma_s + \gamma_l - 2.0\chi(\gamma_s\gamma_l)^{1/2} \qquad \textit{A.8}$$

$$\gamma_s = 35.0 - 325\,\mathrm{M_{wt}}^{-2/3} - 0.098(T - 298) \qquad \textit{A.9}$$

$$\gamma_l = 72.0 - 0.16(T - 298) \qquad \textit{A.10}$$

where χ = constant with value of 0.55

M_{wt} = molecular weight of hydrocarbon tail

γ_{agg} = aggregate core interfacial tension

γ_{sl} = interfacial tension between the aliphatic hydrocarbon of same molecular weight as the hydrocarbon tail and the surrounding water.

4) Free Energy associated with the increased steric repulsion of polar head groups.

From van de Waals: (based on steric repulsion)

$$\frac{\left(\Delta\mu_g^0\right)_{steric}}{k_b\,T} = -\ln\left(1-\frac{a_o}{a}\right) \qquad \textit{A.11}$$

where a_o = the effective area of the polar (hydrophilic) head group

This relationship assumes the head groups are compact in nature acting as hard particles with a definable core. For polyoxyethylene head groups having a long chain head structure this is not valid. To account for this Puvvada and Blankschtein [1992] use the same relationship successfully but replace a_o with a_h where a_h is a temperature dependent parameter estimated from the volume of its hydrophilic head divided by its effective length.

$$a_h = a_{h0}\left[1 - H(T-298)\right] \qquad \textit{A.12}$$

H reflecting the decrease in hydration on the head group with temperature. H is estimated to be $0.00075K^{-1}$. From reference a_{ho}= 38Å for $C_{10}E_6$ (E_6 part). For change in a_h the following can be applied:

$$a_h \alpha j^z \qquad \textit{A.13}$$

where j = number of ethoxylated monomeric units (C_iE_j)

z = dimensionless constant

(equations for calculating free energy contributions for each step were taken from Nagarjan and Ruckenstein [1991])

Required Properties

Molecular Volume

$$v_s = v(CH_3) + (n_c - 1)v(CH_2) \qquad (Å^3) \qquad \textit{A.14}$$

$$v(CH_3) = 54.6 + 0.12(T-298) \qquad (Å^3) \qquad \textit{A.15}$$

$$v(CH_2) = 26.9 + 0.0146(T-298) \qquad (Å^3) \qquad \textit{A.16}$$

The maximum radius of the spherical micelles will be limited by the extended length of the hydrocarbon tail which can be estimated:

Extended Length of Surfactant Tail (l_c)

$$l_c = 1.50 + 1.265 n_c \qquad (\text{Å}) \qquad \textit{A.17}$$

The forces holding amphiphilic molecules together in micelles and bilayers are not due to strong covalent or ionic bonds but arise from van der Waals, hydrophobic, hydrogen-bonding and electrostatic interactions. Thus if solution conditions such as electrolyte concentration, pH effect the intermolecular forces between each aggregate and hence the intermolecular forces within each aggregate they will therefore modify the shape and size of the aggregates.

Table A.4 Aggregation Numbers from the Literature

Surfactant	Temp°C	Agg. No.	Technique	References
$C_{12}E_6$	25	400	Light scattering	Porter 1994
$C_{12}E_6$	35	1400	Light scattering	Porter 1994
$C_{12}E_6$	25	1200	Modelling	Puvvada, Blankenstein 1992
$C_{12}E_6$	35	10000	Modelling	Puvvada, Blankenstein 1992
$C_{12}E_8$	25	40	Modelling	Puvvada, Blankenstein 1992
$C_{12}E_8$	35	45	Modelling	Puvvada, Blankenstein 1992
$C_{12}E_8$	50	170	Modelling	Puvvada, Blankenstein 1992
$C_{12}E_{10}$	25	80	Modelling	Nagarajan, Ruckenstein 1991
$C_{12}E_8$	25	120	Experimental	Nagarajan, Ruckenstein 1991
$C_{12}E_6$	25	120	Modelling	Nagarajan, Ruckenstein 1991
$C_{12}E_6$	25	200	Experimental	Nagarajan, Ruckenstein 1991
$C_{10}E_6$	15	85	Time Resolved Fluorescence	Alami et al 1993
$C_{10}E_6$	25	100	Time Resolved Fluorescence	Alami et al 1993
$C_{10}E_6$	35	150	Time Resolved Fluorescence	Alami et al 1993
$C_{10}E_8$	25	85	Time Resolved Fluorescence	Alami et al 1993
$C_{10}E_8$	35	105	Time Resolved Fluorescence	Alami et al 1993

Crude Oil Viscosity Measurement

Since crude oil is not necessarily Newtonian, the viscosity cannot be determined using a U-tube viscometer as was done for the nonionic surfactant. A plate - plate *Bohlin* rheometer (*Lund, Sweden*) was selected with a diameter of 40 mm and a gap of 0.15 mm. This allowed viscosities to be calculated over a range of shear rates, shown in Figure A-1. As the shear rate increases, the viscosity is reduced indicating the crude oil is slightly shear thinning. Since the change in viscosity with shear rate is small, the crude oil is assumed to be Newtonian. The average changes in viscosity with temperature are reported in Chapter 4. Through careful calibration, common inaccuracies found with rotational viscometers due to end effects were minimised. Accurate temperature control was obtained through a water bath ±0.1°C.

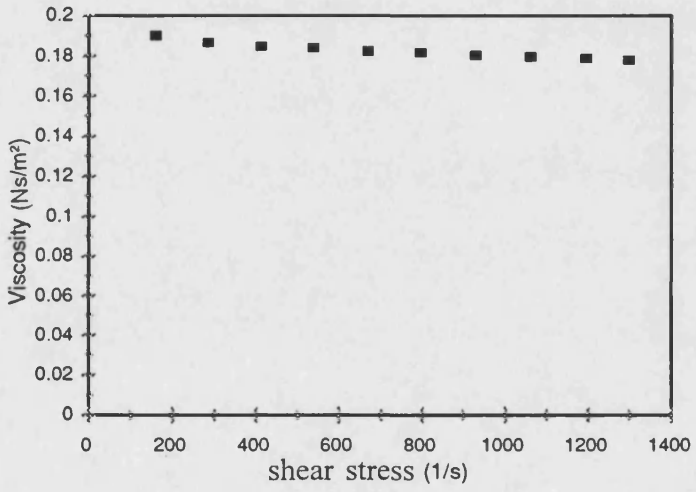

Figure A.1 Viscosity against Shear Rate, 30°C

ASTM D5307 Test Method to Determine Molecular Mass Distribution

Procedure

Essentially, the crude oil sample is dried, diluted with carbon disulphide and injected into a gas chromatographic column. The column temperature is raised at a linear rate while the sample is carried through the column by a constant flow of inert carrier gas (He). The rate of component movement through the column is mass transfer dependent therefore lighter fractions of petroleum will have a greater tendency to pass through the column than heavier ones. A flame ionisation detector detects exiting components (C-H bonds) from the column reporting 0-1 mV which is then logged by a computer and represented on a chromatogram. Boiling points of exiting components

are determined by comparison to a calibration curve. The calibration curve is produced by running a mixture of 16 n-parafins of known boiling points through the column under the same chromatographic conditions. Components with boiling points above 545°C remain in the column. The amount of residue is determined by the injection but with the addition of a known volume of internal standard to the crude. From the subsequent increase in area of the chromatogram the residual mass is determined.

Apparatus

A standard gas chromatograph is used with a column temperature programmer capable of 30 to 350°C ramped at 15°C/min (Figure A.1). The flow controller was required to maintain a constant flow of carrier gas of 30 ml/min (±1%) over the full operating temperature range. A cryogenic oven was not required since the crude oil is light and an exact boiling point distribution of the very light fraction of the crude oil is not necessary. The detector and the injector operated continuously at 360°C. The column used was a SIMDIS Petrocol C, 20"×1/8" (*Supelco, Dorset*). 1 µm samples were injected into the head of the column. The response from the detector was logged on a local PC and analysed through a spreadsheeting package and a BASIC program.

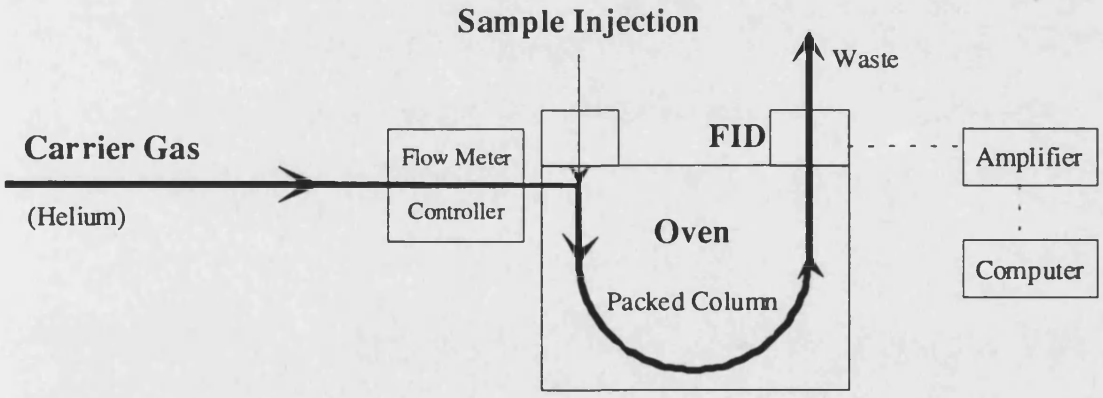

Figure A.1 Schematic of Gas Chromatograph

Materials

The following materials were used at various stages to determine the crude oil boiling point distribution:

Purity of Reagents- All chemicals used were of reagent-grade purity. Particularly air must be hydrocarbon free since it is used in the FID to support combustion.

Anhydrous Calcium Chloride- Used as a drying agent for the oil samples. Water injected into the column causes wide scatter due to its high polarity.

Calibration Mixture- A series of 16 n-parrafins that cover a boiling point range 174-545°C all of 6.25 wt% (*Supelco, Dorset*) (Table A.5).

Table A.5 Boiling Points of Calibration Mixture

n-paraffin	BP (°C)	n-paraffin	BP (°C)
n-C_{10}	174	n-C_{18}	316
n-C_{11}	196	n-C_{20}	344
n-C_{12}	216	n-C_{24}	391
n-C_{13}	235	n-C_{28}	431
n-C_{14}	254	n-C32	466
n-C_{15}	271	n-C_{36}	496
n-C_{16}	287	n-C_{40}	522
n-C_{17}	302	n-C_{44}	545

Internal Standard- A mixture of equal proportions of 4 n-paraffins, n-C_{14} through to n-C_{17} (25 wt% split).

Carbon Disulphide- CS_2 99% purity. It is miscible with crude oils and has a minimal response to the FID but it is extremely hazardous.

Sample Preparation

In addition to the calibration mixture two samples have to be prepared for each crude oil. Firstly the crude sample and secondly the crude sample plus an internal standard. Initially the crude was dried with anhydrous calcium chloride but this was discovered to be unnecessary due to the low water content.

The sample was prepared by placing a few grams of crude oil into a vial and dissolving it in carbon disulphide using a ratio of 1:9 respectively. For the crude oil plus internal standard sample a more accurate measure of the sample was required. A known quantity of crude was placed into a vial (accurate to ±1 mg). A few drops of the internal standard were added, and the increased weight was determined (±1 mg). This

mixture was then diluted with CS_2 as before. All preparations undertaken with CS_2 were performed in a fume cupboard due to the hazardous nature of the mixture.

Column Operation

After column conditioning (ASTM D5307 [1992]), the gas chromatograph was allowed to reach pre-programmed temperatures. The injection and detection temperature were set to 360°C, and the initial oven temperature to 30°C. The carrier gas flow was verified and the FID was checked for the presence of a continuous signal. The oven was programmed to maintain the initial temperature for 3 minutes, to allow all the components with boiling points below 90°C to pass through the column. The oven temperature was then increased at a rate of 15°C/min up to a value of 350°C whereupon the temperature was maintained for 10 minutes to ensure that as many of the components with boiling points above 545°C did not remain in the column.

Baseline Drift

Baseline drift is a common problem with GC's operating at high temperatures and wide ranges. Drift can also be caused by the residual crude in the column and 'bleeding' of the packing material. As long as the drift is reproducible, it does not present a problem. Drift can be accounted for by subtracting an area slice profile of a blank run from a sample run to obtain the corrected area slices. An example of a baseline drift is shown below in Figure A.2.

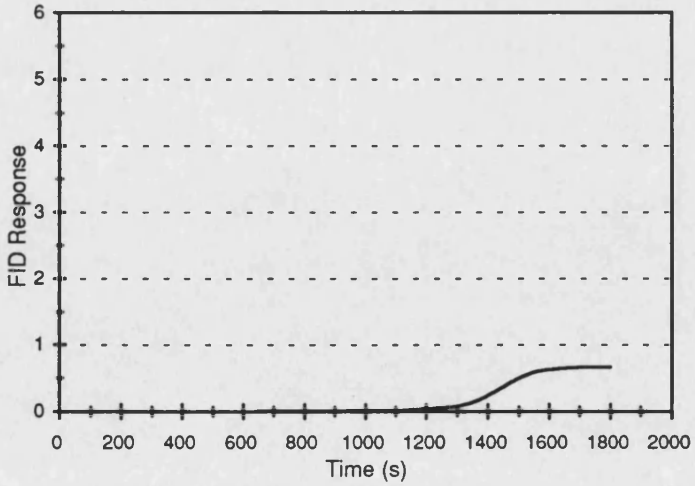

Figure A.2 Blank Run, Baseline Drift

Calibration run

As stated previously a calibration curve is required to correlate retention time against boiling point of the component. The calibration mixture is dissolve in carbon disulphide 1:9, care must be taken to ensure all the mixture has dissolved, gentle warming of the vial in the hands is sufficient. A 1µl sample is then injected into the GC and the same column conditions are applied. A series of well defined peaks results , Figure A.3, and a graph of boiling point against retention time can then be plotted, Figure A.4.

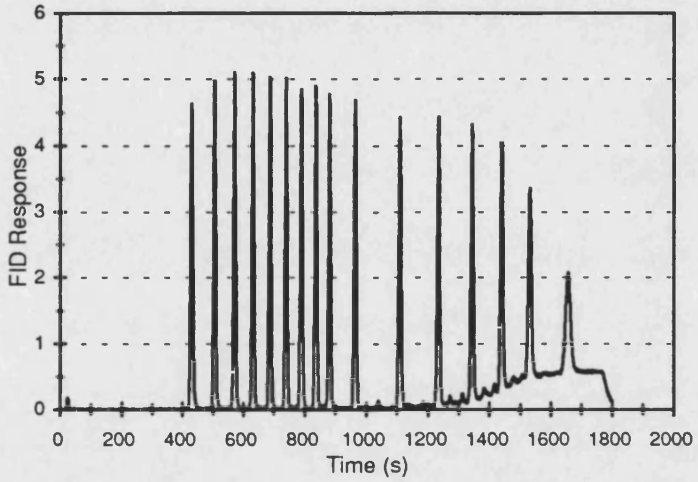

Figure A.3 Calibration Sample, 16 hydrocarbons

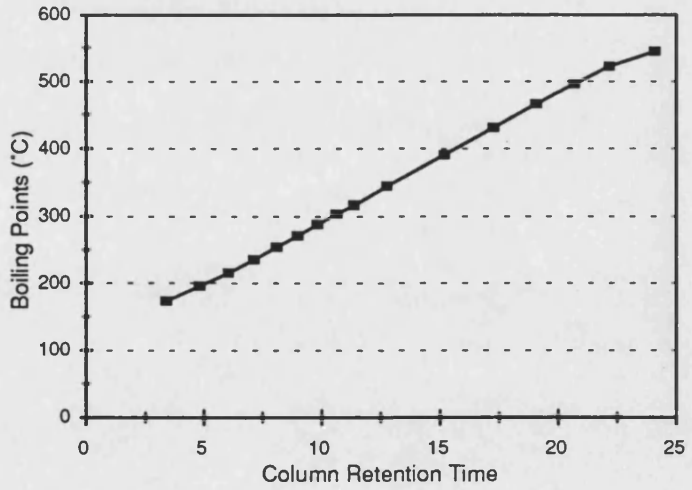

Figure A.4 Calibration Curve

Internal Standard and Crude Samples

The same column operating conditions as used previously are employed for both samples, injection was carried out using a 1 µl syringe. The chromatographs of the internal standard plus crude oil and the crude oil only sample are depicted in Figure A.5 and Figure A.6 respectively.

Residual Composition of Crude Sample

The calculation procedure is detailed in the standard ASTM D5307 [1992]. Briefly, by comparing a chromatogram of a crude oil and a chromatogram of a known mass of the same crude oil and a known mass of internal standard it is possible to determine the increase in chromatogram area represented by the addition of the internal standard. This then allows calculation of the theoretical total area that should be represented on the chromatograph and hence the residue remaining in the column.

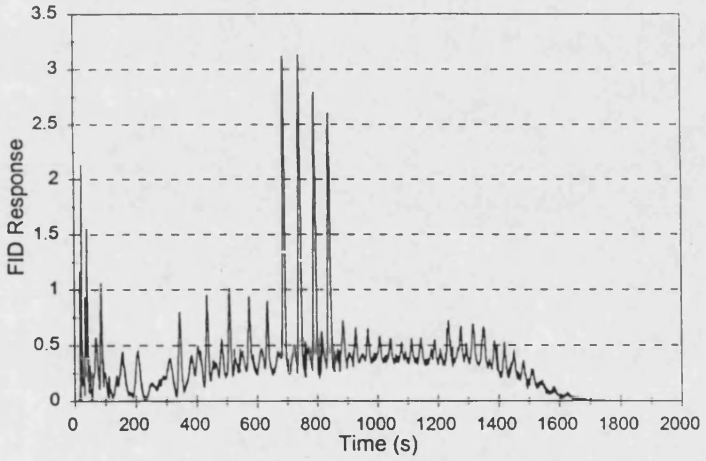

Figure A.5 Crude Oil plus Internal Standard Chromatogram

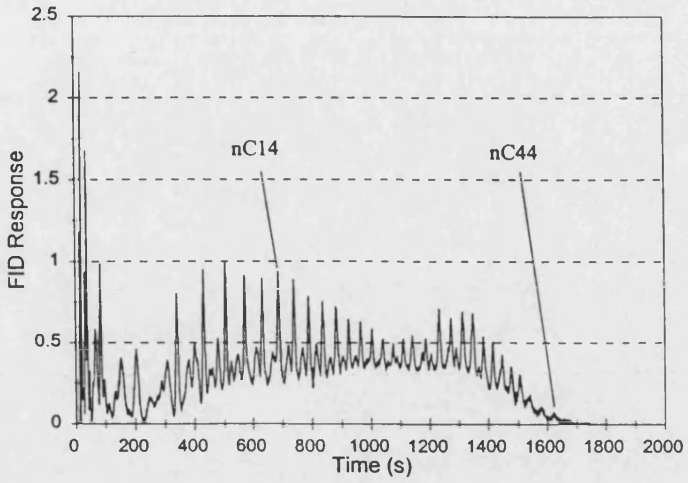

Figure A.6 Crude Oil Chromatogram, neat

Boiling Point Curve

The boiling point distribution curve for the neat crude oil is depicted in Figure A.7. The curve represents the cumulative amount of oil recovered as a percentage of the amount of oil injected plotted against retention time. The IBP of the crude is defined as the boiling point equivalent of time when the cumulative area at the beginning of the chromatogram is 0.5% of the theoretical total area. However since the initial detectable boiling point of the column is 90°C which is above the IBP of the sample crude this cannot be reported. Instead the weight percent of the sample that has a boiling point above 90°C is depicted. An even spread of hydrocarbons nC_7 to nC_{42} is present in the crude with a residual content (boiling point above 538°C) of 17.5% which is typical of the type of crude, (Izadpanah [1996]).

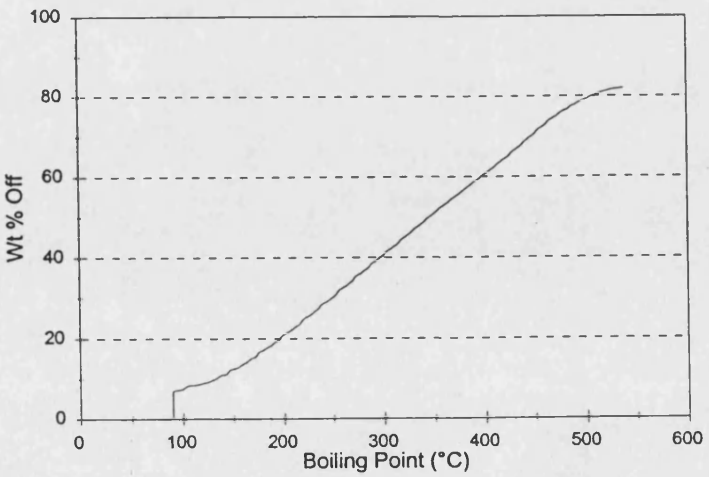

Figure A.7 Crude Oil Boiling Point Distribution Curve

Appendix B

Rig Design

Flowrate Control

Centrifugal pumps were chosen for use in the cleaning rig. They give a steady delivery and can easily be made out of alkali resistant materials. The pumps were sized by calculating the pressure drop at the maximum flowrate, 10 l/min. The pressure drop was estimated using a form of Bernoulli's equation assuming incompressible, turbulent flow (equation A.18).

$$g\Delta z + v\Delta P = -F_r \qquad A.18$$

where, g = Acceleration due to gravity

z = Distance in vertical direction

v = Volume per unit mass of fluid

F_r = Energy loss per unit mass

P = Pressure

The energy lost per unit mass, F_r, was calculated from equation A.19. The equivalent pipe length of the process stream was estimated by adding to the actual length to equivalent lengths of all the valves, elbows and T-pieces. The friction factor, φ, was estimated assuming a surface roughness, e, for smooth pipes of 1.5×10^{-6} m (Coulson and Richardson [1977]). The process stream pressure drop at 10 l/min was calculated to be 4 bara.

$$F_r = \frac{4\,(\varphi) l\,\rho_l\,u^2}{d} \qquad A.19$$

where, φ = Friction factor

l = Equivalent length of pipe

ρ_l = Density of fluid

d = Internal diameter of pipe

The net positive suction head (NPSH) was verified to avoid possible cavitation of the pump. The NPSH is given by the difference between the total head at the suction inlet and the head corresponding to the vapour pressure of the liquid at the pump inlet. It

is given by the following equation A.20 (Coulson and Richardson, [1977]). The figure for the rig was well within the specified margins for the pump.

$$NPSH = \frac{P_0}{\rho g} - \frac{P_v}{\rho g} + H_0 - H_f \qquad \textit{A.20}$$

where, P_0 = Pressure at pump suction tank

P_v = Vapour pressure of liquid

H_0 = Height of liquid above pump inlet

H_f = Friction head

g = Acceleration due to gravity

Appendix C

Estimation of Modelling Parameters

Boundary Layer Thickness

For turbulent flow the boundary layer thickness, b, can be estimated using the relationship below (A.21), by assuming boundary region is in laminar flow. The core is assumed to be perfectly mixed and all the transfer of mass, momentum etc occurs across the laminar region and occurs through molecular processes only. The velocity decreases across the boundary linearly to zero at the wall. (Kay and Nedderman, [1988]).

$$b = 25.32\, d\, Re_l^{-\frac{3}{4}} \qquad A.21$$

Viscosity and Density Determination

Since the aqueous surfactant solutions are very dilute, the viscosity and density were assumed to be that of water at the operating temperature. From data found in Perry and Green [1984] the following correlations, (equations A.22 and A.23) were developed to describe the variation of density and viscosity with temperature.

$$\rho_l = 1000 - 0.0896\, T - 0.00339\, T^2 \qquad A.22$$

$$\mu_l = 1.441 \times 10^{-3} \exp(-0.0176 \times [T - 273]) \qquad A.23$$

Diffusivity of Liquids

Unlike gases, liquid diffusion coefficients vary significantly with concentration and are difficult to estimate. The following empirical correlation (A.24) is recommended for dilute solutions of nonelectrolyte, (Trebal, [1980]):

$$D_{AB}^{o} = \frac{\left(117.3 \times 10^{-18} \left(\omega (M_{wt})\right)^{0.5} T\right)}{\mu_l (v_A)^{0.6}} \qquad A.24$$

where D_{AB}^{o} = diffusivity of A in very dilute solution in solvent B, m•/s

M_{wt} = molecular weight of solvent, kg/kmol

T = temperature, K

μ_l = solution viscosity, kg/m s

v_A = solute molar volume at normal boiling point, m^3/kmol

ω = association factor for solvent, 2.26 for water as the solvent

Using the correlation the diffusivity of a $C_{10}E_6$ ($C_{22}H_{46}O_7$) monomer in water can be simplified to (A.25):

$$D_{AB}^{o} = \frac{7.45 \times 10^{-13} T}{\exp(-0.0176[T-273])} \quad (m^2/s) \qquad \textit{A.25}$$

The solute molar volume (v_A) was estimated using group contribution of atomic molar volumes (Treybal, [1980]) as shown in equation A.26 below.

$$v_A = 0.0148(22) + 0.0037(46) + 0.0074(7) = 0.548 \ m^3 / kmol \qquad \textit{A.26}$$

References

Adam, N.K. (1937). Detergent action and its relation to wetting and emulsification. *Journal of the society of dyers and colourists*, **4**, 121-129.

Adams, C.L. (1990). Hot water helped clean up the Prince William Sound. *Plumbing Engineer*, **18**(1), 49-50.

Alami, E., Kamenka, N., Raharimihamina, A. and Zana, R. (1993) Investigation on the Microstructures in mixtures of water with the nonionic surfactants C_8E_5, $C_{10}E_6$, and $C_{10}E_8$ in the whole range on composition. *Journal of Colloid and Interface Science*, **158**, 342-250.

Aronson, M.P., Gum, M.L. and Goddard, E.D. (1983). Bahaviour of surfactant mixtures in model oily-soil detergency studies. *Journal of the American Oil Chemists Society*, **60**(7), 1333-1339.

ASTM D5307. (1992). Standard test method for determination of boiling range distribution of crude petroleum by gas chromatography.

B.S. 188. (1977). Methods for determination of the viscosity of liquids.

B.S. 733. (1987). Pyknometers. Part 1-2

Bartlett, M. Bird, M.R. and Howell, J.A. (1994). Effective cleaning of microfiltration membranes fouled during whey protein processing. *IChemE Food Process Engineering Oral Presentation,* University of Bath.

Beaudoin, S.P., Grant, C.S. and Carbonell, R.G. (1995). Removal of Organic Films from Solid Surfaces Using Aqueous Solutions of Nonionic surfactants. 1. Experiments. *Ind. Eng. Chem. Res.*, **34**, 3307-3317.

Belyakov, V.L. and Sagdeev, R.S. (1988). Conductometric measurement of oil contents in water-rich emulsions. *Measurement Techniques*, **31**,3, 299-302.

Benton, W.J., Raney, K.H. and Miller, C.A. (1986) Enhanced videomicroscopy of phase-transitions and diffusional phenomena in oil-water nonionic surfactant systems. *Journal of colloid and interface science*, **110**(2), 363-388.

Bird, M.R. and Fryer, P.J. (1991). An experimental study of the cleaning of surfaces fouled with whey proteins. *Trans IChemE, Part C*, **69**, 13-21.

Bird M.R. and Espig S.W.P. (1994). Cost optimisation of dairy cleaning in place (CIP) cycles. *Trans IChemE*, **72**(C), 3, 17-20.

Bird, M.R. (1993). Cleaning of a Food Process Plant. *Ph.D. Thesis*, University of Cambridge

Bott, T.R. (1990). Fouling notebook. London: IChemE.

Bourne, M.C. and Jennings, W.G. (1961) Some Physicochemical Relationships in Cleaning Hard Surfaces. *Food Technology*, **11**, 495-499.

Bourne, M.C. and Jennings, W.G. (1963). Kinetics studies of detergency. I. Analysis of cleaning curves. *Journal of the American Oil Chemists Society*, **40**(10), 517-523.

Bourne, M.C. and Jennings, W.G. (1965). Kinetic Studies of detergency. III. Dependance of the Dupré mechanism on surface tension. *Journal of the American Oil Chemists Society*, **42**(6), 546-548.

Bulat, T.Y. (1955). Evaluating metal cleaning efficiency. *Metal Progress*, **12**, 94-95.

Carroll, B.J. (1981). The kinetics of solubilisation of nonpolar oils by nonionic surfactant solutions. *Journal of Colloid and Interface Science*, **79**(1), 126-135.

Carroll, B.J. (1993). Physical aspects of detergency. *Colloids and Surfaces*, **74**(2-3), 131-167.

Chahine, R. and Bose, T.K. (1983). Measurement of small dielectric loss by time domain spectroscopy; application to water/oil emulsions. *IEE Transactions on instrumentation and measurement*, **IM-32(2)**, 360-363.

Chan, A.F., Evans, D.F. and Cussler, E.L. (1976). Explaining Solubilisation Kinetics. *AIChE Journal*, **22**(6), 1006-1012.

Chiu, Y.C. and Huang, J.F. (1993). Solubilisation of Crude oil in ultralow interfacial tension systems formulated with carboxymethyl ethoxylates under extremely high calcium ion concentration. *Journal of Dispersion Science and Technology*, **14**(3) 295-312.

Cleaver, J.W. and Yates, B. (1973). Mechanism of Detachment of Colloidal Particles from a Flat Substrate in a Turbulent Flow. *Journal of Colloid and Interface Science*, **44**(3), 464-474.

Clint J.H. (1992). Surfactant Aggregation, New York: Chapman and Hall.

Comelles, F., Solans, C., Azemar, N., Sánchez Leal, J. and Parra, J.L. (1986). Microemulsions with commercial nonionic surfactants: Study of their formation and detergency properties. *Journal of dispersion science and technology*, **7**(4), 369-382.

Coulson, J.M. and Richardson, J.F. (1980). Chemical Engineering- Volume 1. 3rd. ed. Oxford: Pergamon Press.

Cox, M.F. (1986). Surfactants for hard surface cleaning. Mechanisms of Solid Soil Removal. *Journal of American Oil Chemists Society*, **63**, 4, 559-565.

Cox, M.F. and Matson, T.P. (1984). Optimisation of Non-ionic surfactants for hard-surface cleaning. *Journal of the American Oil Chemists Society*, **61**(7), 1273-1278.

Cox, M.F., Smith, D.L. and Russell, G.L. (1987). Surface chemical processes for removal of solid sebum soil. *Journal of the American Oil Chemists Society*, **64**(2), 273.

Dillan, K.W., Goddard, E.D. and McKenzie, D.A. (1979). Oily soil removal from a polyester substrate by aqueous non-ionic surfactant systems. *Journal of American Oil Chemists Society*, **56**(1), 59-70.

Dillan, K.W., Goddard, E.D. and McKenzie, D.A. (1980). Examination of the parameters governing oily soil removal from synthetci substrates. *Journal of American Oil Chemists Society*, **57**(7), 230-237.

Fogler, H.S. (1992). Elements of Chemical Reaction Engineering. 2nd ed. New Jersey: Prentice-Hall International.

Gallot-Lavellée, T. and Lalande M. (1985). A mechanistic approach to milk deposit cleaning. Fouling and Cleaning in food processing. (Lund, D.B., Plett, E.A. and Sandu, C. ed.) Wisconsin: Madison.

Gallot-Lavellée, T., Lalande M. and Corrieu, C. (1984). Cleaning kinetics modelling of holding tubes fouled during milk pasteurisation. Journal of Food Proc. Eng. 7, 123-142.

Garrett-Price, B.A. (1985). Fouling of Heat Exchangers- Characteristics, Costs, Prevention, Control, and Removal. New Jersey: Noyes Publications.

Grifin, W.C. (1949). *Journal Soc. Cosm. Chem.* **1**, 311.

Harris, D.A., and Bashford, C.C. (1987). Spectrophotometry and spectrofluorimetry, a practical approach. IRC Press Limited.

Harvath, A.L. (1982). Halogenated Hydrocarbons Solubility- miscibility with water. New York: Marcel Dekker Inc.

Hauser, G. and Sommer, K. (1990). Basic aspects on plant cleaning in the food industry. Process engineering in the food industry 2 (Field R.W. and Howell, J.A. eds.). Oxford: Elsevier.

Hegg, P.O. Castberg, H. and Lund G. (1985). *Journal of Dairy Research*, **52**, 213.

Herd, M.D., Lassahn, G.D., Thomas, C.P., Bala, G.A., and Eastman, S.L. (1992) Interfacial tensions of microbial surfactants determined by real-time video imaging of pendant drops. *Society of Petroleum Engineers*, **24206**, 513-519.

Hirasaki, G.J. (1988). Wettability: Fundamentals and Surface Forces. *Society of Petroleum Engineers*, **17367**, 513-528.

Israelachvili, J.N. (1992). Intermolecular and Surface Forces. 2nd. ed. London: Academic Press.

Israelachvili, J.N., Mitchell, D.J. and Ninham, B.W. (1976). *Journal Chem. Soc. Faraday Trans. I* **72**, 1525-1568.

Izadpanah, S. (1996). Characterisation of Light and Medium Heavy Crude Oils. Experimental Project: University of Bath.

Jafvert, C.T., Van Hoof, P.L. Heath, J.K. (1994). Solubilization of Non-Polar compounds by Non-ionic surfactant micelles. *Water Research*, **28**(5), 1009-1017.

Jennings, W.G. (1965). Theory and practice of hard surface cleaning. *Adv. Food. Res.* **14**, 325-458.

Jennings, W.G., McKillop, A.A. and Luick, J.R. (1957). Circulation Cleaning. Journal of Dairy Science, 40, 1471-1479.

Jennings, W.G., Whitaker, S. and Hamilton, W.C. (1966). Interfacial mechansim of soil removal. *Journal of the American Oil Chemists Society*, 23(3), 130-132.

Johnson, M.A. (1984). A greasy soil hard surface cleaning test. *Journal of the American Oil Chemists Society*, **61**(4), 810-813.

Kao, R.L., Wasan, D.T., Nikolov, A.D. and Edwards, D.A. (1989). Mechanisms of oil removal from a solid surface in the presence of anionic micellar solutions. *Colloids and Surfaces*, **34**(4), 389-398.

Kay, J.M. and Nedderman, R.M. (1988). Fluid mechanics and transfer processes. Cambridge: Cambridge University Press.

Kern, D.Q. and Seaton, R.E. (1959) Surface Fouling... how to calculate limits. *Chemical Engineering Progress*, **55**, 6, 71-73.

Koretskii, A.F., Kolosanova, V.A. and Koretskaya, T.A. (1983). Mechanical work of cleaning and washing effect of surfactant solutions. *Kolloidn Zh*, **45**(1), 74-80.

Koretskii, A.F., Smirnova, A.V., Kolosanova, V.A. and Koretskaya, T.A. (1984). Detergency of nonionic surfactants. *Colloid Journal of the USSR*, **45**(6), 935-940.

Lange, K.R. (1994). Detergents and cleaners. New York: Hanser.

Lide, D.R. (1990). CRC handbook of chemistry and physics: a ready-reference book of chemical and physical data. 71st ed. CRC Press.

Lim, J.C. and Miller, C.A. (1991). Dynamic Behaviour and Detergency in Systems Containing Nonionic Surfactants and Mixtures of Polar and Nonpolar oils. *Langmuir*, **7**, 2021-2027.

Lodhi, A.N. (1994). Equilibrium and dynamic surface tension of nonionic surfactants. *Master of Science*, Bristol University: Bristol.

Mahé, M., Vignes-Adler, M., Rousseau, A., Jacquin, C.G., and Adler, P.M. (1988). Adhesion of droplets on a solid wall and detachment by shear flow- I-III. *Journal of Colloid and Interface Science*, **126**, 314-345.

McCoy, J.W. (1984). Industrial Chemical Cleaning. London: Chemical Pub.

Miller, C.A. and Neogi, P. (1985). Interfacial Phenomena: Equilibrium and Dynamic Effects. Surfactant Science Series, 17, New York: Dekker.

Miller, C.A. and Raney, K.H. (1993). Solubilisation-emulsification mechanisms of detergency, *Colloids and Surfaces*, **74**, (2-3), 169-215.

Mori, F., Lim, J.C., Raney, K.H. Elsik, C.M. and Miller, C.A. (1989). Phase behaviour, dynamic contacting, and detergency in systems containing triolein and nonionic surfactants, *Colloids surf.* **40**, 323.

Myers, D. (1988). Surfactant science and technology. New York: VCH Publishers.

Nagarajan, R. and Ruckenstein, E. (1984). Selective solubilisation in aqueous surfactant solutions. In: Surfactants in Solution 2 (Mittal, K.L. and Lindman, B. ed.). pp. 923-947. New York: Plenum Press.

Nagarajan, R. and Ruckenstein, E. (1991). Theory of Surfactant Self-Assembly: A Predictive Molecular Thermodynamic Approach. *Langmuir*, **7**(12) 2934-2969.

Nagarajan, R. and Welker R.W., (1992). Precision Cleaning in a Production Environment with High-Pressure Water. *Journal of the IES*, **35**(4) 34-44.

Nasr-El-Din, H.A. and Taylor, K.C. (1992). Dynamic interfacial tension of crude oil/alkali/surfactant systems. *Colliods and Surfaces*. **66**, 23-37.

Neogi, P., Kim, M. and Friberg, S.E. (1985). Hydrocarbon extraction into surfactant phase with nonionic surfactants. II. Model. *Sep. Sci. Technol.* **20**(7/8) 613.

Orgino, K. and Agui, W. (1976). A study of the removal of oily soil by rolling up in detergency. *Bullentin of the chemical society of Japan*, **49**(6) 1703-1708.

Otani, M., Saito, M. and Yabe, A. (1985). Surface Energy analysis of the detergency process- Surface tension components of binary mixtures of organic liquids and aqueous solutions of surfactatns. *Textile Research Journal*, **11**, 582-589.

Otani, M., Saito, M. and Yabe, A. (1985). Work of adhesion of oily dirt and correlation with washability. *Textile Research Journal*, **3**, 157-164.

Paciej, R., Jansen, F. and Krommenhoek, S. (1993). Evaluation of plasma cleaning, An Environmentally Friendly Process, for Removing Lubricants from Metallic Surfaces, *ASTM Special Technical Publication*, **1181**, 124-140.

Pasquet, R. and Denis, J. (1983). New developments in beach cleanup techniques. *Proc. 1983 Oil Spill Conf, San Antonio U.S.A.* 279-282.

Paulsson, B. (1989). Removal of Wall Deposits in Turbulent Pipe Flow. *Ph.D. Thesis*. Sweden: Lund University,

Perlat, M.N. (1986). Etude du nettoyage des exchangeurs a plaques destines a la pasteurisation et a la sterilisation a ultra-haute-temperature du lait. Ph.D. thesis UST 1 Lille, France.

Perry, R.H. and Green, D.W. (1984). Perry's Chemical Engineers' Handbook. 6th. ed. New York: McGraw-Hill.

Phillips, D.Z. (1996). Mitigation of crude oil fouling by the use of HiTRAN inserts. First year transfer report. University of Bath: Bath

Plett, E.A. (1985). Relevant mass transfer mechanisms during rinsing. *Fouling and cleaning in food processing*, (Lund, DB, Sandu, C and Plett, EA Eds.), USA: University of Wisconsin, , 395-409.

Pohlman, R., Werden, B. and Marziniak, R. (1972). The ultrasonic cleaning process: its dependence on the energy density, time of action, temperature, and modulation of the sonic field. *Ultrasonics*, **7**, 156-161.

Porter, M.R. (1994). Handbook of Surfactants. 2nd ed. Glasgow: Chapman and Hall.

Prieto, N.E., Lilienthal, W. and Tortorici, P.L. (1996). Correlation between spray cleaning detergency and dynamic surface tension of nonionic surfactants. *Journal of the American Oil Chemists Society*, **73**(1), 9-13.

Puvvada, S. and Blankschtein, D. (1990). Molecular-thermodynamic approach to predict micellization, phase behaviour and phase separation of micellar solutions. I. Application to nonionic surfactants. *Journal of Chemical Physics*, **92**, 3710-3724

Puvvada, S. and Blankschtein, D. (1992). Theoretical and Experimental investigations of micellar properties of aqueous solutions containing binary mixtures of nonionic surfactants. *Journal of Physical Chemistry*, **96**(13), 5579-5592.

Raney, K.H. (1991). Optimization of nonionic/anionic surfactant blends for enhanced oily soil removal. *Journal of the American Oil Chemists Society*, **68**(7), 525-531.

Raney K.H. and Miller, C.A. (1987). Optimum detergency conditions with nonionic surfactants II. *Journal of Colloid and Interface Science*, **117**(1), 539-549.

Raney, K.H., Benton, W.J. and Miller, C.A. (1987). Optimum detergency conditions with nonionic surfactants. *Journal of Colloid and Interface Science*, **117**(1), 282-290.

Romney, A.J.D. (1990). CIP: Cleaning in Place. 2nd ed. Society of Dairy Technology

Rosen, M.J. (1978). Surfactants and interfacial phenomena. New York: Wiley.

Saito, M., Otani, M. and Yabe A. (1985). Work of Adhesion of Oily Dirt and Correlation with Washibility. *Textile Research Journal*, 157-164.

Sayeed, F.A.A. and Schott, H. (1986). Micellar solubilisation of cholesteryl esters of C_{18} fatty acids by a nonionic surfactant. *Journal of Colloid and Interface Science*. **109**(1), 140.

Schambil, F. and Schwuger, M.J. (1987). Correlation between the phase behaviour of ternary systems and removal of oil in the washing process. *Colloid Polym. Sci.* **265**(11), 1009.

Schick, M.J. (1987). Nonionic Surfactants, Physical Chemistry. Vol 23. New York: Dekker.

Schott, H., (1972). In: Detergency: Theory and Test Methods. (Cutler, W.G. ed.). Part 1, New York: Dekker.

Schwartz, A.M. (1972). The Physical Chemistry of Detergency. *Surface and Colloid Science*, **5**, New York: Wiley.

Scott, B.A. (1963). Mechanism of fatty soil removal. *Journal of applied Chemistry*, **13**(3), 133-144.

Shaeiwitz, J.A., Chan, F.C., Cussler, E.L. and Evans, D.F. (1981). The mechsnism of solubilisation in detergent solutions. *Journal of Colloid and Interface Science*, **84**(1), 47-56.

Smith, J.M. and Van Ness, H.C. (1987). Introduction to Chemical Engineering Thermodynamics. 4th. ed. Singapore: McGraw-Hill

Southworth, G.R., Herbes, S.E. and Allen, C.P. (1983). Evaluating a mass transfer model for the dissolution of organics from oil films into water. *Water Res.*, **17**(11), 1647-1651.

Speight, J.G. (1980). The Chemistry and Technology of Petroleum. New York: Dekker.

Sterritt, J.R. (1992). Aqueous Cleaning Performance. *International Sampe Electronics Conference* **6**, 202-213.

Tadros, T.F. (1984). Surfactants. London: Academic Press.

The Soap and Detergent Association, (1987). A Handbook of Industry Terms. 3rd. ed. New York.

Thompson, L. (1992). Surface Chemistry and the Detergency of Surfactants. *Special Publication Royal Society of Chemistry*, **118**, 56-77.

Thompson, L., (1994) The role of oil detachment mechanisms in determining optimum detergency conditions. *Journal of Colloid and Interface Science*, **163**, 61-73.

Trebal, R.E. (1980). Mass-Transfer Operations. 3rd. ed. New York: McGraw-Hill.

Vaccari, J.A. (1993). Ultrasonic cleaning with aqueous detergents. *American Machinist* (Penton). **4**, 41-42.

Voss, T.E. and Korpi, G.K. (1972). Radioisotope Evaluation of Metal Cleaning Processes. *Metal Finishing*, **70**, 2, 76-79.

Walas, S.M., (1988). Chemical Process Equipment- Selection and Design. Boston: Butterworths Publishers.

Walker, R. (1985). The efficiency of ultrasonic cleaning. *Plating and surface finishing*, **1**, 63-70.

Withers, P. (1994). Ultrasonic sensor for the detection of fouling in UHT processing plants. *Food Control*, **5**, 2, 67-72.

Yatagai, M., Komaki, M. and Hashimoto, H. (1992). Applying Differential Scanning Calorimetry to Detergency Studies of Oily Soil. *Textile Research Journal.* **62**(2), 101-104.

NOMENCLATURE

		S.I.Dimensions
A	area of fouled surface	m^2
A	pre-exponential factor (equations 7.7 and 7.8)	dimensionless
A_g	aggregate surface area (equations 4.5, 4.6, 4.9 and 4.10)	m^2
A_{res}	residual layer mass per unit surface area	$kg\ m^{-2}$
a	aggregate area per surfactant molecule (equations 4.5, 4.6 4.9, A.7 and A11)	$kg\ m^{-2}\ s^{-1}$
a_c	cleaning region A zero order removal constant	$kg\ m^{-2}\ s^{-1}$
a_h	revised area of hydrophilic head for ethoxylate group (equation A.12)	m^2
a_o	area of hydrophilic head group	m^2
b	boundary layer thickness (equation A.21)	m
b	length of semi-major axis for globular micelles (equations 4.7 and 4.8)	m
C_1	proportionality constant (equation 2.1)	$m^{2.24}\ s^{1.48}\ kg^{-1.24}$
C_2	proportionality constant (equation 2.1)	$m\ s^{-1}$
C_3	proportionality constant (equation 3.1)	$m\ kg^{-1}$
C_4	proportionality constant (equation 3.1)	$m\ s\ kg^{-1}$
C_5	proportionality constant (equation A.1)	$m^2\ s^{-2}$
C_6	dimensionless constant (equations 7.14 and 7.15)	dimensionless
C_7	dimensionless constant (equation 7.18)	dimensionless
C_8	dimensionless constant (equation 7.18)	dimensionless
c	concentration	$mol\ dm^{-3}$
c_b	concentration of monomers in the bulk	$mol\ dm^{-3}$
c_i	concentration of monomers at the interface	$mol\ dm^{-3}$
c_{io}	concentration of monomers in the oil at the interface	$mol\ dm^{-3}$
c_s	concentration of applied surfactant (equations 7.17 and 7.18)	v/v%
D	diffusivity	$m^2\ s^{-1}$
d	diameter of tubing	m
d_r	diameter of droplet	m

E	eccentricity factor	dimensionless
E_{act}	apparent activation energy	J mol^{-1}
F	total free energy of a system	J
F_r	Energy loss per unit mass	J kg^{-1}
G	mass flow rate (equation 3.1)	kg s^{-1}
g	acceleration due to gravity (equations A18 and A.20)	m s^{-2}
g	aggregation number	dimensionless
H	Dimensional constant (equation A.12)	K^{-1}
H_o	height of liquid above pump inlet (equation A.20)	m
h	dirt content (equation 3.1)	dimensionless
J	flux	mol m^{-2} s^{-1}
j	number of ethoxylated groups per molecule (C_iE_j)	dimensionless
K	equilibrium constant	dimensionless
k	removal constant	s^{-1}
k_A	apparent reaction rate (equation 2.2)	m s^{-1}
k_b	Boltzmann's constant	J K^{-1}
L	linear dimension of lattice site (equation A.5)	m
l	deposit thickness (equations 2.1 and 3.1)	m
l	equivalent length of piping (equation A.19)	m
l	tube length	m
l_c	length of hydrophobic chain of molecule (Figure 2.1)	m
l_s	length of surfactant hydrophobic tail (equation A.17)	m
M_d	mass of fouled deposit (equation 2.2)	kg
M_w	force (equation A.2)	N
M_{wt}	molecular weight of hydrocarbon tail (equation A.9)	dimensionless
M_{wt}	molecular weight of solvent (equation A.24)	dimensionless
m	mass of deposit per square area	kg m^{-2}
m_a	mass of deposit per square area in cleaning region A (equations 6.1, 6.2, 7.4 and 7.5)	kg m^{-2}
m_b	mass of deposit per square area in cleaning region B (equations 6.2 and 7.5)	kg m^{-2}
N	segments (defined in equation A.6)	dimensionless

n	reaction order	dimensionless
n_c	number of carbon atoms	dimensionless
OH-	Cleaning Agent Hydroxide ion concentration (equation 2.2)	kg m^{-3}
P	packing parameter	dimensionless
P_o	Pressure at pump suction (equation A.20)	N m^{-2}
P_v	Vapour pressure of liquid (equation A.20)	N m^{-2}
p	perimeter of ring (equation A.2)	m
P	Pressure (equation A.18)	N m^{-2}
R	gas constant (equations 7.7 and 7.8)	J K^{-1} mol^{-1}
R	radius (inc. hydrophobic core of the micelle)	m
R_a	arithmetic mean roughness	m
Re_i	Reynolds number ($\rho_i ud/\mu_i$)	dimensionless
Re_o	Reynolds number of oil ($\rho_i ud/\mu_o$)	dimensionless
R_p	droplet contact radius (equation 2.5)	m
R_s	radius of hydrophobic core of micelle	m
T	temperature	K
t	time	s
t_{rev}	time of cleaning region A	s
u	velocity	m s^{-1}
v	kinematic viscosity (equation A.1)	m^2 s
v	volume of hydrophobic tail	m^3
W_a	work of adhesion (equation 2.6)	N m^{-1}
W_c	work of cohesion (equation 2.7)	N m^{-1}
X	mole fraction	dimensionless
X_1	mole fraction of monomers singly dispersed in solution	dimensionless
X_g	mole fraction of monomers contained within a micelle	dimensionless
z	dimensionless constant 0.3-0.5 (equation A.13)	dimensionless
z	distance in the vertical direction (equation A.20)	m

Greek symbols

ψ	chemical potential	J

θ	contact angle	degree
φ	friction factor	dimensionless
μ_g	Gibbs free energy	J
$(\Delta\mu_g)_{tr}$	Gibbs free energy of transfer	J
$(\Delta\mu_g)_{defr}$	Gibbs free energy of deformation	J
$(\Delta\mu_g)_{int}$	Gibbs free energy of formation	J
$(\Delta\mu_g)_{steric}$	Gibbs free energy of steric repulsion	J
$\nu(CH^*)$	volume of hydrocarbon unit	m^3
ω	association factor	dimensionless
ρ	density	$g\ m^{-3}$
ρ_l	density of liquid	$g\ m^{-3}$
ρ_o	density of oil	$g\ m^{-3}$
τ_w	shear stress at the wall	$N\ m^{-2}$
μ	viscosity	$N\ s\ m^{-2}$
μ_l	viscosity of liquid	$N\ s\ m^{-2}$
μ_o	viscosity of oil	$N\ s\ m^{-2}$
γ	surface or interfacial tension	$N\ m^{-1}$
γ_l	surface tension of the liquid	$N\ m^{-1}$
γ_{sl}	interfacial tension between solid and liquid	$N\ m^{-1}$
γ_{sg}	interfacial tension between solid and gas	$N\ m^{-1}$
γ_{gl}	interfacial tension between gas and liquid	$N\ m^{-1}$
γ_{ol}	interfacial tension between oil and liquid	$N\ m^{-1}$
γ_{os}	interfacial tension between oil and solid	$N\ m^{-1}$
γ_{og}	interfacial tension between oil and gas	$N\ m^{-1}$
ν	volume per unit mass of fluid	$m^3\ kg^{-1}$
ν_A	solute molar volume at normal boiling point	$m^3\ mol^{-1}$
ν_s	volume of hydrophilic chain (equation A.14)	m^3
τ_c	critical wall shear stress (equation 2.5)	$N\ m^{-2}$
χ	dimensionless constant (equation A.8)	dimensionless
χ	dimensionless constant (equation A.8)	dimensionless

γ_{agg}	aggregate core interfacial tension (equations A.7 and A.8)	$N\ m^{-1}$
θ_r	receding contact angle (equation 2.5)	degree
θ_a	advancing contact angle (equation 2.5)	degree